SESM 67-8

STRUCTURES AND MATERIALS RESEARCH
DEPARTMENT OF CIVIL ENGINEERING

ANALYSIS OF ELASTIC-PLASTIC SHELLS OF REVOLUTION UNDER AXISYMMETRIC LOADING BY THE FINITE ELEMENT METHOD

by

M. KHOJASTEH-BAKHT

Report to
National Aeronautics and Space Administration
NASA Research Grant No. NsG 274 S-2

APRIL 1967

STRUCTURAL ENGINEERING LABORATORY
UNIVERSITY OF CALIFORNIA
BERKELEY CALIFORNIA

Structures and Materials Research
Department of Civil Engineering

ANALYSIS OF ELASTIC-PLASTIC SHELLS OF REVOLUTION UNDER AXISYMMETRIC LOADING BY THE FINITE ELEMENT METHOD

by

Mahmoud Khojasteh-Bakht

Graduate Student

E.P. Popov

Faculty Investigator

Report to

National Aeronautics and Space Administration
NASA Research Grant No. NsG 274 S-2

Structural Engineering Laboratory
University of California
Berkeley, California

April 1967

Errata

Page	Line	Reads	Should Read
4	9	deVenbeke	deVeubeke
24	8	$\{t\}$	$\{t\}^T$
32	12	$\{P^{(m-1}\}$	$\{P^{(m-1)}\}$
40a	13,14,15,19	[A]	[a]
40b	12	[A]	[a]
118,119,120	Legend	□	△
129	Legend	27 Elements	47 Elements

ABSTRACT

The finite element method using a displacement model is employed to analyze the behavior of elastic-plastic shells of revolution under axisymmetric loading. Both perfectly plastic and work hardening materials are treated. The solution is based on the use of a new curved element which can take specified slopes and curvatures at its nodal circles.

Various methods of expressing the geometry of a curved element are discussed, and the elements developed are well-conditioned for all ranges of latitude angle. Representation of the displacement pattern in both rectilinear local and curvilinear surface coordinates are compared. The former is found to be superior in accommodating the rigid body translation and the constant straining modes.

A general treatment of the elastic-plastic problem in connection with the finite element method is given. The tangent stiffness method and the initial strain method, which treats the plastic deformation as a fictitious load, are compared. The former method was selected for use in the analysis. Several numerical examples are given to illustrate the convergence and the accuracy of the method.

ACKNOWLEDGEMENTS

The author wishes to express his deep appreciation to Professor E.P. Popov for his supervision and encouragement throughout the course of this work. He is also grateful to Professors E.L. Wilson and B.N. Parlett for reading the manuscript. In addition, the help of other faculty members and graduate students is acknowledged.

This work was sponsored by the National Aeronautics and Space Administration by Grant NsG 274-S2. The Berkeley Computer Center provided facilities for the computer work.

Finally, the author wishes to thank Mrs. M. French who did an excellent job in typing the manuscript.

TABLE OF CONTENTS

NOMENCLATURE

The following list contains the list of symbols used in this dissertation. Some of the symbols which were introduced and were not referred to afterwards were defined in the text and are not listed here. Unless otherwise stated, the repeated indices imply summation over the range of the indices. In Chapter 3 quantities with subscripts are covariant components and quantities with superscripts are contravariant components. The symbol $|_i$ denotes covariant derivative.

$A_{ijk\ell}$ - as defined in (4.43)

$C_{ijk\ell}$ - elastic-plastic moduli tensor

$\bar{C}_{\alpha\beta\gamma\delta}$ - elastic-plastic moduli for generalized plane stress, see (4.65)

C - edge of the shell

c - as defined in (4.29)

dA - surface element of the reference surface of shell

dC - element of edge length of the shell

dS - surface element

ds - element of arc length

dv - volume element

E - Young's modulus

E_t - tangent modulus

$E^{ijk\ell}$ - elastic moduli tensor

e_{ij} - deviatoric strain tensor, see (4.3)

$\mathcal{E}$ - strain energy density

F - free energy function, see (3.32); also yield function in Chapter 4

f - yield function

f^i - component of body force per unit volume

g - plastic potential

$H_{ijk\ell}$ - elastic compliance tensor

H - as defined in (4.21)

h - as defined in (4.42), also shell thickness in Chapter 5

J_1, J_2, J_3 - invariants of deviatoric stress tensor

k - yield stress in simple shear

ℓ - cord length of an element

M_s, M_θ - meridional and circumferential bending moments per unit length, respectively

N_s, N_θ - meridional and circumferential in plane forces per unit length, respectively

n_j - direction cosines of outward normal to the boundary surface

p_s, p_r - meridional and normal surface load per unit area of reference surface of shell, Fig. 10

Q_s - transversal shearing force, Fig. 10

r_1, r_2 - principal radii of curvature of shell

r - as shown in Fig. 10

S_T - part of boundary surface where stresses are specified

$S_{ijk\ell}$ - elastic-plastic compliance tensor, see (4.36)

s_{ij} - deviatoric stress tensor, see (4.2)

s - arc length, also mean normal stress, see (4.2)

S_1, S_2 - as defined in (4.69) or (4.70)

t^i - component of stress vector

u_1, u_2 - displacements as shown in Fig. 12

u - meridional displacement

u_i - displacement components

V - volume

W_p - plastic work, see (4.20)

α_i - generalized coordinates

α_{ij} - see (4.28)

β - an angle as shown in Fig. 12

δ_{ij} - Kronecker delta; $\delta_{ij} = \begin{cases} 1 & \text{for } i=j \\ 0 & \text{for } i \neq j \end{cases}$

Δ, δ - if precede any symbol designate a finite and an infinitesimal increments, respectively

δ_η - as defined in (4.30)

δ_λ - a positive parameter, see (4.13)

ϵ_{ij} - strain tensor

$\epsilon_s, \epsilon_\theta$ - meridional and circumferential strains, respectively

$\epsilon_s^o, \epsilon_\theta^o$ - meridional and circumferential strains of the reference surface of shell, respectively

$\bar{\epsilon}^p$ - equivalent plastic strain, see (4.22)

ζ - as defined in (4.55) for Chapter 4; also coordinate along the thickness of shell in Chapter 5, see Fig. 13

η_{ij} - initial strain tensor, see (3.26)

η - local coordinate for an element, see Fig. 12

θ - circumferential angle, see Fig. 10

κ - parameter of work-hardening, see (4.16)

κ_s, κ_θ - meridional and circumferential change of curvatures of shell, respectively

λ, μ - Lamé constants

ν - Poisson ratio

ξ - local coordinate for an element, see Fig. 12

π - potential energy

π_Δ - potential energy of an element

σ_y - yield stress in tension

$\bar{\sigma}$ - equivalent stress

τ^{ij}, τ_{ij} - stress tensor

φ - latitude angle, see Fig. 10

χ - meridional rotation

ψ - as shown in Fig. 12

Ω - as defined in (4.74)

$\{\ \}$ - vector; column matrix

$[\ ]$ - matrix

$[A]$ - displacement transformation matrix, see (3.15)

$[B]$ - as defined in (3.8)

$[C]$ - matrix of elastic-plastic moduli

$[D]$ - rigidity matrix, see (5.24)

$[E]$ - matrix of elastic moduli

$\{J\}$ - as defined in (3.38)

$[K]$ - stiffness matrix of the entire system

$[k]$ - element stiffness matrix

$[k_\alpha]$ - element stiffness matrix in generalized coordinates, see (3.11)

$[L]$ - as defined in (3.24)

$[\eta]$ - as defined in (5.23)

$\{P\}$ - as defined in (3.37) in Chapter 3, also as defined in (5.29) in Chapter 5

$\{p\}$ - as defined in (5.28)

$\{Q\}$ - equivalent nodal point force

$\{Q_\alpha\}$ - equivalent nodal point force in generalized coordinates

$\{q\}$ - nodal point displacement

$\{R\}$ - external nodal point load of the system

$\{r\}$ - nodal point displacement of the system

$[T]$ - as defined in (5.54)

$\{\alpha\}$ - generalized coordinates

$\{\varepsilon\}$ - strain tensor expressed in column matrix

$\{\varepsilon\}$ - as defined in (5.22)

$\{\tau\}$ - stress tensor expressed in column matrix

$[\varphi]$ - as defined in (3.7)

$[\varphi_f],[\varphi_t]$ - interpolating functions for body forces and surface loads, respectively, see (3.13) and (3.14)

1. INTRODUCTION

The stress analysis of shells of revolution and particularly those of spherical, cylindrical, toroidal, and conical shells has received a great deal of attention. The abundance of literature in this area is due mainly to the great variety of applications: domes, fluid containers, nuclear reactors, rocket casings, submarine hulls, and pressure vessels.

Early investigations have been limited to small deformations of shells composed of linear, homogeneous isotropic elastic materials. The classical work of H. Reissner [1]* on spherical shells and the extension by E. Meissner [2] for shells of revolution of arbitrary shapes were the first significant contributions to the theory of rotational shells. Asymptotic integration was found to be very fruitful in the solution of the governing equations of spherical shells for a wide range of geometrical and material parameters. This method has also been employed for other types of rotational shells [3,4].

Analytical solutions of the governing differential equations for shells of revolution are available only for special cases [5,6,7]. However, numerical solutions, with the aid of digital computers, have been achieved for arbitrary meridional shapes using: 1) the finite difference method [8,9], 2) numerical integration procedures [10], and 3) numerical integration combined with the finite difference method [11]. These methods are applicable if variation in the shell geometry and material properties can be expressed analytically. In many practical problems, however, the variation of geometry

*The numbers in brackets refer to the references listed at the end.

and material properties are quite arbitrary and do not lend themselves to simple analytical representations. The process of curve-fitting must then be used to characterize these variations. This introduces inaccuracies which will permeate through the remainder of the numerical analysis, especially where the derivatives of the fitted curve are used.

Additional difficulties may also arise in the numerical integration of the shell equations. Since such methods were originally devised to handle initial value problems, their application to shell analysis, a boundary value problem, requires trial and error procedures. If the values of the unspecified variables at the initial boundary are not judiciously assigned, unsatisfactory results may be produced. Truncation, cancellation, and round-off errors may also accumulate over a large integration range and destroy the desired accuracy in the results. The importance of the error due to cancellations when the length of the shell is increased is pointed out in [11]. It is found that for every set of geometric and material properties of the shell there is a critical length beyond which the solution loses all accuracy.

A different numerical scheme, which is known as the finite element method, has also been employed for the analysis of arbitrary shells of revolution. In this procedure, the continuous shell structure is divided into a number of short frustums, to be referred to as the "shell elements", which are connected at their edges called the "nodal circles". The assemblage is made through equilibrium and compatibility requirements at nodal circles. Because each frustum may be considered as a separate unit,

different material properties, as well as thicknesses can be ascribed to different elements. The principal task in this procedure consists of establishing a force-displacement relationship between the nodal circle forces/moments and the corresponding displacements/rotations. The influence coefficients relating these two sets of quantities may be expressed in matrix form, which is well suited for routine computations in a digital computer, as a stiffness or a flexibility matrix of the element. In the literature there are two methods for obtaining the influence coefficients of a shell element.

The first method utilizes the homogeneous solution of the governing differential equations. As a result, the element shape is restricted to certain simple shell geometries such as a truncated cone, a circular cylinder, and a spherical cap. The truncated cone element is the more general shape for approximating an arbitrary shell geometry. This element has been employed by Meyer and Harmon [12] for edge loading and by Popov, Penzien, and Lu [13] for any general axisymmetric loading. Ref. [13] has also used cylindrical elements and a spherical cap to supplement the conical element. The use of a piece of circular toroid has also been reported [14]. In addition to the restriction of the element shape, the influence coefficients obtained by this method turn out to be very complicated and require the evaluation of infinite series, which for some geometrical and material parameters converge very slowly. For a conical shell element, these series are Bessel functions of complex argument, known

as Thompson functions. At the transitions of conical elements into cylindrical and circular plate elements, the Thompson Functions become ill-conditioned and require special treatment. This phenomenon is due to the change of the form of the solution of the differential equations from Bessel to exponential and logarithmic functions.

The second approach makes use of a special type of direct method of variational problems, referred to as the extended Ritz method. This approach is based on the original work of Turner et al [15] and Argyris et al [16], which was further developed and extended by Melosh [17], de Venbeke [18,19] and others. In this approach, the primary variables are approximated by some relatively complete sets of functions in a subregion, here called the element, to extremize the variational problem. Depending on which set of variables, displacements or stresses is taken as the primary variable two types of models known as the "displacement models" and the "equilibrium models" have been advanced. In displacement models the displacements are taken as the primary variables, expressed in terms of linear combinations of the interpolating functions. These displacements are then used to minimize the potential energy of the system. This procedure provides upper bounds for the stiffness influence coefficients. In the equilibrium models, on the other hand, the stresses are taken as the primary variables and their approximate forms, which satisfy the equilibrium equations, are used to minimize the complementary potential energy of the system. The stiffness influence coefficients thus obtained constitute a lower bound to the exact solution. By taking a finer mesh, provided certain conditions are

satisfied [19], the bounds can be made closer. However, this is insufficient to guarantee convergence for the true solution. Finally, the use of a "mixed model" has also been advocated [20].

In the analysis of shells only the "displacement models" have been studied thus far. Until very recently the truncated cone has been the only element which was reported in the literature to idealize shells of revolution. In contrast with the finite element of the first type, discussed above, the use of an approximate and, in fact, simple displacement field removes the ill-conditioning and enables a truncated cone to be degenerated directly into the limiting case of a circular cylinder or of an annular plate. In addition, the relative simplicity of the influence coefficients obtained from the second approach decreases the number of numerical operations and consequently reduces the numerical errors. It also enables the use of a larger number of elements for the same computer core storage. Based on many numerical examples, the accuracy of the second method was found to be comparable, if not superior, to the first approach.

The use of a conical element for a displacement model, together with the direct stiffness method of matrix analysis of structure, is reported by Grafton and Strome [21] for axisymmetric deformation of shells of revolution of cylindrically orthotropic materials. In the derivation Grafton and Strome approximated the integral of the strain energy of the shell in a manner which later was shown to reduce accuracy. The solution for asymmetric deformations, utilizing Fourier expansion, was achieved by Percy et al [22]. These authors also studied the effect of including higher order polynomials in the dis-

placement field, which is reported to improve the results for edge loading. Extension of [22] has been made by Klein and Sylvester [23] for the dynamic analysis of shells of revolution. The conical element was also employed for analysis of laminated shells of revolution by Dong [24].

The idealization of the shell geometry by a series of truncated cones introduces the discontinuity of slopes along the meridian of the shell. This may introduce an unrealistic stress concentration at the element junctures. This effect is very pronounced in membrane type shells. The study of Jones and Strome [25] on the membrane type spherical cap clearly indicates the undesirable phenomena of oscillating displacement and development of large bending moments at the nodal circles. The peak values of these bending moments, which do not exist in the true solution, appear at the element junctures where the slopes are made discontinuous. The manner in which one can improve the analysis is to develop a curved element to provide a better geometric idealization of the system. Jones and Strome [26] report the first attempt to construct such a curved element for rotational shells. Their element provides the continuity of slopes at nodal circles but for an arbitrary shell the meridional curvatures are not continuous at these nodes. Moreover, due to an inadequate geometrical representation, their element is only applicable to open shells and to cases where the latitude angle, ϕ, is not equal or close to zero.

Although the elastic analysis has been shown to predict satisfactorily the load-deformation behavior of the structures for loading below the proportional limit; it ceases to be useful once the stresses exceed the

elastic limit. In certain design problems, such as space vehicle structures, a small amount of plastic deformation may be tolerated in order to utilize the material more efficiently. In fact, a small amount of plastic deformation may have the beneficial effect of alleviating the stress concentration at the junctures and in the zones where the gradient of loading is high. Moreover, the analysis of plastic deformation for cyclic loading is essential in predicting low cycle fatigue failure [38,39]. The fact that the problem of determining the displacements and stress distributions in these types of problems is highly non-linear in the past made it almost impossible to obtain solutions to any but the simplest problems. The availability of the digital computer and the techniques of finite element now makes these problems tractable.

Originally, the finite element method was devised to treat the linear system by means of matrix algebra. With the aid of incremental or iterative techniques the utility of the finite element can be extended to handle non-linear problems [27, 28,29]. In this dissertation attention is confined to physical or material nonlinearity, in particular non-linearity as the result of plastic deformation. This area of research is now in its development stage and much future work is to be expected. In general, two approaches can be adapted to extend the finite element method to treat the elastic-plastic problems. One approach makes use of an analogy between the plastic strain and the thermal, creep, or shrinkage strain [30,31,32]. This approach will be termed the "initial strain method". The stiffness influence coefficients used in this approach are identical with the elastic

case, and the effect of plastic deformation appears as a modification to the loading. The other approach utilizes the relations between stress and strain increments to establish the tangent influence coefficients for each load increment [33,34]. Here the influence coefficients are changed during incremental loading to account for physical nonlinearity and path-dependency of plastic deformation. Because different stiffness influence coefficients are used in the formulation of the problem, depending on the stress level achieved, this method will be referred to as the "tangent stiffness method". Some experience with the initial strain method has shown a slow convergence of the results [35]. It can be surmized that for materials exhibiting a small amount of work-hardening, the initial strain method should give inferior results. In addition, since in the initial strain method the plastic strain appears as a correction to the elastic part of strain, the process may become ill-conditioned for cases where the plastic strain is predominant. The initial strain method has the advantage of requiring the stiffness matrix to be inverted only once. On the other hand, the stiffness influence coefficients must be changed for each loading increment if the material properties change due to variation of temperature or other environmental conditions, or in the cases where geometrical nonlinearity is to be included. In this case, the initial strain method loses its only advantage.

A brief review of the previous work on plastic behavior of shells is given in Chapter 2. To treat plastic deformations, a detailed study of the initial strain and the tangent stiffness methods in connection with the

finite element technique will be made in Chapter 3.

This dissertation is concerned with the elastic-plastic deformation of shells of revolution under axisymmetric loading. An extensive study was made to develop a refined element for use in the finite element method of analysis. Several curved elements were developed and their accuracies were compared through numerical examples. The elements developed do not have the shortcomings of the one given in Ref. [26]. The best element developed here which satisfies the continuity of slopes and curvatures at nodal circles was used in connection with the "tangent stiffness method" to analyze the plastic deformation of shells of revolution. It may be pointed out that no applications of the finite element method to the analysis of plastic deformation of shells appear to be available in the literature.

A computer program in FORTRAN IV language was written for IBM 7090-7094 DCS system, available at the Computer Center of the University of California at Berkeley. Several illustrative examples were worked out and the accuracy of the method was studied.

2. REVIEW OF THE PLASTIC SHELL THEORIES

The plasticity of shells is a relatively new area of investigation. Research in this field has been started in the late 1940's. The theory was initially developed as an extension of the elastic shell theory by replacing the Hooke's law with Hencky's relations of the deformation theory of plasticity [112]. This development was accompanied by the generalization of the limit analysis theorems for rigid frames [40,41], for the treatment of shell problems [42,43]. Further developments were essentially along these two lines and various special cases were studied. Except for the very simple cases, the complexity of finding analytical solutions for shells using the flow theory of plasticity has retarded the progress in this field. The advent of the digital computers and the development of new methods of structural analysis greatly changed this situation. These aids are now indispensible for the numerical solution of practical problems.

In this chapter the work reported in the literature on the plasticity of rotational shells under axisymmetric loading will be reviewed. As the development of solutions for general loading conditions is still fragmentary, this topic will not be discussed here.

Much of the research has been devoted to the limit analysis approach. In the sequel the work related to limit analysis, rigid-work hardening materials, and elastic-plastic analysis using both deformation and flow theories of plasticity will be briefly reviewed. In addition, the results of some experiments will be discussed. For further details the reader may wish to examine the appropriate references listed at the end.

2.1 Limit Analysis of Shells

In the limit analysis approach, the objective is to find the load carrying capacity of the structure in question based on the assumptions that the material is perfectly plastic (i.e., non-work-hardening) and the deformation prior to collapse is so small as to allow the use of small deflection theory. In some cases, the effect of the change in geometry and work-hardening could make the calculation of the ultimate load meaningless. The complete solution involves the determination of the stress and the velocity fields at the point of collapse.

Except for a few cases such as the hyperbolic paraboloid and the helicoidal shells [95], all of the literature on the limit analysis of shells have been devoted to the case of rotational shells under axisymmetric loading.

The steps in the limit analysis of shells are as follows: (1) express the yield condition in terms of the stress resultants (including the stress couples), (2) apply the lower and upper bound theorems to establish the bounds on the ultimate load, and (3) determine the stress and velocity fields, if a unique collapse load has been attained in (2).

As a general rule, the first step has been achieved by making a kinematic assumption, namely the Kirchhoff-Love hypotheses. The yield hypersurface in the stress resultant space (the 6-space) was first constructed for Mises yield condition by Ilyushin in 1948 [112]. The same surface was later reconstructed and specialized for rotational shells by Rozhdestvyensky [50] and Hodge [65,70]. Onat and Prager 1954 [45] constructed the yield hypersurface in the stress resultant space for Tresca yield condition.

Even for Tresca yield condition the hypersurface in the stress resultant space is nonlinear and leads to a formidable mathematical problem. Two approaches have been used to linearize this hypersurface. One replaces a uniform shell with a sandwich shell having two thin face sheets carrying only the in plane stresses and a central core transmitting the shearing forces [46,51,65,68,70]. The other replaces the hypersurface by a series of intersecting planes inscribed and circumscribed on it [85].

Other methods to simplify the hypersurface also have been suggested. The method used by Drucker and Shield [62] ignores the circumferential bending moment in comparison with the meridional moment, and the one proposed by Hodge [70] neglects the interaction between the membranc forces and the bending moments.

Among the various shapes of shells of revolution the cases of cylindrical, spherical, and conical shells have received much attention. The remainder of this section is devoted to the discussion of these problems.

Drucker [43] is believed to be the first to consider the limit analysis of the cylindrical shells under internal pressure. Expressions for the yield hypersurface for a cylindrical shell of a material obeying Tresca yield condition were derived independently by Hodge [46] and Onat [48]. The effect of free ends on the load carrying capacity of cylindrical shells has been discussed by Eason and Shield [49]. The case of a circular cylinder under ring load was studied by Eason [63] and Prager [66]. The shells under combined loading: - pressure, axial load, and/or torque - have been treated by Sankaranarayanan [72], Panarelli et al [79], Ball et al [84], and Ho et al [99]. The last reference derives the complete stress and velocity

fields at the limit load for certain types of loads, end conditions, and shell proportions. The problem of orthotropic cylindrical shells has been reported by Niepostyn [53] and Mróz [69] where the modified linear yield condition was used. The cases for anisotropic material has been discussed in a series of papers by Mikeladze [51,87]. The use of Mises yield condition for cylindrical sandwich shell is also reported by Rzhanitzyn [60].

The problem of spherical shells was first treated by Onat and Prager [45]. The material was assumed to obey Tresca yield condition and crude bounds on the ultimate uniform pressure were obtained. Closer bounds were later reported for sandwich shells [61,64,70]. Mróz and Xu [82] discussed the load carrying capacity of spherical shells by using a variety of yield conditions and established a complete solution for certain simply supported shells. Shallow spherical shells were treated by Hazalia [52] and Feinberg [55]. Hodge et al [75] discussed the problem of a spherical cap with a cut out. The case of a shell loaded through a rigid boss was investigated by Leckie [100]. Finally, the complete solution of a clamped spherical sandwich shell subjected to hydrostatic pressure is reported by Lee and Onat [104].

The limit load for a uniform shallow conical shell was derived by Onat [73] and Lance and Onat [80]. The load was applied through a finite rigid boss, connected rigidly to the shell proper, and the material was assumed to obey Tresca yield condition and its associated flow rule. Simultaneous with [73], the same problem, but with the rigid boss connected

through a hinge to the shell body, was considered by Hodge [71]. It was shown that if the radius of the boss tends to zero the solution will be reduced to the case of a conical shell subjected to a concentrated load at its apex. The value of the ultimate load is found to be independent of the support condition and is equal to $P = 2\pi M_o \cos^2 \varphi$, where φ denotes the latitude angle. Such a reduction was not possible in [73]. The work in [73,80] was extended to sandwich shells by Hodge [95]. It was reported that for a given shell, the collapse load increases with the increase of boss size. The case of a closed conical shell under internal pressure is presented by Resenblum [47] and Hodge et al [82] and an exact solution based on the two moment interaction (see Ref. [70]) is reported by Kuech and Lee [103].

In addition to the above types of shells, some other cases have also been reported in the literature. The case of torispherical shell was discussed by Drucker and Shield [62]. For intersecting shell structures, the work of Hodge [88] for a closed cylindrical shell and Gill [89], Lind [90], Cloud [91,96], Dinno and Gill [93,94], and Ellvin and Sherbourne [97,98] concerning cylindrical nozzles in spherical shells may be mentioned. Moreover, the general theory of axisymmetric shallow shells has been treated by Feinberg [55] and Hodge et al [81].

For more information the books by Hodge [61,85] and Olszak et al [86] are recommended.

2.2 Shells of Rigid-Work Hardening Materials

In the elastic-plastic analyses some simplifications may be introduced by neglecting the elastic part of the strain. This is generally referred to as the rigid-plastic approach. For work-hardening materials, the rigid-work hardening approach together with the concept of piecewise linear yield conditions have been employed. The utilization of the piece-wise linear yield conditions and the associated flow rules for the solution of work-hardening problems were suggested by Prager [107] and Hodge [108]. It allows the total stress-strain relations to be used in the small and at the same time retaining the characteristic features of incremental laws in the large. As indicated by Hodge [109], the plastic flow rules can be explicitly integrated under restrictive conditions, defined as a "regular progression". That is a stress point, which has reached the yield surface, should not move from one side of the surface to another, nor from one corner to a side, or back into the elastic zone. These conditions impose a serious restriction which may not hold in general.

The application of rigid-work hardening approach to the shell problems is reported by Onat [110] and Thorn et al [111]. Utilizing Tresca yield condition and kinematic hardening, Onat discusses the rotational shells and the special case of a circular cylinder. Thorn [92] and Thorn and Lee [111] report cases of simply supported cylindrical shells under the internal pressure. Tresca yield condition in terms of the stress resultants is approximated by means of a square yield curve. Linear isotropic hardening is assumed. In this analysis solutions are obtained for several plastic

regimes and are applied to shells of various relative lengths.

2.3 Elastic-Plastic Analysis of Shells Using the Deformation Theory

Attempts to formulate the elastic-plastic shell analysis problems was initiated by using the deformation theory of plasticity. Ilyushin [112] established the basic equations for the analysis of elastic-plastic shells based on Hencky's relation. Ilyushin's work was continued by other investigators in the Soviet Union [113 to 120] for different cases such as shallow shells [118] and for shells of anisotropic material [120]. Various approximations were introduced in order to make the task of reaching an analytical solution feasible. Iteration techniques together with the "initial strain method", referred to in the Soviet literature as "the method of elastic solution", also have been suggested [30].

Employing this technique, Mendelson and Manson [121] formulated the problem in a nonlinear integral equation form. Several examples, among them the analyses of cylindrical shells with axial temperature gradient, were worked out by using the method of successive approximations. This method was later applied to general shells of revolution by Stern [122] and Roberts [125]. Utilizing a finite difference method, Spera [124] extended the approach for shells of revolution containing discontinuities.

2.4 Elastic-Plastic Analysis of Shells Using the Flow Theory

The concept of piecewise linear yield condition [107,108,109] together with idealization of the shell as a sandwich structure have been utilized in the solution of elastic-plastic shells using the flow theory of plasticity.

This enables one to integrate the flow law locally. Several special cases have been studied. Hodge and Romano [126], Lee and Thorn [135], and Thorn et al [138] discussed the problem of circular cylinder under uniform radial pressure. Linear isotropic hardening and simplified piecewise linear yield function in terms of stress resultants were adopted in these investigations. Comparisons with the limiting cases such as for perfectly plastic and to rigid-work hardening cases are reported. The same problem was also discussed by Hodge [127] and Shaffer et al [131] for sandwich shells with clamped edges using Tresca yield condition; and by Hodge and Nardo [128] and Paul and Hodge [129] by including the beam-column effect. In the latter case the stress field is first determined for the rigid-plastic shell. Then, assuming that the state of stress is represented by the same part of the yield surface, the elastic-plastic problem is dealt with. Onat and Yamantürk [130] included the effect of temperature both on strain and yield strength. This approach has also been extended to conical shells by Stephens [137] and Stephens and Friedericy [140] where the beam-column effect is also included.

Attempts to establish a general procedures to deal with the elastic-plastic shells using the flow theory also has been made by using the techniques of numerical analysis. The finite difference method was used by Witmer et al [132], Stern [134], and Stricklin et al [136]. Reference [132] deals with a dynamic loading and treats the problem of impact-loaded hemispherical shells. The method is limited to the shells of perfectly plastic material.

Reference [136] deals with static problems and adopts Tresca yield condition together with a special linear hardening rule (three slip planes). These authors included the effect of large deflection. The method of numerical integration was utilized for the analysis of rotational shells by Marcal and Turner [133] and Marcal and Pilgrims [139]. Reference [133] uses the Runge step-by-step integration for the solution of a corrugated bellows consisting of toroidal elements. Reference [139] employs a step-by-step predictor-corrector method to solve the problem of a bellows under axial load and a torispherical pressure vessel head. It is reported that the computer program developed in [139] is capable of solving shells made up of segments of a flat plate, a cone, a cylinder, a sphere, and a torus. For other shell geometry either the shell should be replaced with the above segments or the program is to be modified. Moreover, the program is limited to the case of shells under distributed loading.

2.5 Experiments

In comparison with the amount of literature on theoretical aspect of shell plasticity, only a few experimental results have been published. Experimental work reported in the literature may be classified into two groups. One is concerned about the investigation of special design problems such as reliability of welded or riveted connections, effect of openings, and fatigue failure. Much of these experiments have been performed in connection with pressure vessels. The other is related to the verification of theoretical results. The latter will be reviewed here. Because the general

theoretical solutions were lacking, the experiments were mostly confined to the verification of ultimate load of the shells. Some contradictory results have been reported. The effects of the change in geometry and a work hardening may have a profound influence on the load carrying capacity. It has been pointed out that "secondary" membrane effect, which comes into action after deformation takes place, is not as severe in shell problem as it is in the degenerate case of plate bending. This is based on the fact that membrane stresses, which are generally the primary stresses in shells, are included in the formulation for the undeformed geometry. However, the effect of the change in geometry can not be ignored in general.

To verify the results obtained in [71] and [73], Gerstle et al [141] tested several circular conical shells. The specimens were loaded through a rigid boss and connections similar to those described in Refs. [71] and [73] were provided. Besides the study of the limit load, the effects of the change in geometry were also studied. Demir and Drucker [142] tested eight steel and seven aluminum cylindrical shells under ring loading. The above authors report a reasonable correlation between the theoretical prediction of the limit load and the experimental results. Augusti and d'Agostino [143], on the other hand, report the results of the tests on nine short cylindrical shells with fixed ends made of mild steel subjected to internal pressure, where appreciable radial deflections have been observed at a pressure far below the calculated limit pressure given by Hodge [46]. Their report cast some doubt on the validity of limit analysis for the radius to thickness ratios in the range of their tests. The error indicated by their comparison

with the theory has been qualitatively discussed by Drucker [144].

Experiments on spherical shells were performed by Wasti [145] and Kaufman et al [146]. The specimen in Ref. [146] consisted of a hemispherical dome made of 6061 aluminum having a reinforced opening. Satisfactory agreement between the experiments and the theoretical results based on Ref. [124] is reported.

Tests on corrugated bellows consisting of toroidal element are reported by Marcal et al [147]. The results were compared with predictions of Ref. [133]. The experimental and calculated results are reported to be in reasonable agreement.

Stoddart and Owen [148] performed an experiment on a torispherical pressure vessel head. The limit load observed confirms the prediction made by Drucker and Shield [62].

Finally, the results of tests on intersecting shells, consisting of cylindrical nozzles in spherical pressures vessels, are given by Cloud [96], Dinno et al [149], and Ellyin et al [150]. They all report reasonable agreements between experimental evidence and the predictions made in references [96], [89], and [98].

3. GENERAL TECHNIQUES FOR THE APPLICATION OF THE FINITE ELEMENT METHOD TO ELASTIC-PLASTIC PROBLEMS

The direct stiffness method of the displacement models is found to be the most powerful and in fact the most widely used procedure in the finite element approach. Its general theory has been extensively discussed elsewhere, see for example the paper by Clough [36]. Only a brief summary of its concepts and procedures will be given here. The quantities will be expressed in terms of their covariant and contravariant components to allow generalization of results for any curvilinear coordinates. In what follows, the attention is confined to deformations of a body which cause small strain and small rotation.

3.1 General Concept

The theorem of minimum potential energy is well known in the theory of elasticity.* It may be stated thus

> "Of all displacements satisfying the given boundary conditions those which satisfy the equilibrium equations make the potential energy an absolute minimum."

The potential energy, which is a functional, is defined as

$$\pi(u_1,u_2,u_3) = \int_V \mathcal{e}\, dv - \int_V f^i u_i dv - \int_{s_T} {}^{*i}t\, u_i\, ds \qquad (3.1)$$

where

$\mathcal{e}$ - strain energy density

V - volume

*See e.g., I.S. Sokolnikoff, "Mathematical Theory of Elasticity," McGraw-Hill, 1956, pp. 382-386.

S_τ - part of boundary where stresses are specified

u_i - displacement components

f^i - components of body force per unit volume

$\overset{*i}{t}$ - components of stress vector specified on the boundary

In linear elasticity the strain energy density is expressed as

$$\mathcal{E} = \frac{1}{2} \tau^{ij} \epsilon_{ij} \tag{3.2}$$

Note that the displacement, u_i, must belong to a class of admissible functions, that it must satisfy the displacement boundary conditions and must have as many continuous derivatives as required in the solution of a problem.

Following the method of calculus of variations, it can be easily shown that the Euler's equation of the above variational problem yields the equilibrium equations

$$\tau^{ij}\big|_j + f^i = 0 \tag{3.3}$$

and its natural boundary conditions constitute the stress boundary conditions

$$\tau^{ij} n_j = \overset{*i}{t} \tag{3.4}$$

These results verify the theorem. That π is indeed a minimum can be demonstrated from the positive definiteness of the strain energy density.

One of the advantages of stating the problem in the variational form consists in being able to solve the problem with the aid of a direct method, without recourse to the differential equations. Among the direct methods of the calculus of variation the Raleigh-Ritz method has been widely used.

In the functional space terminology, the idea of the Ritz method is to extremize the functional on a finite dimensional subspace of admissible functions. For the approximate solution to converge to the true solution, the subspace should contain a set of functions which are relatively complete in the space. In the ordinary Ritz method this set of functions extends over the entire space of the body. For an arbitrary geometry of a body, selection of these functions so as to satisfy the geometric boundary conditions is very difficult. In the finite element technique, however, these functions are selected over a subregion of the body and vanish over the remaining part. They are sometimes referred to as the "almost disjoint support functions." The linear combination of these functions should satisfy certain requirements, here compatibility conditions, at the boundary of a subregion.

The potential energy of the body is expressed as the summation of the potential energies of the subregions.

$$\pi = \sum_{\Delta=1}^{N} \pi_{\Delta} \tag{3.5}$$

where N is the number of subregions each one of which is called an "element". The fact that the shape and the dimension of the element may be chosen arbitrarily can be used to advantage in approximating the shape of a body of any geometry. The convergence can be studied by increasing the dimension of the subspace of the admissible functions and also by increasing the number of elements.

The potential energy of an element may be expressed in matrix form as

$$\pi_\Delta = \frac{1}{2} \int_{V_\Delta} \{\epsilon\}^T \{\tau\}\, dv - \int_{V_\Delta} \{u\}^T \{f\}\, dv - \int_{S_\Delta} \{u\}^T \{t\}\, dv \qquad (3.6)$$

where,

$$\{u\}^T = \{u_1, u_2, u_3\}$$

$$\{\tau\}^T = \{\tau^{11}, \tau^{22}, \tau^{33}, \tau^{23}, \tau^{31}, \tau^{12}\}$$

$$\{\epsilon\}^T = \{\epsilon_{11}, \epsilon_{22}, \epsilon_{33}, 2\epsilon_{23}, 2\epsilon_{31}, 2\epsilon_{12}\}$$

$$\{f\}^T = \{f^1, f^2, f^3\}$$

$$\{t\} = \{t^1, t^2, t^3\}$$

and the superscript T stands for the matrix transpose and Δ designates the subregion.

The elements are connected with each other at a selected number of points, called nodes. Depending on the type of element, each one contains certain number of nodal points. The product of the number of components of displacements at each node times the number of nodal points of the element is called the number of degrees of freedom of the element. The displacement components defined at a nodal point may not always have a physical interpretation.

Following the idea of the finite element method, the displacements in a subregion (element) are expressed in terms of the generalized coordinates α_i

$$\underset{3x1}{\{u(x^i)\}} = \underset{3xn}{[\phi(x^i)]}\ \{\alpha\} \tag{3.7}$$

where n should be equal or greater than the number of degrees of freedom of the element. If n is equal to the number of degrees of freedom, it is preferrable to express $\{u\}$ in terms of interpolating functions. Making use of (3.7) the strains can be expressed in terms of α's as

$$\{\epsilon(x^i)\} = [B(x^i)]\ \{\alpha\} \tag{3.8}$$

Stresses are related to strains through the constitutive relations

$$\{\tau(x^i)\} = [E]\ \{\epsilon(x^i\} \tag{3.9}$$

where $[E]$ is the matrix of the elastic moduli. The material may be anisotropic and the body may be inhomogeneous. In the latter case the matrix $[E]$ will be a function of space coordinates x^i.

Substituting (3.7), (3.8) and (3.9) into (3.6), one obtains

$$\pi_\Delta = \{\alpha\}^T\ [k_\alpha]\ \{\alpha\} - \{\alpha\}^T\ \{Q_\alpha\} \tag{3.10}$$

where

$$[k_\alpha] = \int_{V_\Delta} [B(x^i)]^T\ [E]\ [B(x^i)]\ dv \tag{3.11}$$

$$\{Q_\alpha\} = \int_{V_\Delta} [\phi(x^i)]^T\ \{f\}\ dv + \int_{S_\Delta} [\phi(x^i)]^T\ \{t\}\ ds \tag{3.12}$$

Note that the vectors $\{f\}$ and $\{t\}$ may also be expressed in terms of the interpolating functions, namely

$$\{f(x^i)\} = [\phi_f(x^i)]\ \{F\} \tag{3.13}$$

$$\{t(x^i)\} = [\phi_t(x^i)]\ \{T\} \tag{3.14}$$

where $\{F\}$ and $\{T\}$ are the values of the body forces and the stress vectors, respectively, at selected points, say the nodal points.

Assuming n to be equal to the number of degrees of freedom of the element and making use of (3.7), we can express α's in terms of the displacements of the nodal points q_i

$$\underset{nxl}{\{q\}} = \underset{nxn}{[A]}\ \underset{nxl}{\{\alpha\}} \tag{3.15}$$

or

$$\{\alpha\} = [A]^{-1}\ \{q\} \tag{3.16}$$

Substitute (3.16) into (3.10) and define

$$[k] = [A^{-1}]^T\ [k_\alpha]\ [A^{-1}] \tag{3.17}$$

$$\{Q\} = [A^{-1}]^T\ \{Q_\alpha\} \tag{3.18}$$

to get

$$\pi_\Delta = \{q\}^T\ [k]\ \{q\} - \{q\}^T\ \{Q\} \tag{3.19}$$

Now, minimize the potential energy, π_Δ, with respect to q's

$$\frac{\partial \pi_\Delta}{\partial q_i} = 0 \qquad i = 1, 2, \ldots\ldots n \tag{3.20}$$

This yields the following force-displacement relations

$$\underset{nxn}{[k]}\ \underset{nx1}{\{q\}} = \underset{nx1}{\{Q\}} \tag{3.21}$$

The displacements q_i and forces Q_i are then transformed to a global coordinates system. The assemblage of elements may be easily achieved through the direct stiffness method, and the force-displacement relations of the entire structure can be established.

$$[K]\ \{r\} = \{R\} \tag{3.22}$$

Having imposed the displacement boundary conditions, the equations (3.22) can be solved for $\{r\}$. Then, the stress field may be determined from

$$\{\tau\} = [E]\ \{\epsilon\} = [L]\ \{q\} \tag{3.23}$$

where

$$[L] = [E]\ [B]\ [A^{-1}] \tag{3.24}$$

and the solution is complete.

3.2 The Use of Finite Elements in the Analysis of Elastic-Plastic Problems

In the mathematical theory of plasticity two types of theories have been advanced. The one which is called deformation (total) theory is based on the premise that the final state of strain is uniquely determined by the final state of stress. In the other, which is referred to as flow (incremental) theory, it is stated that the plastic strain increments are related to the final state of stress, plastic strain, and the stress increment. In general, these relations are not integrable and the integral depends on the loading path. For this reason the term "nonholonomic" theory also has

been suggested to designate this theory.

The inadequacy of the deformation theory to treat an arbitrary plastic deformation has been the topic of discussion during the early 1950's. It is now a fairly well established fact that the deformation theory is incapable of tracing the totality of the load-deformation history, especially during the reversal of loading.

From the analytical view point the deformation theory is more tractable than the flow theory and its application to solve practical problems has not yet been totally abandoned. However, using the incremental techniques of the numerical analysis there appears to be no significant simplification in using the deformation theory. Both the flow and the deformation theories can be treated in a similar manner. However, the iteration techniques are more convenient for the solution of the problems formulated according to the deformation theory.

In the remainder of this chapter, the finite element method will be adapted for the analysis of elastic-plastic problems. The discussion on the constitutive laws of plasticity will be left for Chapter 4.

3.2.1 Initial Strain Method

For small strains it is customary to express the strain tensor as the sum of elastic, thermal, plastic, and shrinkage strains as

$$\epsilon_{ij} = \epsilon^{E}_{ij} + \epsilon^{T}_{ij} + \epsilon^{P}_{ij} + \epsilon^{S}_{ij} \tag{3.25}$$

where the superscripts E, T, P, and S refer, respectively, to the elastic, thermal, plastic, and shrinkage or swelling parts of the strain. Strains due to other causes such as creep may also be included.

The elastic strain is recoverable upon the removal of the loading. If the environmental conditions remain unchanged and the body is free to deform, the removal of loading does not affect the other parts of the strain tensor. Therefore, it may be helpful to express these parts in the following manner

$$\eta_{ij} = \epsilon^{T}_{ij} + \epsilon^{P}_{ij} + \epsilon^{S}_{ij} \tag{3.26}$$

The quantity η_{ij} will be referred to as "the initial strain". Expression (3.25) may now be written as

$$\epsilon_{ij} = \epsilon^{E}_{ij} + \eta_{ij} \tag{3.27}$$

If the deformation theory of plasticity is adopted the plastic strain may be expressed as

$$\epsilon^{P}_{ij} = \epsilon^{P}_{ij} (\tau^{k\ell}) \tag{3.28}$$

Whereas, adopting the flow theory of plasticity

$$\epsilon^{P}_{ij} = \int_{\text{path}} \delta\epsilon^{P}_{ij} \tag{3.29}$$

where

$$\delta\epsilon^{P}_{ij} = \delta\epsilon^{P}_{ij} (\tau^{k\ell}, \epsilon^{P}_{k\ell}, \delta\tau^{k\ell}) \tag{3.30}$$

The expression (3.29) is only integrable if the integration path is known. The symbol "δ" is used to indicate that the plastic strain increment, $\delta\epsilon^{P}_{ij}$, is not in general a total differential. In addition, the symbol δ designates an infinitesimal increment. For numerical purposes $\delta\epsilon^{P}_{ij}$ is replaced

by a finite increment and the expression (3.29) may be rewritten as

$$\epsilon^{P}_{ij(k)} = \sum_{m=1}^{k} \Delta_m \epsilon^{P}_{ij} \tag{3.31}$$

where m denotes the number of increments.

In the theory of uncoupled thermoelasticity it is known* that the theorem of the minimum potential energy, in the form stated in Equation (3.1), is readily applicable if the strain energy density, $\mathcal{E}$, is replaced by the free energy function (Helmholtz's function), F, defined as follows

$$F = \frac{1}{2} \tau^{ij} (\epsilon_{ij} - \epsilon^{T}_{ij}) \tag{3.32}$$

Expression (3.32) may be generalized by replacing the thermal strain ϵ^{T}_{ij} by the initial strain η_{ij}; thus

$$\bar{\mathcal{E}} = \frac{1}{2} \tau^{ij} (\epsilon_{ij} - \eta_{ij}) \tag{3.33}$$

where $\bar{\mathcal{E}}$ denotes the generalization of the strain energy density.

The stress tensor can be expressed in terms of the elastic strain tensor

$$\tau^{ij} = E^{ijk\ell} \epsilon^{E}_{k\ell} = E^{ijkl} (\epsilon_{kl} - \eta_{kl}) \tag{3.34}$$

Upon substitution of (3.34) into (3.33) and expressing the results in matrix form we get

$$\bar{\mathcal{E}} = \frac{1}{2} \{\epsilon\}^{T} [E] \{\epsilon\} - \{\epsilon\}^{T} [E] \{\eta\} + \frac{1}{2} \{\eta\}^{T} [E] \{\eta\} \tag{3.35}$$

*See, for example, B.A. Boley and J.H. Weiner, "Theory of Thermal Stresses", John Wiley, 1960, pp. 262-268.

Substituting (3.35) into (3.1) and following the general scheme of the finite element method, as described in Eqns. (3.5) through (3.21), we obtain

$$[k]\ \{q\} = \{Q\} + \{P\} \tag{3.36}$$

where $\{q\}$, $[k]$, and $\{Q\}$ are the same as defined before in (3.15), (3.17), and (3.18) respectively, and

$$\{P\} = [A^{-1}]^T\ \{J\} \tag{3.37}$$

$$\{J\} = \int_{V_\Delta} [B(x^i)]^T\ [E]\ \{\eta\}\ dv \tag{3.38}$$

Equation (3.36) clearly indicates that the initial strain plays the role of an additional external load and may be treated as such. For a system with single degree of freedom, Eqn. (3.36) is schematically shown in Fig. 1. The analogy between the thermal effect and the body force has long been known. The analogy between plastic strain and body force is believed to have been first brought out by Ilyushin in 1943 [30]. It was also independently discussed by Lin [37].

In the solution of the problems by the initial strain method the η_{ij} should be known. The thermal strain ϵ^T_{ij} and the shrinkage (or lack of fit) strain ϵ^S_{ij} are generally given. But the plastic strain ϵ^P_{ij} is not known beforehand. If the deformation theory of plasticity is adopted, Equation (3.36), after its assemblage for the entire body, may be solved by iteration [30]. This is done by assuming $\{P\}$ to be initially zero and going through

an iteration cycle to determine the new value of $\{P\}$. Using the value of $\{P\}$ determined, the iteration can be repeated until the solution converges to the desired accuracy. At times this approach may not be very fruitful, because in general there is no guarantee of achieving convergence. Moreover, it cannot be applied to flow theory. Alternatively, we may use an incremental scheme by adding the load in small increments. Let

$$\{Q^{(m)}\} = \sum_{k=1}^{m} \{\Delta_k Q\} \tag{3.39}$$

$$\{P^{(m)}\} = \sum_{k=1}^{m} \{\Delta_k P\} \tag{3.40}$$

where the symbol Δ denotes a finite increment and the superscript m refers to the number of the load increments, it is possible to establish the following algorithm.

$$[k]\ \{q^{(m)}\} = \{Q^{(m)}\} + \{P^{(m-1)}\} \tag{3.41}$$

For each increment the vector $\{P^{(m-1)}\}$ is calculated from the previous step. Eqn. (3.41), after assemblage, can be solved for $\{q^{(m)}\}$. The value of $\{P^{(m)}\}$ is then calculated for the next increment. For a single degree of freedom system, this procedure is demonstrated in Fig. 2.

For the calculation of $\{P^{(m)}\}$ two schemes, which are called the constant stress and the constant strain methods, have been proposed [31]. These two methods can be easily described for a one dimensional state of stress. Having solved for $\{q^{(m)}\}$, the states of strain $\{\epsilon^{(m)}\}$ and stress $\{\tau^{(m)}\}$ can be determined. In the constant stress method, the plastic

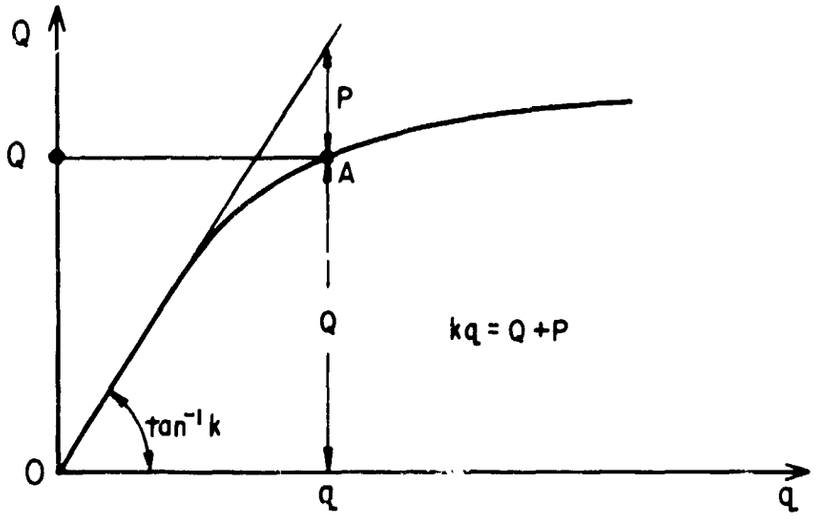

FIG. 1 INITIAL STRAIN METHOD

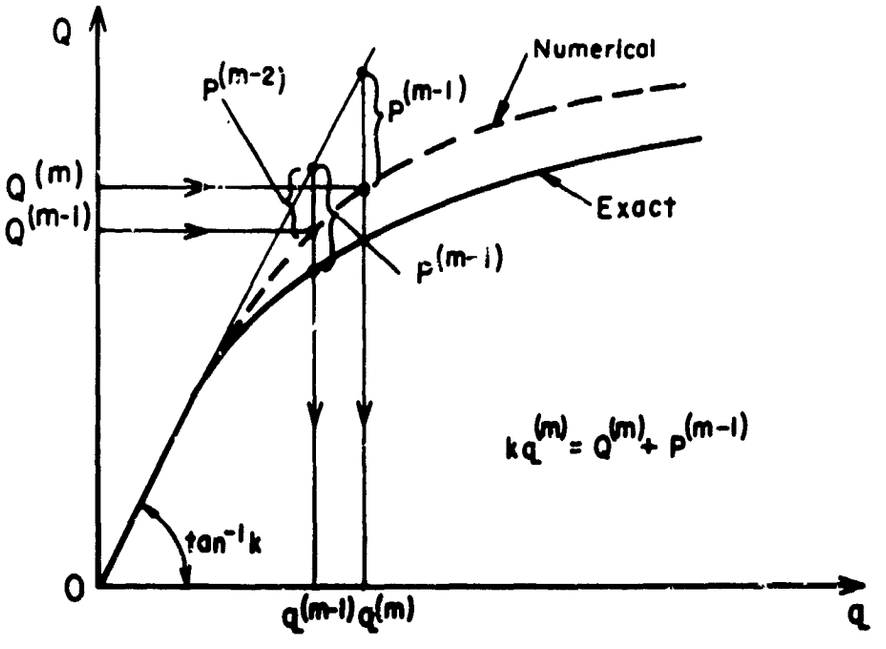

FIG. 2 STEP-BY-STEP PROCEDURE (TOTAL) IN INITIAL STRAIN METHOD

strain is determined by reading from the given stress-strain curve the value of $\epsilon^{P}_{(m)}$ corresponding to the calculated $\tau^{(m)}$ Fig. 3. In the constant strain method, the strain calculated in step m, that is $\epsilon^{(m)}$, is used to read the plastic strain $\epsilon^{P}_{(m)}$ from stress-strain curve Fig. 4. In Figs. 3 and 4 the quantities $\tilde{\epsilon}^{(m)}$ and $\tilde{\tau}^{(m)}$ denote the adjusted values of strain and stress, respectively. As may be expected, the constant stress method is reported [35] to have an inherent defect of sudden and catastrophic divergence. This makes it unsuitable for numerical work. The constant strain method is also reported to have a slower convergence [35].

An alternative approach for the solution of problems by the initial strain method has also been suggested [32]. For this purpose Equation (3.36) may be written for an increment of loading as

$$[k]\ \{\Delta q\} = \{\Delta Q\} + \{\Delta P\} \tag{3.42}$$

In evaluating (3.42), reference [32] suggests two procedures. The first, which is called "the direct incremental approach", advocates the use of the following algorithm

$$[k]\ \{\Delta_m q\} = \{\Delta_m Q\} + \{\Delta_{m-1} P\} \tag{3.43}$$

If the pattern of loading changes from one loading increment to another the above algorithm is not very meaningful. According to the theory of the "linear multistep methods"*, it can be shown that although (3.43) satisfies the requirement of consistency with the differential system, it becomes

*See, for example, J. Todd, "Survey of Numerical Analysis," McGraw-Hill, 1962, pp. 327-340.

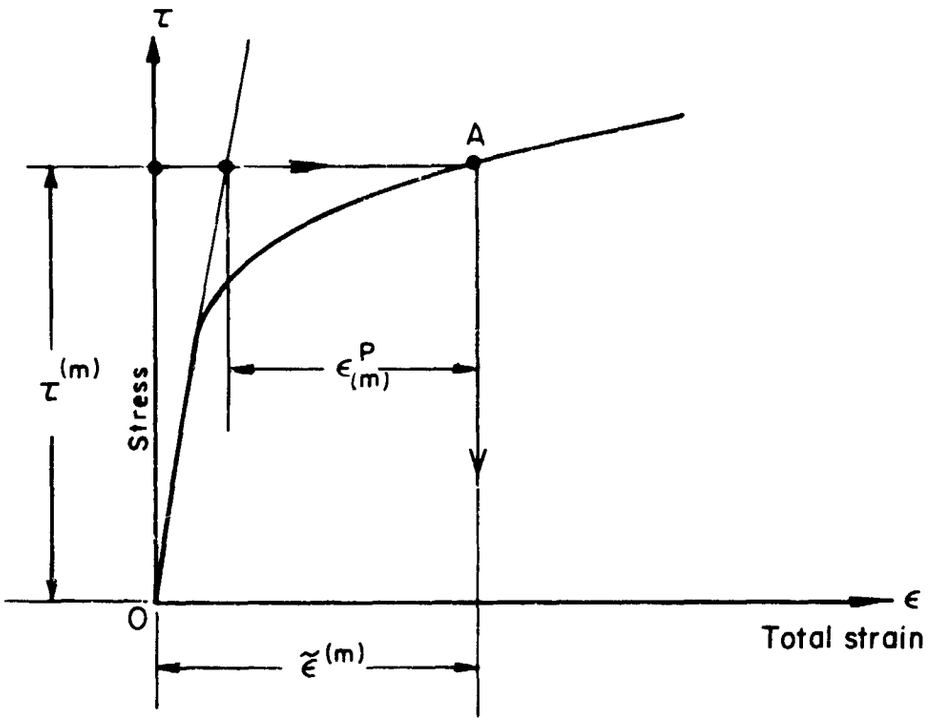

FIG 3 CONSTANT STRESS METHOD

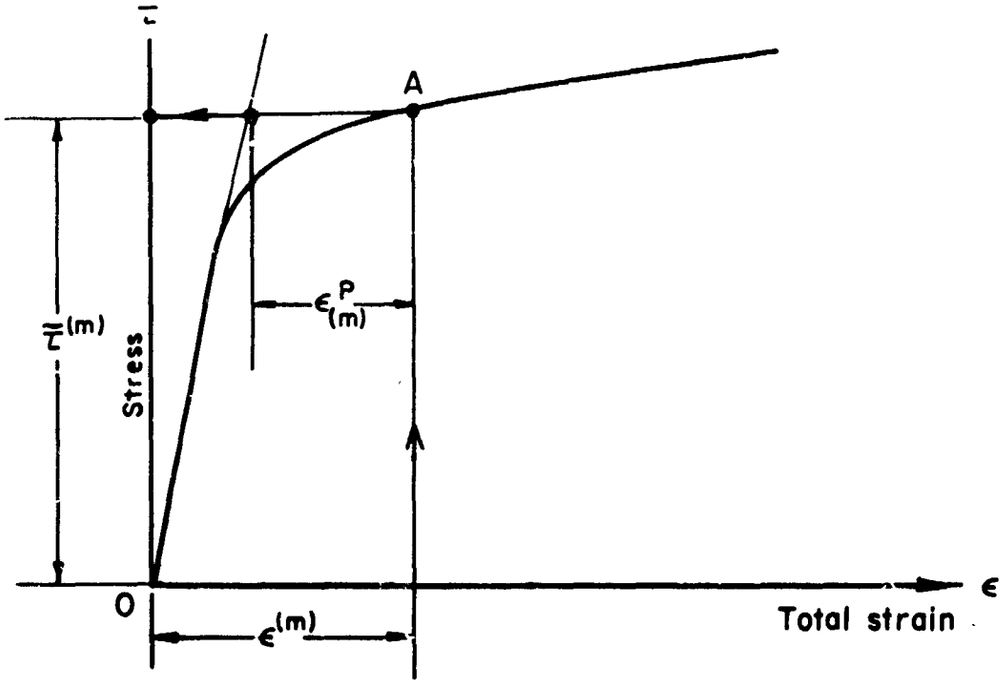

FIG. 4 CONSTANT STRAIN METHOD

asymptotically unstable if the load-displacement curve at a generic point tends to become parallel to the displacement axis. The procedure in (3.43) is shown schematically in Fig. 5. The second procedure, which is called "the iterative incremental approach" solves Eqn. (3.42) by an iterative scheme. This is found to be very time consuming. In general, if incremental approach is to be used "the tangent stiffness method", which will be described below appears to be more efficient.

3.2.2 Tangent Stiffness Method

As will be described in Chapter 4, the constitutive law of plasticity can be stated as follows

$$\delta\tau^{ij} = C^{ijk\ell}\,\delta\epsilon_{k\ell} \tag{3.44}$$

where

$$C^{ijk\ell} = C^{ijk\ell}\,(\tau^{mn},\ \epsilon^{P}_{mn},\ E^{mn\ pq};\ x^{m}) \tag{3.45}$$

For a thermostress problem $C^{ijk\ell}$, which will be referred to as the elastic-plastic moduli, may be also a function of temperature T. In the deformation theory of plasticity the expressions given by (3.44) are total differentials and can be integrated directly.

By mean value theorem, equations (3.44) can be expressed as

$$\Delta\tau^{ij}_{(t)} = \bar{C}^{ijk\ell}_{(t)}\ \ \Delta\epsilon^{(t)}_{k\ell} \tag{3.46}$$

where

$$\bar{C}^{ijk\ell}_{(t)} = \bar{C}^{ijk\ell}_{(t)}\ \ (\tau^{*mn},\ \epsilon^{*P}_{mn},\ E^{mnpq};\ x^{m}) \tag{3.47}$$

Here t denotes the increment number, τ^{*mn} and ϵ^{*P}_{mn} are some values of stress and plastic strain, respectively, within the loading increment. For a

sufficiently small loading increment the values at the beginning of the loading step may be substituted for $\overset{*}{\tau}^{mn}$ and $\overset{*}{\epsilon}^{P}_{mn}$

$$\bar{C}^{ijk\ell}_{(t)} \doteq \bar{C}^{ijk\ell}_{(t)} \left(\tau^{mn}_{(t-1)},\ \epsilon^{P}_{mn(t-1)},\ E^{mnpq};\ x^{m}\right) \tag{3.48}$$

This is called here the "first approximation method". It is possible to employ the techniques of numerical integration to improve Eqn. (3.48). The Euler's modified method was found to yield good accuracy for this class of problem [34]. This method may be stated in the following form

$$\bar{C}^{ijk\ell}_{(t)} \doteq \bar{C}^{ijk\ell}_{(t)} \left(\bar{\tau}^{mn},\ \bar{\epsilon}^{P}_{mn},\ E^{mnpq};\ x^{m}\right) \tag{3.49}$$

where

$$\begin{aligned} \bar{\tau}^{mn} &= \tau^{mn}_{(t-1)} + \frac{1}{2}\,\Delta_t\,\tau^{mn} \\ \bar{\epsilon}^{P}_{mn} &= \epsilon^{P}_{mn(t-1)} + \frac{1}{2}\,\Delta_t\,\epsilon^{P}_{mn} \end{aligned} \tag{3.50}$$

This procedure requires each step of loading to be repeated once and it is referred to as the "second approximation method."

Utilizing either (3.48) or (3.49), the elastic-plastic moduli of Eqn. (3.46) become known. Equations (3.46) is then analogous to (3.9), except that stress and strain tensors are replaced by their respective increments. In other words, Equations (3.46) defines a pseudo anisotropic, nonhomogeneous elastic material for each loading increment. Therefore, the theorem of minimum potential energy can be used for each increment of loading. The solution procedures are identical with those given in Equation (3.7)

through (3.21) except that now $[k_\alpha]$ is replaced by

$$[\bar{k}_\alpha] = \int_{V_\Delta} [B(x^i)]^T [\bar{C}(x^i)] [B(x^i)] \, dv \tag{3.51}$$

and Equations (3.21) is now restated as

$$[\bar{k}] \{\Delta q\} = \{\Delta Q\} \tag{3.52}$$

The assemblage of the elements and the remaining procedures follow the usual scheme. Equations (3.52) for the first and second approximation methods are shown schematically in Figs. 6 and 7, respectively.

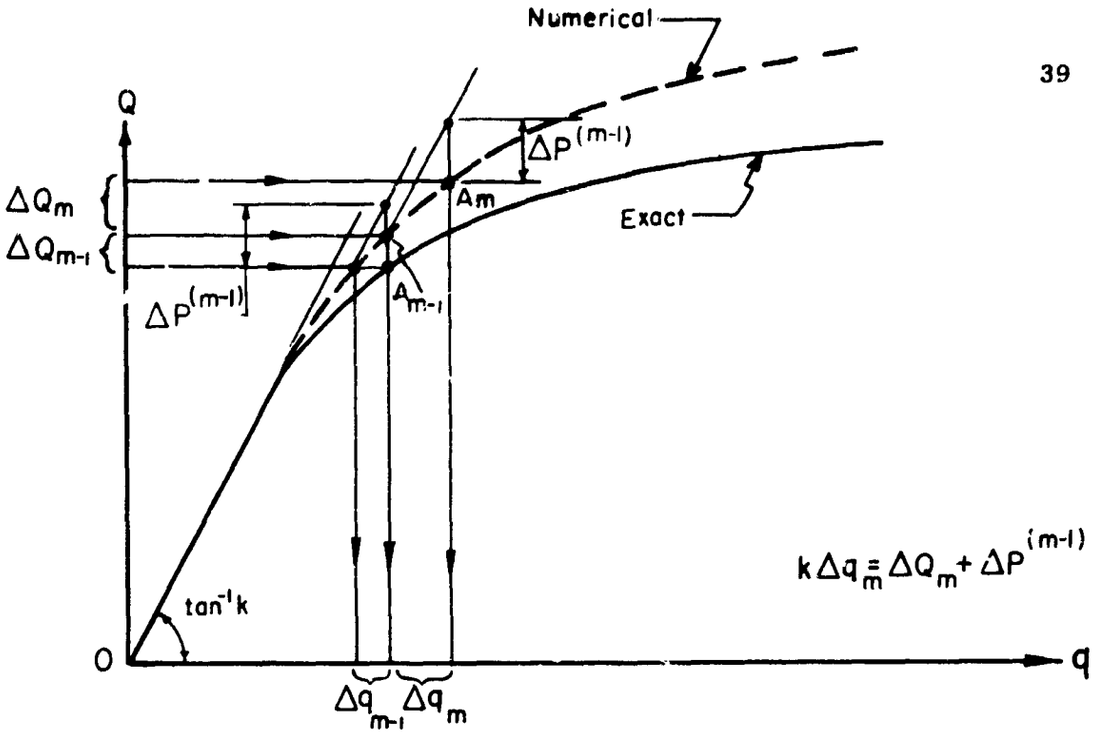

FIG. 5 STEP-BY-STEP PROCEDURE (INCREMENTAL) IN INITIAL STRAIN METHOD

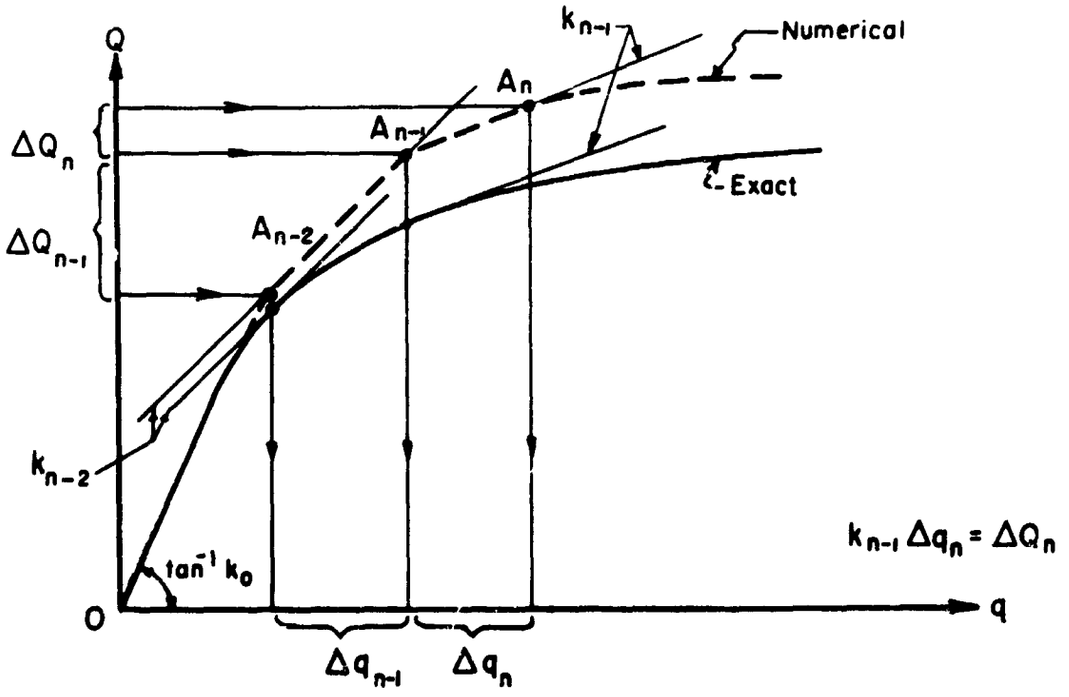

FIG. 6 TANGENT STIFFNESS METHOD (FIRST APPROXIMATION)

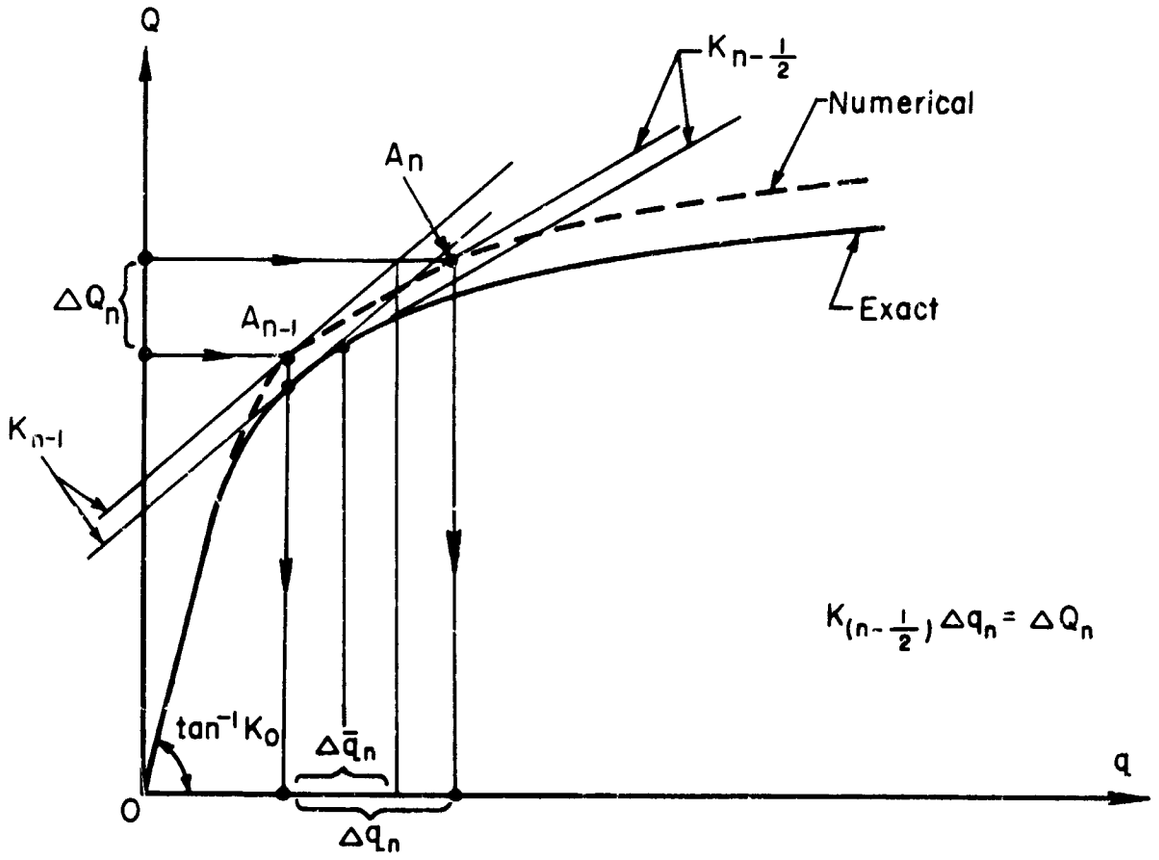

FIG. 7 TANGENT STIFFNESS METHOD
(SECOND APPROXIMATION)

3.2.3 Comparison of the Initial Strain and the Tangent Stiffness Methods

The "initial strain" method stated in incremental form

$$[k]\ \{\Delta q\} = \{\Delta Q\} + \{\Delta P\} \tag{3.42}$$

where

$$\{\Delta P\} = [A^{-1}]^T\ \{\Delta J\} \tag{3.37}'$$

$$\{\Delta J\} = \int_{V_\Delta} [B(x^i)]^T\ [E]\ \{\Delta \eta\}\ dv \tag{3.38}'$$

and other quantities as defined before, is shown here to be identical to the "tangent stiffness" method stated in (3.52). To illustrate, let us assume that the contribution to $\{\Delta\eta\}$ comes entirely from plastic deformation

$$\{\Delta\eta\} \equiv \{\Delta\epsilon^P\}$$

The plastic strain tensor can be expressed in terms of strain tensor itself

$$\{\Delta\epsilon^P\} = [A]\ \{\Delta\epsilon\} \tag{3.53}$$

Matrix [A] can be defined according to the type of material and the plasticity law used. A form of [A] is given in (4.44). Utilizing (3.8) in (3.53) and substituting the results into (3.38) one obtains

$$\{\Delta J\} = [k^P_\alpha]\ \{\alpha\} \tag{3.54}$$

where

$$[k^P_\alpha] = \int_{V_\Delta} [B(x^i)]^T\ [E]\ [A]\ [B(x^i)]\ dv \tag{3.55}$$

Now express $\{\alpha\}$ in terms of $\{\Delta q\}$ as in (3.16) and substitute (3.54) into the (3.37)' to get

$$\{\Delta P\} = [k^P]\ \{\Delta q\} \tag{3.56}$$

where

$$[k^P] = [A^{-1}]^T\ [k^P_\alpha]\ [A^{-1}] \tag{3.57}$$

Substitution of (3.56) into the (3.42) and transposition of $\{\Delta P\}$ yields

$$[\tilde{k}]\ \{\Delta q\} = \{\Delta Q\} \tag{3.58}$$

where

$$[\tilde{k}] = [k] - [k^P] \tag{3.59}$$

It can be easily shown that $[\tilde{k}]$ is identical to $[\bar{k}]$ defined in (3.52) by considering that

$$[\bar{C}] = [E] - [E]\ [A] \tag{3.60}$$

Expression (3.60) can be readily verified if we consider the relations between the increments of stresses and strains. Therefore, the identity of (3.42) and (3.52) is established.

Now consider the different algorithms discussed in connection with the initial strain and the tangent stiffness methods. Expression (3.43) after summing over m

$$\sum_{m=1}^{n} ([k]\ \{\Delta_m q\} = \{\Delta_m Q\} + \{\Delta_{m-1} P\})$$

will be identical to the algorithm expressed in (3.41). The only difference is that of computational procedures.

In order to compare the algorithm of the tangent stiffness method (3.52) with that of the initial strain method (3.43), one may proceed as follows. Using the first approximation method (3.48), expression (3.52) can be written as

$$[k_{(m-1)}]\ \{\Delta_m q\} = \{\Delta_m Q\} \tag{3.61}$$

where $[k_{(m-1)}]$ signifies that this matrix has been computed from the information obtained in previous load increment. Expression (3.61), after considering (3.60), may be recast in the equivalent form

$$[k]\ \{\Delta_m q\} - [k^P_{(m-1)}]\ \{\Delta_m q\} = \{\Delta_m Q\} \tag{3.62}$$

On the other hand, utilizing (3.56), expression (3.43) can be stated as

$$[k]\ \{\Delta_m q\} - [k^P_{(m-1)}]\ \{\Delta_{m-1} q\} = \{\Delta_m Q\} \tag{3.63}$$

Comparing the last two expressions, it is seen that the difference between the tangent stiffness method, (3.62), and the initial strain method, (3.63), is in the quantity $\{\Delta q\}$, used in the second part of the left hand side.

4. CONSTITUTIVE LAWS OF PLASTICITY

In this chapter the constitutive equations of the flow theory of plasticity are discussed and the forms suitable for finite element method are derived. Although generality of the exposition has been retained, only the most relevant aspects for the problem considered are given. For a more complete introduction and further details on the subject the reader may consult the classical work of Hill [157] and the papers by Koiter [162] and Naghdi [163].

A constitutive equation is a relation between forces and deformations for a given material. Although attempts have been made to construct the most general form of these relations through axiomatic approach, the complexity of the general form looses its utility for the solution of particular problems. Fortunately, under a given environmental conditions, only a special form of the general relations is needed to approximate closely the material behavior. Ideal materials, such as elastic, visco-elastic, elasto-plastic, thermo-visco-elastic, and so forth; are defined by particular relations between the stress tensor and the deformation of the body. In the sequel, the discussion is limited to the quasi-static, small deformations of elastic-plastic solid. The material is assumed to be inviscid and attention is confined to isothermal deformation. For simplicity the quantities are defined in Cartesian coordinates in this chapter.

A constitutive equation for elastic-plastic solid should include the state of stress and strain as well as their increments, in order to account

for history dependence. The response of elastic-plastic material can be described [161] by

(a) an initial yield condition, specifying the state of stress for which plastic flow first sets in,

(b) a flow rule, connecting the plastic strain increments with the stresses, plastic strains, and the stress increments, and

(c) a hardening rule, specifying the modification of the yield condition in the course of plastic flow.

4.1 Initial Yield Condition

The initial yield condition is generally represented as a surface in stress space convex and containing the origin. Experimental evidence with metals [153] indicates that the hydrostatic stress of an order of magnitude of the yield stress has no influence on the initial yield nor indeed does it affect plastic deformation itself. Also based on the experimental results it is customary to assume that the plastic deformation takes place without volume change

$$\epsilon^{P}_{ii} = 0 \tag{4.1}$$

For these reasons, it is convenient to decompose the stress and strain tensors into two parts

$$s_{ij} = \tau_{ij} - s\delta_{ij}, \quad s = \frac{1}{3}\tau_{ii} \tag{4.2}$$

and

$$e_{ij} = \epsilon_{ij} - e\delta_{ij}, \quad e = \frac{1}{3}\epsilon_{ii} \tag{4.3}$$

where s_{ij} and e_{ij} are, respectively, the deviatoric stress and strain and δ_{ij} is the Kronecker delta.

If the material is initially isotropic, the initial yield function may be expressed entirely in terms of invariants of the deviatoric stress

$$f^o = f^o(J_2, J_3) \tag{4.4}$$

where

$$\begin{aligned} J_1 &= s_{ii} = 0 \\ J_2 &= \frac{1}{2} s_{ij} s_{ij} \\ J_3 &= \frac{1}{3} s_{ij} s_{jk} s_{ki} \end{aligned} \tag{4.5}$$

are the invariants of the deviatoric stress. A state of stress for which $f^o < o$ will not produce plastic flow, and a state of stress corresponding to $f^o = 0$ indicates the incipience of the plastic deformation. Various forms have been suggested for the expression (4.4). Those which are customarily used and have been verified by experiments are; the von Mises yield condition [152]

$$f^o = J_2 - k^2 = o \tag{4.6}$$

the Tresca yield condition [151]

$$f^o = 4J_2^3 - 27J_3^2 - 36k^2J_2^2 + 96k^4J_2 - 64k^6 = o \tag{4.7}$$

and the Prager yield condition [155]

$$f^{o} = J_2^{3} - 9/4J_3^{2} - k^{6} = 0 \tag{4.8}$$

The constant k can be assigned based on the results of some simple experiments such as the uniaxial tension or the pure shear test. Different physical explanations have been given to interpret expression (4.6) among these the strain energy density of distorsion, the octahedral shear, and the spherical mean shear are best known. Equation (4.6) is also referred by the names of other investigators, namely; Huber, Hencky, Nadai, and Novozhilov. However, the name Mises criterion is the most widely used designation. Expression (4.6) is sometimes given in terms of the principal stresses as

$$f^{o} = (\sigma_1-\sigma_2)^2 + (\sigma_2-\sigma_3)^2 + (\sigma_3-\sigma_1)^2 - 2\sigma_y^2 = o \tag{4.9}$$

where σ_1, σ_2, σ_3 are the principal stresses and σ_y is the yield stress in uniaxial tension test. Expression (4.7) was first suggested by Tresca based on the maximum shear stress criterion in the following form

$$\sigma_{max} - \sigma_{min} = 2k \tag{4.10}$$

where σ_{max} and σ_{min} are the maximum and minimum principal stresses, respectively.

For initially anisotropic material the initial yield function cannot be expressed in terms of stress invariants alone but may be represented as

$$f^{o}(\tau_{ij}) = f^{o}(s_{ij}) = o \tag{4.11}$$

For this case, several forms have been suggested. The one proposed by Hill [156] is widely cited, and can be stated as

$$f^{o} = \frac{1}{2} A_{ijk\ell} s_{ij} s_{k\ell} - k^2 = o$$

or,

$$f^{o} = F(\tau_{22}-\tau_{33})^2 + G(\tau_{33}-\tau_{11})^2 + H(\tau_{11}-\tau_{22})^2 + 2 (L \tau_{23}^2 + M \tau_{31}^2 + N \tau_{12}^2) - 1 = o \tag{4.12}$$

where F, G, H, L, M, N are experimental constants. Expression (4.12) is a generalization of (4.9) and reduces to (4.9) for isotropic materials. Similar generalization of Tresca yield condition also have been proposed.

4.2 Flow Rule

In plasticity, in a manner analogous to the existence of Green's strain energy function in the theory of elasticity, it is postulated that the plastic strain increment tensor is derivable from a plastic potential. Stated symbolically,

$$\delta\epsilon_{ij}^{p} = \delta\lambda \frac{\partial g}{\partial \tau_{ij}} \tag{4.13}$$

where

$$g = g(\tau_{ij}, \epsilon_{ij}^{p}) \tag{4.14}$$

is the plastic potential and $\delta\lambda$ is a non-negative scalar. The plastic potential g may be assumed to be identical with the yield condition. This has been originally proposed by von Mises [154] and restated by Drucker [158]

as a consequence of the stability postulate. In the latter case the flow rule is referred to as the associated flow rule. Expression (4.13) may be interpreted geometrically as the vector of the increment of the plastic strain normal to the surface of the plastic potential (the normality rule).

The form (4.13) is applicable to regular regimes where the normal to the plastic potential is uniquely defined. For singular regimes this form is replaced by

$$\delta\epsilon^{P}_{ij} = \sum_{k=1}^{n} \delta\lambda_k \frac{\partial g_k}{\partial \tau_{ij}} \tag{4.15}$$

where n is the number of regular regimes which meet to form the singular regime. In the sequel only regular regimes will be considered.

4.3 Hardening Rule

From experimental results with uniaxial and biaxial states of stress, it is known that during plastic deformation the yield surface is continuously changing in size and shape . Hardening rule is concerned with the manner of constructing the consecutive yield surfaces. A general form of this yield condition, which is sometimes referred to as the loading function, can be stated as

$$f(\tau_{ij}, \epsilon^{P}_{ij}, K) = o \tag{4.16}$$

where K is the parameter of work hardening and is, in general, a function of the stress and the plastic strain tensors. Since the parameter K can be incorporated in τ_{ij} and ϵ^{P}_{ij}, Equation (4.16) without loss of generality may

be expressed as

$$f(\tau_{ij},\ \varepsilon^{P}_{ij}) = o \tag{4.17}$$

Equation (4.17) reduces to (4.11) for the initial yield condition for an annealed material.

Several hardening rules have been suggested. The isotropic hardening rule (Fig. 8a), which at the progressively higher stresses predicts a uniform expansion of the initial yield surface, is used most widely. For isotropic hardening expression (4.17) reduces to

$$f = F(\tau_{ij}) - K = o \tag{4.18}$$

To define the work-hardening parameter K, two well-known measures have been proposed [157]. One states that K is a function of the plastic work only, and is otherwise independent of the strain path, i.e.,

$$K = G(W_p) \tag{4.19}$$

where

$$W_p = \int_{o}^{\varepsilon^{P}_{k\ell}} \tau_{ij}\ \delta\varepsilon^{P}_{ij} \tag{4.20}$$

is the plastic work. The other is based on the assumption that the work-hardening parameter K is solely a function of the so-called equivalent plastic strain. According to this approach

$$K = H\ (\bar{\varepsilon}^{p}) \tag{4.21}$$

where $\bar{\epsilon}^p$ is the equivalent plastic strain, defined as follows:

$$\bar{\epsilon}^p = \int_0^{\epsilon^P_{ij}} \delta\bar{\epsilon}^p, \quad \delta\bar{\epsilon}^p = \sqrt{\frac{2}{3}} \left[\delta\epsilon^P_{ij} \; \delta\epsilon^P_{ij}\right]^{\frac{1}{2}} \tag{4.22}$$

As pointed out by Hill [157], the above two measures of K are equivalent for materials obeying the von Mises yield condition,* as it can be shown that

$$\delta W_p = \bar{\sigma} \; \delta \; \bar{\epsilon}^p \tag{4.23}$$

where the quantity $\bar{\sigma}$ is referred to as equivalent stress and is given by

$$\bar{\sigma} = \sqrt{3J_2}$$

In this case, by expressing (4.18) in two alternative forms

$$f = \bar{\sigma} - H(\bar{\epsilon}^p) = o \tag{4.25}$$

$$f = \bar{\sigma} - G(W_p) = o \tag{4.26}$$

the relation

$$\frac{dH}{d\bar{\epsilon}^p} = \bar{\sigma} \frac{dG}{dW_p} \tag{4.27}$$

holds true between H and G.

The isotropic hardening rule does not account for the Bauschinger effect. In fact, it predicts a negative Bauschinger effect. Therefore,

*The conditions for equivalence of these two measures for other yield conditions having homogeneous polynomial forms were studied by Bland [160].

isotropic hardening would not be satisfactory for the cases involving unloading followed by reloading along some new path. To account for the Bauschinger effect, Prager [159] suggested a hardening rule which assumes a translation of the initial yield surface which remains undeformed (Fig.8b). Prager employed a kinematic model to describe this hardening rule. For this reason it is termed "kinematic hardening". This hardening rule can be represented by

$$f = f^{o}(\tau_{ij} - \alpha_{ij}) = o \tag{4.28}$$

where α_{ij} is a tensor representing the total translation of the initial yield surface. Prager suggested that the yield surface be translated in the direction of the normal to the initial yield surface for any increment of strain

$$\delta\alpha_{ij} = c\ \delta\epsilon^{P}_{ij} \tag{4.29}$$

where the function c is determined by an experiment. For a case where c is treated as a constant, the process is called linear-hardening. Shortly after Prager's proposal it was recognized that the properties of preserving the shape, and of a pure translation of the yield surface along a normal, do not in general remain invariant for the stress subspaces. To resolve this shortcoming Ziegler [161] proposed to replace (4.29) by

$$\delta\alpha_{ij} = (\tau_{ij} - \alpha_{ij})\ \delta\eta \tag{4.30}$$

where $\delta\eta > o$. Here, the magnitude of the plastic strain increment remains free.

One way to dispose of this indeterminacy is to assume that the vector c $\delta\epsilon^P_{ij}$ is the projection of $\delta\tau_{ij}$ (and thus of $\delta\alpha_{ij}$) on the exterior normal of the plastic potential. This has the advantage that the results of Prager's rule (4.29) and of its modified form (4.30) will coincide in many cases. Both rules give identical results for plane strain and also for a plane stress when $\tau_{12}=0$.

Other hardening rules also have been advanced. The piecewise linear yield condition, which accomodates both translation and expansion of the yield surface (Fig. 8d), and the concept of a yield corner stating that the yield surface changes only locally (Fig. 8c) may be noted. The latter is a consequence of the slip theory of plasticity.

Numerous tests have been conducted to check these theories, the results are contradictory and no definite conclusions have been reached so far.

4.4 Strain-Stress Relations

As stated in Chapter 3, the increment of strain tensor may be decomposed into the elastic and plastic parts

$$\delta\epsilon_{ij} = \delta\epsilon^E_{ij} + \delta\epsilon^P_{ij} \tag{4.31}$$

The increment of elastic strain is related to the increment of stress through the generalized Hooke's law

$$\delta\epsilon^E_{ij} = H_{ijk\ell}\,\delta\tau_{k\ell} \tag{4.32}$$

For elastically isotropic material

$$H_{ijk\ell} = \frac{1+\nu}{2E} \left(\delta_{ik}\delta_{j\ell}+\delta_{i\ell}\delta_{jk}\right) - \frac{\nu}{E}\,\delta_{ij}\,\delta_{k\ell} \tag{4.33}$$

The increment of plastic strain is expressed through the flow rule (4.13). To determine $\delta\lambda$ one may proceed as follows. Since loading from a plastic state must lead to another plastic state (called the consistency condition by Prager), from (4.17) one has

$$\delta f = \frac{\partial f}{\partial \tau_{ij}}\,\delta\tau_{ij} + \frac{\partial f}{\partial \epsilon^{P}_{ij}}\,\delta\epsilon^{P}_{ij} = o \tag{4.34}$$

Solving (4.13) and (4.34) simultaneously one gets

$$\delta\lambda = -\left(\frac{\partial f}{\partial \tau_{k\ell}}\,\delta\tau_{k\ell}\right) \Big/ \left(\frac{\partial f}{\partial \epsilon_{mn}{}^{p}}\,\frac{\partial g}{\partial \tau_{mn}}\right) \tag{4.35}$$

Substituting (4.32) and (4.13) into (4.31) and taking into account (4.35) one obtains

$$\delta\epsilon_{ij} = S_{ijk\ell}\,\delta\tau_{h\ell} \tag{4.36}$$

where

$$S_{ijk\ell} = H_{ijk\ell} - \left(\frac{\partial g}{\partial \tau_{ij}}\,\frac{\partial f}{\partial \tau_{k\ell}}\right) \Big/ \left(\frac{\partial g}{\partial \tau_{mn}}\,\frac{\partial f}{\partial \epsilon^{p}_{mn}}\right) \tag{4.37}$$

4.5 Stress-Strain Relation

In some problems the inverse of (4.36) is required. Although, it may be possible to express (4.36) first and then obtain its inverse through the routine matrix inversion, however, for computational purposes it is desirable to have the inverse readily available. Moreover, for the elastic-perfectly

plastic material equation (4.36) cannot be defined at all. Fortunately, because of special form of the constitutive relations of plasticity, it is possible to find the inverse of (4.36) in a fairly simple manner. The procedure is given below.

The generalized Hooke's law (4.32) can be expressed as

$$\delta\tau_{ij} = E_{ijk\ell}\,\delta\epsilon^{E}_{k\ell} = E_{ijk\ell}\,(\delta\epsilon_{k\ell} - \delta\epsilon^{P}_{k\ell}) \tag{4.38}$$

For the elastically isotropic material

$$E_{ijk\ell} = \mu(\delta_{ik}\delta_{j\ell}+\delta_{i\ell}\delta_{jk}) + \lambda\delta_{ij}\delta_{k\ell} \tag{4.39}$$

where λ and μ are the Lame's constants

$$\mu = \frac{E}{2(1+\nu)} \quad , \quad \lambda = \frac{\nu E}{(1+\nu)\ (1-2\nu)} \tag{4.40}$$

Substitute (4.38) and (4.13) into (4.34) to get

$$\delta\lambda = h\ E_{ijk\ell}\frac{\partial f}{\partial\tau_{ij}}\ \delta\epsilon_{k\ell} \tag{4.41}$$

where

$$h^{-1} = E_{ijk\ell}\frac{\partial f}{\partial\tau_{ij}}\ \frac{\partial g}{\partial\tau_{k\ell}} - \frac{\partial f}{\partial\epsilon^{P}_{ij}}\ \frac{\partial g}{\partial\tau_{ij}} \tag{4.42}$$

Substituting (4.41) into (4.13) we obtain

$$\delta\epsilon^{P}_{ij} = A_{ijk\ell}\ \delta\epsilon_{k\ell} \tag{4.43}$$

where

$$A_{ijk\ell} = h\ \frac{\partial g}{\partial\tau_{ij}}\ \frac{\partial f}{\partial\tau_{mn}}\ E_{mnk\ell} \tag{4.44}$$

Upon substitution of (4.43) into (4.38) we get

$$\delta\tau_{ij} = C_{ijk\ell}\ \delta\epsilon_{k\ell} \tag{4.45}$$

where

$$C_{ijk\ell} = E_{ijk\ell} - E_{ijmn}\ A_{mnk\ell} \tag{4.46}$$

Expression (4.45) is the inverse of (4.36) and it can be shown that

$$C_{ijmn}\ S_{mnk\ell} = \frac{1}{2}\ (\delta_{ik}\delta_{j\ell}+\delta_{i\ell}\delta_{jk})$$

4.6 Special Cases

The general expressions (4.36) and (4.45), may be specialized for specific cases of yield conditions and flow rules. In the sequel it is assumed that the associated flow rule holds; that is

$$g \equiv f \tag{4.47}$$

The special cases of the isotropic hardening using Hill's measure of hardening (4.21), and the kinematic hardening with Prager's hardening rule (4.29) will be discussed next.

4.6.1 Isotropic Hardening

If the material is initially isotropic by taking the equivalent plastic strain-see expression (4.22) - for the measure of work-hardening, we have

$$f = F(J_2,J_3) - H(\bar{\epsilon}^P) = o \tag{4.48}$$

If, in addition, von Mises yield condition is adopted, (4.48) may be expressed as

$$f = \bar{\sigma} - H(\bar{\epsilon}^P) = 0 \tag{4.49}$$

Utilizing (4.49), the quantities needed to express the constitutive relations can be found. Thus

$$\begin{cases} \dfrac{\partial f}{\partial \tau_{ij}} = \dfrac{\partial g}{\partial \tau_{ij}} = \dfrac{3}{2\bar{\sigma}} s_{ij} \\ \dfrac{\partial f}{\partial \epsilon^P_{ij}} = -\dfrac{1}{\bar{\sigma}} \dfrac{dH}{d\bar{\epsilon}^P} \tau_{ij} \end{cases} \tag{4.50}$$

To determine the strain-stress relation, substitute (4.50) into (4.37) to obtain

$$S_{ijk\ell} = H_{ijk\ell} + \frac{1}{H'} \left(\frac{3}{2\bar{\sigma}}\right)^2 s_{ij} s_{k\ell} \tag{4.51}$$

where

$$H' = \frac{dH}{d\bar{\epsilon}^P} \tag{4.52}$$

which can be determined provided the $\bar{\sigma} - \bar{\epsilon}^P$ curve is given. If the data of uniaxial tension test are used to define H', it can be shown that

$$\frac{1}{H'} = \frac{1}{E_t} - \frac{1}{E} \tag{4.53}$$

where E_t is the tangent modulus (see Fig. 9).

The inverse of (4.51) for elastically isotropic material may be derived by substituting (4.50) into (4.42), (4.44), and (4.46). The resulting expressions are

$$\begin{cases} C_{ijk\ell} = \mu(\delta_{ik}\delta_{j\ell}+\delta_{i\ell}\delta_{jk}) + \lambda\,\delta_{ij}\delta_{k\ell} - 9\mu^2 h\,\dfrac{s_{ij}s_{k\ell}}{\bar{\sigma}^2} \\ A_{ijk\ell} = \dfrac{9}{2}\,\mu h\,\dfrac{s_{ij}s_{k\ell}}{\bar{\sigma}^2} \\ h = \dfrac{1}{3\mu+H'} \end{cases} \tag{4.54}$$

For the numerical work it is advantageous to introduce

$$\zeta = \frac{E_t}{E} \tag{4.55}$$

then

$$\begin{aligned} H' &= E\left(\frac{\zeta}{1-\zeta}\right) \\ h &= \frac{2(1+\nu)(1-\zeta)}{E[3-\zeta(1-2\nu)]} \end{aligned} \tag{4.56}$$

For the perfectly plastic material ζ=o,

$$h = \frac{1}{3\mu} \tag{4.57}$$

For the elastic state $\zeta = 1$, and expression (4.56) gives h=o, as to be expected.

4.6.2 Kinematic Hardening

Here, the Prager's hardening rule (4.29) together with the von Mises yield condition is adopted. The yield condition can be expressed as follows

$$f = \frac{1}{2} (s_{ij}-\alpha_{ij}) (s_{ij}-\alpha_{ij}) - k^2 = o \tag{4.58}$$

where k is the yield stress in a simple shear test. Making use of (4.58), we obtain

$$\begin{cases} \dfrac{\partial f}{\partial \tau_{ij}} = \dfrac{\partial g}{\partial \tau_{ij}} = s_{ij} - \alpha_{ij} \\ \\ \dfrac{\partial f}{\partial \epsilon^{P}_{ij}} = - c (s_{ij}-\alpha_{ij}) \end{cases} \tag{4.59}$$

Using (4.59), the expression (4.37) reduces to

$$S_{ijk\ell} = H_{ijk\ell} + \frac{1}{2k^2 c} (s_{ij}-\alpha_{ij}) (s_{k\ell}-\alpha_{k\ell}) \tag{4.60}$$

The inverse relations for the elastically isotropic material may be obtained using (4.46)

$$\begin{cases} C_{ijk\ell} = E_{ijk\ell} - 4\mu^2 h (s_{ij}-\alpha_{ij}) (s_{k\ell}-\alpha_{k\ell}) \\ \\ A_{ijk\ell} = 2\mu h (s_{ij}-\alpha_{ij}) (s_{k\ell}-\alpha_{k\ell}) \\ \\ E_{ijk\ell} = \mu(\delta_{ik}\delta_{j\ell}+\delta_{i\ell}\delta_{jk}) + \lambda\delta_{ij}\delta_{k\ell} \\ \\ h = \dfrac{1}{2(2\mu+c)k^2} \end{cases} \tag{4.61}$$

If the data from uniaxial tension test are used to define the quantities k and c, it can be shown that

$$k = \frac{1}{\sqrt{3}}\,\sigma_y$$
$$c = \frac{2}{3}\,H' = \frac{2}{3}\,E\,\frac{\zeta}{1-\zeta} \tag{4.62}$$

where σ_y is the initial tensile yield stress and H' is the slope of σ-ϵ^P curve.

4.7 Generalized Plane Stress

In the next chapter the stress-strain relations in the state of generalized plane stress will be needed. Here, the expressions (4.54) and (4.61) will be specialized for such a case.

In this case $\tau_{i3} = o$, $\delta\tau_{i3} = o$ and further we assume that $\delta\epsilon_{13} = \delta\epsilon_{23} = o$, hence

$$\delta\tau_{\alpha\beta} = C_{\alpha\beta\gamma\delta}\,\delta\epsilon_{\gamma\delta} + C_{\alpha\beta 33}\,\delta\epsilon_{33} \tag{4.63}$$

$$\delta\tau_{33} = C_{33\gamma\delta}\,\delta\epsilon_{\gamma\delta} + C_{3333}\,\delta\epsilon_{33} = o \tag{4.64}$$

Solve (4.64) for $\delta\epsilon_{33}$ and substitute into (4.63), to get

$$\delta\tau_{\alpha\beta} = \bar{C}_{\alpha\beta\gamma\delta}\,\delta\epsilon_{\gamma\delta} \tag{4.65}$$

where

$$\bar{C}_{\alpha\beta\gamma\delta} = \frac{C_{\alpha\beta\gamma\delta}\,C_{3333} - C_{\alpha\beta 33}\,C_{33\gamma\delta}}{C_{3333}} \tag{4.66}$$

If the stress increment $\delta\tau_{\alpha\beta}$ is represented in its principal direction, and for the case where the principal directions of stress do not change during loading, the expression (4.65) can be stated in matrix form as follows

$$\begin{Bmatrix} \delta\tau_{11} \\ \delta\tau_{22} \end{Bmatrix} = \begin{bmatrix} \bar{C}_{1111} & \bar{C}_{1122} \\ \bar{C}_{2211} & \bar{C}_{2222} \end{bmatrix} \begin{Bmatrix} \delta\varepsilon_{11} \\ \delta\varepsilon_{22} \end{Bmatrix} \tag{4.67}$$

Utilizing (4.54) and (4.61), the components of $\bar{C}_{\alpha\beta\gamma\delta}$ are found to be

$$\begin{cases} \bar{C}_{1111} = \dfrac{E}{\Omega} \left[\zeta + (1-\zeta)\, S_2^{\,2}\right] \\ \bar{C}_{1122} = \dfrac{E}{\Omega} \left[\nu\zeta - (1-\zeta)\, S_1 S_2\right] = \bar{C}_{2211} \\ \bar{C}_{2222} = \dfrac{E}{\Omega} \left[\zeta + (1-\zeta)\, S_1^{\,2}\right] \end{cases} \tag{4.68}$$

where

$$\Omega = (1-\nu^2)\, \zeta + (1-\zeta)\, (S_1^{\,2} + 2\nu\, S_1 S_2 + S_2^{\,2})$$

for isotropic hardening using expression (4.54),

$$\begin{cases} S_1 = (\tau_{11} - 0.5\, \tau_{22}) \,/\, \bar{\sigma} \\ S_2 = (\tau_{22} - 0.5\, \tau_{11}) \,/\, \bar{\sigma} \\ \bar{\sigma}^2 = \tau_{11}^{\,2} - \tau_{11}\, \tau_{22} + \tau_{22}^{\,2} \end{cases} \tag{4.69}$$

and for kinematic hardening, with the aid of expression (4.61),

$$\begin{cases} S_1 = (\tau_{11} - 0.5\, \tau_{22} - \int_{\text{path}} H'\, \delta\epsilon_{11}^{P}) \,/\, \sigma_y \\ S_2 = (\tau_{22} - 0.5\, \tau_{11} - \int_{\text{path}} H'\, \delta\epsilon_{22}^{P}) \,/\, \sigma_y \end{cases} \tag{4.70}$$

If the material is elastic-perfectly plastic, i.e., $\zeta = o$, expressions (4.68) reduce to the form

$$\begin{cases} \bar{C}_{1111} = \dfrac{E}{\Omega} S_2^{\,2} \\ \bar{C}_{1122} = -\dfrac{E}{\Omega} S_1 S_2 = \bar{C}_{2211} \\ \bar{C}_{2222} = \dfrac{E}{\Omega} S_1^{\,2} \end{cases} \tag{4.71}$$

where

$$\Omega = S_1^{\,2} + 2\nu S_1 S_2 + \mathfrak{L}_2^{\,2}$$

and

$$\begin{cases} S_1 = (\tau_{11} - 0.5\ \tau_{22}) / \sigma y \\ S_2 = (\tau_{22} - 0.5\ \tau_{11}) / \sigma y \end{cases}$$

which is identical for both (4.69) and (4.70).

It may be noted that for the elastic state, when $\zeta = 1$, expression (4.68) together with (4.69) will reduce to the well-known expressions of the elasticity

$$\begin{aligned} \bar{C}_{1111} &= \bar{C}_{2222} = \frac{E}{1-\nu^2} \\ \bar{C}_{1122} &= \bar{C}_{2211} = \frac{\nu E}{1-\nu^2} \end{aligned} \tag{4.72}$$

Expression (4.70) for kinematic hardening, however, cannot be reduced directly to the elastic case. Therefore, in the solution of elastic-plastic problems, based on the assumption of kinematic hardening, the expression (4.72) should

be used for the initial stages of loading (elastic), and during the unloading process.

For numerical work, the relations between the increments of the plastic strain and the increments of total strain, equations (4.43), are needed. For this purpose, the equation (4.43) may be specialized for the case of generalized plane stress, referred to the principal directions. The results can be stated as

$$\begin{Bmatrix} \delta\epsilon_{11}^{P} \\ \delta\epsilon_{22}^{P} \end{Bmatrix} = \begin{bmatrix} \bar{A}_{1111} & \bar{A}_{1122} \\ \bar{A}_{2211} & \bar{A}_{2222} \end{bmatrix} \begin{Bmatrix} \delta\epsilon_{11} \\ \delta\epsilon_{22} \end{Bmatrix} \tag{4.73}$$

where

$$\begin{aligned} \bar{A}_{1111} &= (1-\zeta)\, S_1\, (S_1 + \nu S_2) \,/\, \Omega \\ \bar{A}_{1122} &= (1-\zeta)\, S_1\, (S_2 + \nu S_1) \,/\, \Omega \\ \bar{A}_{2211} &= (1-\zeta)\, S_2\, (S_1 + \nu S_2) \,/\, \Omega \\ \bar{A}_{2222} &= (1-\zeta)\, S_2\, (S_2 + \nu S_1) \,/\, \Omega \\ \Omega &= (1-\nu^2)\, \zeta + (1-\zeta)\, (S_1^{\,2} + 2\nu S_1 S_2 + S_2^{\,2}) \end{aligned} \tag{4.74}$$

The quantities S_1 and S_2 are the same as those defined in (4.69) for isotropic hardening and in (4.70) for kinematic hardening.

4.8 Loading Criterion

In the incremental procedure of solution of the elastic-plastic problems, in addition to the constitutive relations, it is necessary to

have a criterion for loading and unloading. For this purpose the following criterion is available

$$\frac{\partial f}{\partial \tau_{ij}} \delta\tau_{ij} \gtrless 0 \begin{cases} \text{Loading} \\ \text{Neutral Loading} \\ \text{Unloading} \end{cases} \tag{4.75}$$

For each step of loading, expression (4.75) is first determined, and depending on the sign of (4.75) the appropriate constitutive relations are used for the next increment. For instance, for isotropic hardening the expressions (4.68) are used for loading; for unloading, the elastic relations (4.72) are utilized. For isotropic hardening, instead of (4.75), the following criterion may be used

$$\delta F \gtrless 0 \begin{cases} \text{Loading} \\ \text{Neutral Loading} \\ \text{Unloading} \end{cases}$$

where F is defined in (4.48).

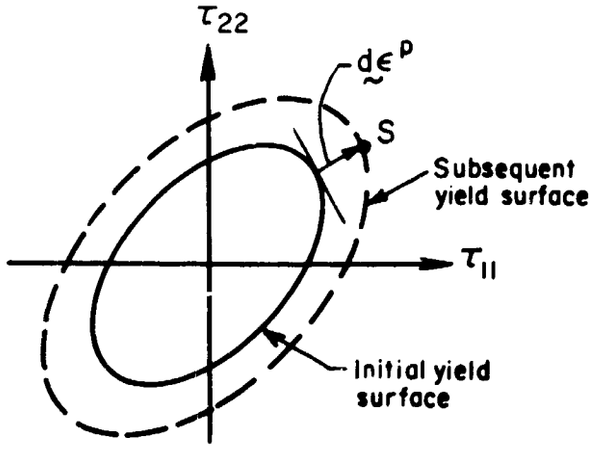

(a) ISOTROPIC HARDENING

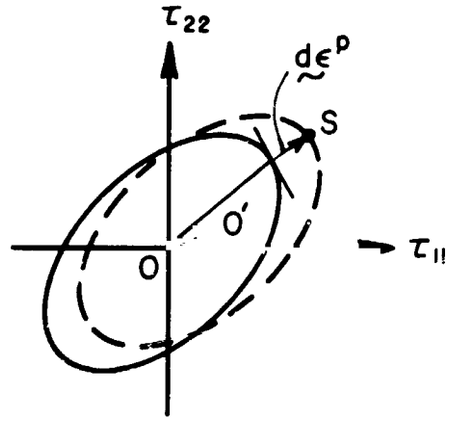

(b) KINEMATIC HARDENING

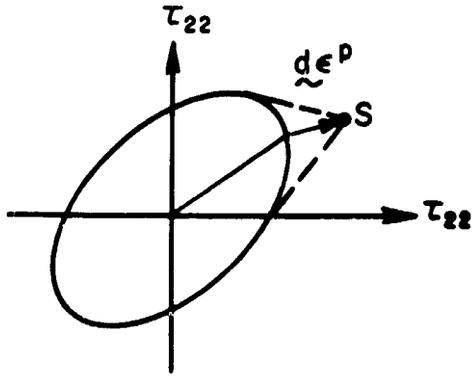

(c) YIELD CORNER

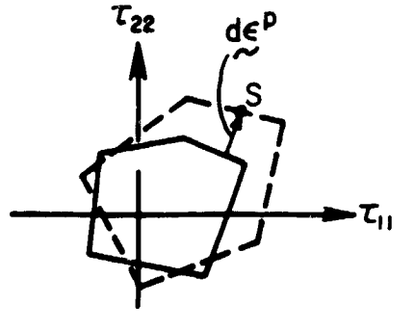

(d) PIECEWISE LINEAR YIELD CONDITION

FIG. 8

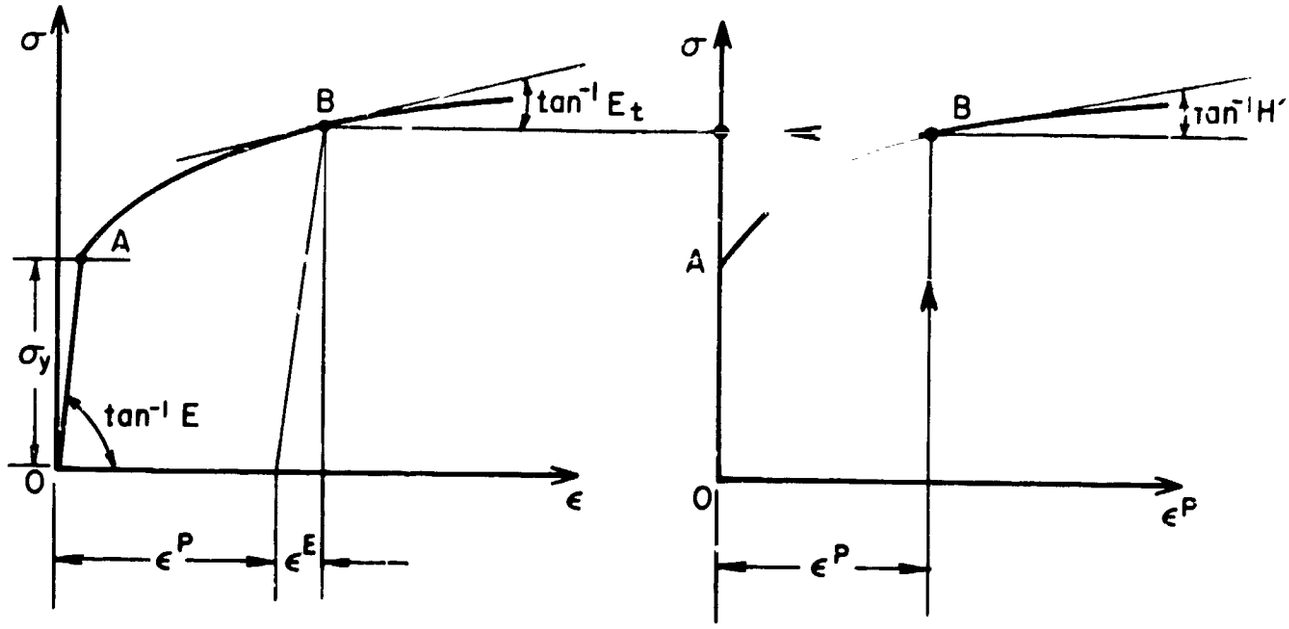

FIG. 9 STRESS - STRAIN CURVE

5. ANALYSIS OF ROTATIONAL SHELLS

Throughtout this chapter the Kirchhoff-Love hypotheses together with the small deflection theory are adopted. The tangent stiffness method, discussed in Chapter 3, is employed and the derivation of element stiffness matrix for a typical increment of loading is presented. For the sake of brevity, the symbol Δ in front of all kinematical and mechanical variables will be dropped. The formulation is confined to axisymmetric loading and support conditions.

The details of the derivation of the element stiffness matrix is given and the corresponding matrices are tabulated in Appendices A through F. Although the formulations are given for rotational shells the cases of cylindrical shells and circular plates are contained as special cases.

5.1 Equilibrium Equations

In rotational shells for axisymmetric loading, among the six equations of equilibrium of shells, three equations are identically satisfied. Adopting the sign convention for positive quantities as shown in Fig. 10, the remaining three equations of equilibrium can be stated as follows*

$$\begin{aligned}
&\frac{d}{ds}(rN_s) - N_\theta \cos\phi - \frac{r}{r_1} Q_s + rp_s = o \\
&\frac{d}{ds}(rQ_s) + N_\theta \sin\phi + \frac{r}{r_1} N_s - rp_r = o \qquad (5.1) \\
&\frac{d}{ds}(rM_s) - M_\theta \cos\phi + rQ_s = o
\end{aligned}$$

*See, for example, Timoshenko and Woinowsky-Krieger, "Theory of Plates and Shells," 2nd ed., McGraw-Hill, 1959, pp. 534.

The quantities N_s, N_θ, M_s, M_θ, Q_s, p_s, and p_r are shown in Fig. 5 and are defined in the nomenclature.

Eliminate Q_s among (5.1) to obtain

$$\begin{aligned} &\frac{d}{ds}(rN_s) + \frac{1}{r_1}\frac{d}{ds}(rM_s) - \left(\frac{M_\theta}{r_1} + N_\theta\right)\cos\phi + r\,p_s = o \\ &\frac{d^2}{ds^2}(rM_s) - \frac{dM_\theta}{ds}\cos\phi + \left(\frac{M_\theta}{r_1} - N_\theta\right)\sin\phi - \frac{rN_s}{r_1} + rp_r = o \end{aligned} \tag{5.2}$$

5.2 Strain-Displacement Relations

Adopting Kirchhoff's hypotheses and Love's first approximation, the strain-displacement relations for axisymmetric small deformation of shells of revolution can be stated as*

$$\begin{Bmatrix} \epsilon_s \\ \epsilon_\theta \end{Bmatrix} = \begin{Bmatrix} \epsilon_s^o \\ \epsilon_\theta^o \end{Bmatrix} + \zeta \begin{Bmatrix} \kappa_s \\ \kappa_\theta \end{Bmatrix} \tag{5.3}$$

where

$$\begin{aligned} \epsilon_s^o &= \frac{du}{ds} + \frac{w}{r_1} \\ \epsilon_\theta^o &= \frac{1}{r}(u\cos\phi + w\sin\phi) \end{aligned} \tag{5.4}$$

are the strains of the middle (reference) surface,

$$\begin{aligned} \kappa_s &= -\frac{d\chi}{ds} \\ \kappa_\theta &= -\frac{\cos\phi}{r}\chi \end{aligned} \tag{5.5}$$

*Ibid. pp. 534-535.

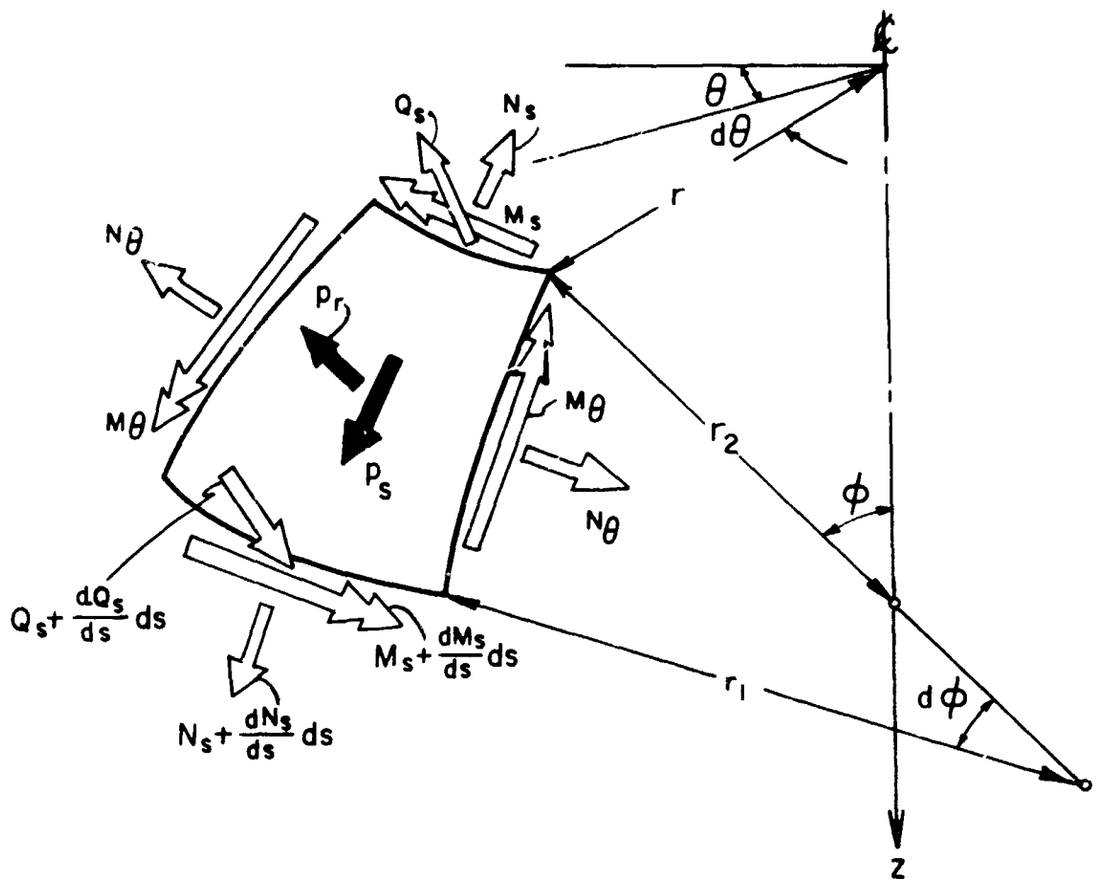

FIG. 10 SHELL FORCES AND MOMENTS
AXISYMMETRIC LOADING

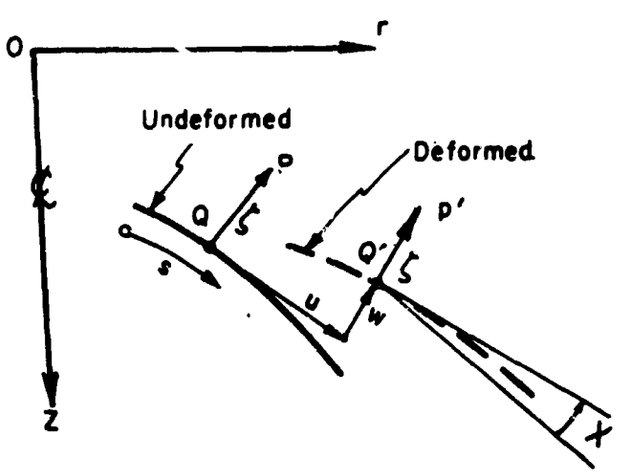

FIG. 11 DISPLACEMENTS OF THE
MIDDLE SURFACE

are the curvature changes, and

$$\chi = \frac{dw}{ds} - \frac{u}{r_1} \tag{5.6}$$

is the meridional rotation. The subscripts s and θ, respectively, refer to the meridional and circumferential variables. The quantities u, w, χ and ζ with positive sign are shown in Fig. 11.

For future use equations (5.4), (5.5), and (5.6) will be represented in terms of a new set of variables. Expressing the displacements of the middle (reference) surface of a shell in local cartesian coordinates ξ-η, the following relations between (u,w) and (u_1,u_2) hold, Fig. 12

$$\begin{Bmatrix} u \\ w \end{Bmatrix} = \begin{bmatrix} \cos\beta & \sin\beta \\ -\sin\beta & \cos\beta \end{bmatrix} \begin{Bmatrix} u_1 \\ u_2 \end{Bmatrix} \tag{5.7}$$

In the following treatment, by applying the chain rule of differentiation, differentiation with respect to arc length s is replaced by differentiation with respect to normalized cord variable ξ using

$$ds = \frac{\ell d\xi}{\cos\beta} \tag{5.8}$$

where ℓ is the cord length AB, Fig. 12. Making use of (5.7), (5.8) and the relation

$$\frac{d\beta}{d\xi} = \frac{d^2\eta}{d\xi^2} \cos^2\beta \tag{5.9}$$

one can recast expressions (5.4), (5.5), and (5.6) as follows:

$$\varepsilon_s^o = \frac{1}{\ell}\left(\frac{du_1}{d\xi} + \frac{du_2}{d\xi}\tan\beta\right)\cos^2\beta$$

$$\varepsilon_\theta^o = \frac{1}{r}\left(u_1 \sin\psi + u_2 \cos\psi\right) \tag{5.10}$$

$$\kappa_s = \frac{1}{\ell^2}\left[\frac{du_1}{d\xi}\eta''(1-\tan^2\beta)\cos^2\beta + \frac{d^2u_1}{d\xi^2}\tan\beta + 2\frac{du_2}{d\xi}\eta''\tan\beta\cos^2\beta - \frac{d^2u_2}{d\xi^2}\right]\cos^3\beta \tag{5.11}$$

$$\kappa_\theta = \frac{1}{\ell r}\left(\frac{du_1}{d\xi}\tan\beta - \frac{du_2}{d\xi}\right)(\sin\psi + \cos\psi\tan\beta)\cos^3\beta$$

and

$$\chi = \frac{1}{\ell}\left(-\frac{du_1}{d\xi}\tan\beta + \frac{du_2}{d\xi}\right)\cos^2\beta \tag{5.12}$$

where

$$\eta'' = \frac{d^2\eta}{d\xi^2}$$

The relation $\eta = \eta(\xi)$ will be discussed in section 5.6 of this chapter.

5.3 Stress-Strain Relations

For shells of uniform thickness, any thin layer parallel to the middle surface is assumed to be in the state of generalized plane stress. If the shell is of variable thickness, this assumption is still taken to be valid for a thin layer whose thickness varies in proportion to the shell thickness itself. Therefore, the relations between the increment of stresses and strains for axisymmetrical deformation, as stated in (4.67),

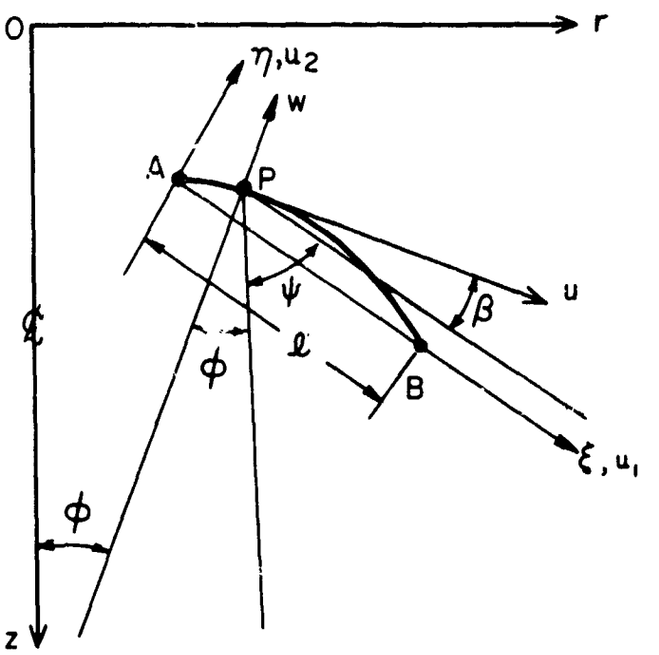

FIG.12 DISPLACEMENTS OF THE MIDDLE SURFACE (ALTERNATIVE)

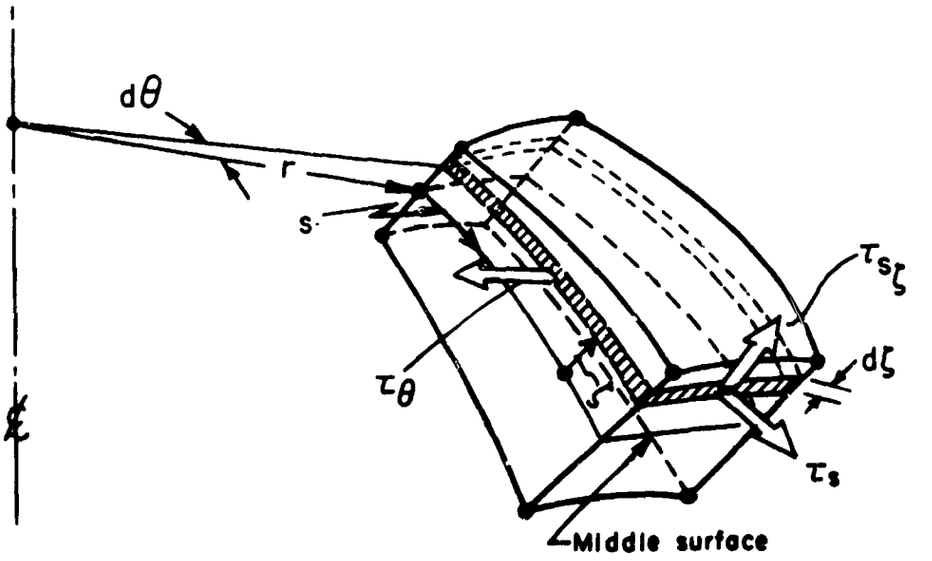

FIG. 13 A PIECE OF ROTATIONAL SHELL

can be written as

$$\begin{Bmatrix} \tau_s \\ \tau_\theta \end{Bmatrix} = \begin{bmatrix} C_{ss} & C_{s\theta} \\ C_{\theta s} & C_{\theta\theta} \end{bmatrix} \begin{Bmatrix} \epsilon_s \\ \epsilon_\theta \end{Bmatrix} \tag{5.13}$$

or symbolically

$$\underset{2x1}{\{\tau\}} = \underset{2x2}{[C]}\ \underset{2x1}{\{\epsilon\}} \tag{5.13}^2$$

The matrix [C] is in general a function of the state of stress and history of loading for a generic point and hence it is a function of the coordinates of the point in question. The dependency of [C] matrix on the state of stress and history of loading can be accounted for by the procedures stated in (3.48), or (3.49). Since the deformation is axisymmetric, the matrix [C] for a material point in the plastic state is independent of the coordinate θ, that is

$$\underset{2x2}{[C]} = \underset{2x2}{[C(s,\zeta)]} = \underset{2x2}{[C(\xi,\zeta)]} \tag{5.14}$$

It may be noted that although the transversal shear stress $\tau_{s\zeta}$ does not vanish, it does not enter into the stress-strain relations as the result of the Kirchhoff hypothesis.

5.4 Potential Energy

The potential energy of a rotational shell undergoing an axisymmetric deformation under an increment of surface loading and in the absence of body and inertial forces can be expressed as

$$\pi(u,w) = \int_V \mathcal{E}\, dv - \int_{A_\tau} (\bar{p}_s\, u+\bar{p}_r\, w+\bar{m}\chi)\, dA - \int_C (\bar{N}_s\, u+\bar{Q}_s\, w+\bar{M}_s\chi)dC \qquad (5.15)$$

where

$$\mathcal{E} = \frac{1}{2}(\tau_s\epsilon_s + \tau_\theta\epsilon_\theta) \qquad \text{strain energy density} \qquad (5.16)$$

$$dv = (1 + \frac{\zeta}{r_1})(1 + \frac{\zeta}{r_2})\, d\zeta\, dA \doteq d\zeta\, dA \qquad \text{volume element} \qquad (5.17)$$

$$dA = 2\pi r\, ds = 2\pi r \frac{\ell d\xi}{\cos\beta} \qquad \text{an area element of the middle (reference) surface} \qquad (5.18)$$

A_τ - part of middle (reference) surface where loading is specified

$\bar{m}$ - meridional moment per unit area of middle (reference) surface

C - edge(s) of shell-parallel circle(s) -

and the bar over p_s, p_r, m, N_s, Q_s and M_s indicates that these quantities are specified. The approximation expressed by (5.17) is consistent with the Love's first approximation.

Substitute (5.3) into the (5.16) and then integrate over the thickness of the shell to get

$$\int_{-\frac{h}{2}}^{\frac{h}{2}} \mathcal{E}\, d\zeta = \frac{1}{2}(N_s\epsilon_s^o + N_\theta\epsilon_\theta^o + M_s\kappa_s + M_\theta\kappa_\theta) = \frac{1}{2}\underset{1x4}{\{\varepsilon\}^T}\underset{4x1}{\{\eta\}} \qquad (5.19)$$

where

$$\begin{Bmatrix} N_s \\ N_\theta \end{Bmatrix} = \int_{-\frac{h}{2}}^{\frac{h}{2}} \begin{Bmatrix} \tau_s \\ \tau_\theta \end{Bmatrix} d\zeta \qquad (5.20)$$

are the in-plane forces per unit length,

$$\begin{Bmatrix} M_s \\ M_\theta \end{Bmatrix} = \int_{-\frac{h}{2}}^{\frac{h}{2}} \begin{Bmatrix} \tau_s \\ \tau_\theta \end{Bmatrix} \zeta \, d\zeta \tag{5.21}$$

are the bending moments per unit length, and

$$\underset{1x4}{\{\varepsilon\}^T} = \langle \varepsilon_s^o \; \varepsilon_\theta^o \; \kappa_s \; \kappa_\theta \rangle \tag{5.22}$$

$$\underset{1x4}{\{\eta\}^T} = \langle N_s \; N_\theta \; M_s \; M_\theta \rangle \tag{5.23}$$

superscript T denotes the matrix transpose. Again, it may be noted that expressions (5.20) and (5.21) are valid within the limitations of the Love's first approximation.

Substitute (5.13) into (5.20) and (5.21), then making use of (5.3) to get

$$\begin{Bmatrix} N_s \\ N_\theta \\ \hline M_s \\ M_\theta \end{Bmatrix} = \left[\begin{array}{c|c} D_{11} & D_{12} \\ 2x2 & 2x2 \\ \hline D_{21} & D_{22} \\ 2x2 & 2x2 \end{array}\right] \begin{Bmatrix} \varepsilon_s^o \\ \varepsilon_\theta^o \\ \hline \kappa_s \\ \kappa_\theta \end{Bmatrix} \tag{5.24}^1$$

4x1 4x4 4x1

or symbolically

$$\underset{4x1}{\{\eta\}} = \underset{4x4}{[D]} \; \underset{4x1}{\{\varepsilon\}} \tag{5.24}^2$$

where

$$\underset{2x2}{[D_{11}]} = \int_{-\frac{h}{2}}^{\frac{h}{2}} \underset{2x2}{[C(\xi,\zeta)]}\, d\zeta$$

$$\underset{2x2}{[D_{12}]} = \int_{-\frac{h}{2}}^{\frac{h}{2}} \underset{2x2}{[C(\xi,\zeta)]}\, \zeta\, d\zeta = \underset{2x2}{[D_{21}]} \qquad (5.25)$$

$$\underset{2x2}{[D_{22}]} = \int_{-\frac{h}{2}}^{\frac{h}{2}} \underset{2x2}{[C(\xi,\zeta)]}\, \zeta^2\, d\zeta$$

[D] will be referred to as the rigidity matrix.

Upon substitution of (5.24) into (5.19), expression (5.15) may be stated as follows

$$\pi(u,w) = \frac{1}{2} \int_A \{\varepsilon\}^T [D] \{\varepsilon\}\, dA - \int_{A_\tau} \{v\}^T \{\bar{p}\}\, dA - \int_C \{v\}^T \{\bar{P}\}\, dC \qquad (5.26)$$

where

$$\{v\}^T = \langle\, u\ w\ \chi\, \rangle \qquad (5.27)$$

$$\{\bar{p}\}^T = \langle\, \bar{p}_s\ \bar{p}_r\ \bar{m}\, \rangle \qquad (5.28)$$

$$\{\bar{P}\}^T = \langle\, \bar{N}_s\ \bar{Q}_s\ M_s\, \rangle \qquad (5.29)$$

It can be verified that the first variation of π in (5.26)

$$\delta\, \pi_{u,w} = o$$

yields the equilibrium equations (5.2) as its Euler equations.

5.5 Evaluation of the Rigidity Matrix [D]

The rigidity matrix expressed by equations (5.25) can be evaluated by employing any method of the numerical integration for definite integrals.

At sections where the stresses due to bending moment dominate those due to membrane (in-plane) forces, the stress distributions across the thickness have a high gradient. These sections, in general, are more susceptible to the early on-set of plastic deformation. For an adequate representation of the elastic-plastic moduli [C] at such sections by means of interpolating functions, the values of these moduli must be calculated at a number of points sufficiently close to each other. This requirement is particularly needed to adequately account for the history of the deformation process. Since the values of [C] should be available at a great number of points, the integrals (5.25) can be determined with the aid of some simple methods of the numerical integration. The discussion of two of these methods will follow.

5.5.1 Application of the Rectangular Rule

The shell thickness is divided into a number of layers. The values of $[C(\xi,\zeta)]$ are evaluated at the center of each layer of the selected cross sections. It is assumed that the material properties do not vary along the thickness of the layer. The problem may then be thought of as one consisting of a shell made of anisotropic elastic thin layers. The integration

of (5.25) can be carried out as follows

$$
\begin{aligned}
&[D_{11}(\xi)]_{2x2} = [D_1(\xi)]_{2x2} \\
&[D_{12}(\xi)]_{2x2} = [D_{21}(\xi)]_{2x2} = [D^*(\xi)]_{2x2} - \frac{1}{2} h(\xi) [D_1(\xi)]_{2x2} \\
&[D_{22}(\xi)]_{2x2} = [D_2(\xi)]_{2x2} - h(\xi) [D^*(\xi)]_{2x2} + \frac{1}{2} h^2(\xi) [D_1(\xi)]_{2x2}
\end{aligned}
\tag{5.30}
$$

where

$$
\begin{aligned}
[D_1(\xi)] &= \sum_{k=1}^{n} [C(\xi,\bar{h}_k)] (h_k - h_{k-1}) \\
[D^*(\xi)] &= \frac{1}{2} \sum_{k=1}^{n} [C(\xi,\bar{h}_k)] (h_k^2 - h_{k-1}^2) \\
[D_2(\xi)] &= \frac{1}{3} \sum_{k=1}^{n} [C(\xi,\bar{h}_k)] (h_k^3 - h_{k-1}^3)
\end{aligned}
\tag{5.31}
$$

$$
\bar{h}_k = \frac{1}{2} (h_k + h_{k-1} - h)
$$

The quantities h_k are as shown in Fig. 14.

If the layers are taken to be of equal thickness, i.e., $h_k = (k\,h)/n$, the expressions (5.31) can be represented in the following form

$$
\begin{aligned}
[D_1(\xi)]_{2x2} &= \frac{h(\xi)}{n} \sum_{k=1}^{n} [C(\xi,\bar{h}_k)]_{2x2} \\
[D^*(\xi)]_{2x2} &= \frac{h^2(\xi)}{n^2} \sum_{k=1}^{n} [C(\xi,\bar{h}_k)]_{2x2} (k - \tfrac{1}{2}) \\
[D_2(\xi)]_{2x2} &= \frac{h^3(\xi)}{n^3} \sum_{k=1}^{n} [C(\xi,\bar{h}_k)]_{2x2} (k^2 - k + \tfrac{1}{3})
\end{aligned}
\tag{5.32}
$$

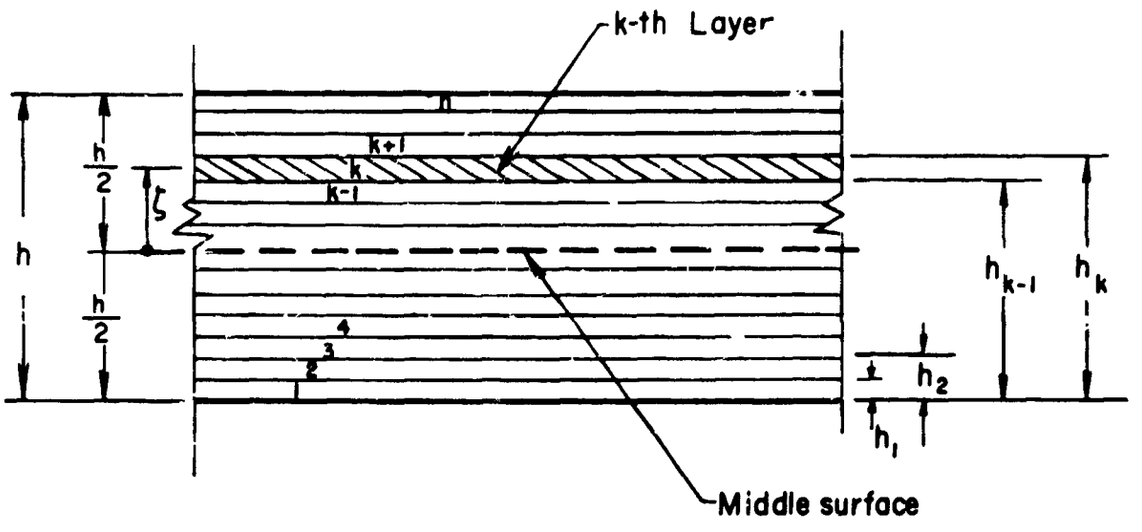

FIG. 14 SHELL THICKNESS

where

$$\bar{h}_k = \left(\frac{2k-1}{2n} - \frac{1}{2}\right) h(\xi)$$

Note that it is preferable to take n to be an even integer.

5.5.2 Application of the Trapezoidal Rule

As in the previous case, the thickness of shell is divided into n number of layers of equal thickness. The values of $[C(\xi, \zeta)]$ are determined at the interfaces of layers as well as at the upper and lower faces of the shell proper. Then, the expression (5.25) can be integrated and the results are as follows

$$[D_{11}(\xi)]_{2x2} = \frac{h(\xi)}{n}\left(\frac{1}{2}[C(\xi,\zeta_1)]_{2x2} + \sum_{k=2}^{n}[C(\xi,\zeta_k)]_{2x2} + \frac{1}{2}[C(\xi,\zeta_{n+1})]_{2x2}\right)$$

$$[D_{12}(\xi)]_{2x2} = \frac{h^2(\xi)}{n}\left(\frac{1}{2}[C(\xi,\zeta_1)]_{2x2}\frac{\zeta_1}{h} + \sum_{k=2}^{n}[C(\xi,\zeta_k)]_{2x2}\frac{\zeta_k}{h} + \frac{1}{2}[C(\xi,\zeta_{n+1})]_{2x2}\frac{\zeta_{n+1}}{h}\right)$$

$$[D_{22}(\xi)]_{2x2} = \frac{h^3(\xi)}{n}\left(\frac{1}{2}[C(\xi,\zeta_1)]_{2x2}\left(\frac{\zeta_1}{h}\right)^2 + \sum_{k=2}^{n}[C(\xi,\zeta_k)]_{2x2}\left(\frac{\zeta_k}{h}\right)^2 + \frac{1}{2}[C(\xi,\zeta_{n+1})]_{2x2}\left(\frac{\zeta_{n+1}}{h}\right)^2\right) \quad (5.33)$$

where

$$\zeta_k = \left(\frac{k-1}{n} - \frac{1}{2}\right) h(\xi)$$

It may be noted that for the integration of the rigidity matrix, it is not necessary to think of a shell consisting of layers. Other interpolation functions may be selected to approximate the variation of the material properties along the thickness.

5.6 Representation of the Element Geometry

Here the objective is to define the geometry of the middle (reference) surface of a typical shell element. Since the shell proper is axially symmetric, it is sufficient to define the shape of its meridional curve.

It is possible to develop the stiffness matrix for any special type of a shell without idealizing its geometry. But if versatility is required, it is necessary to select an element which can closely idealize any meridional shape of a shell of revolution. For this purpose two alternative approaches may be conceived.

One consists of expressing the geometric variables, which enter into the strain-displacement relations and are functions of surface coordinates, in polynomial forms. These geometric variables are the coefficients of the first and the second fundamental forms of the reference (middle) surface. The unknown coefficients of these polynomials are determined by specifying the values of the geometric variable for any given shell at selected points. This approach has two shortcomings:

(a) The geometric variables are not independent and in general they have to satisfy the Gauss-Coddazi relations. These relations can not be identically satisfied.

(b) For some regions of a shell the procedure of determination of the unknown coefficients becomes ill-conditioned.

This approach was used in Ref. [26] by expressing cos φ as

$$\cos \varphi = C_1 + C_2 \, s + C_3 \, s^2$$

where s is the arc length. As the result, in regions of a shell where φ is close to zero, the determination of C_1, C_2 and C_3 becomes ill-conditioned and the stiffness matrix obtained on the basis of these coefficients is inaccurate. In addition sin φ can not be expressed exactly by a polynomial of s in terms of constants C_1, C_2, and C_3. Although this approach is quite general and can be used for any type of shells, this special case may clarify the two shortcomings mentioned above.

The alternative approach consists of replacing the given meridional curve by a substitute curve which matches with the original curve at selected points. This substitute curve may be represented either in a local or global coordinates. The latter scheme turned out to be ill-conditioned for the limiting cases.

In this dissertation the scheme of selecting a substitute curve in local coordinates is adopted. Figure 15 shows a manner of representing this curve. Two types of orientation for the curved element are shown in this figure. With the sign convention indicated in Fig. 15, the following relation applies

$$\overleftarrow{\varphi} + \overleftarrow{\psi} + \overleftarrow{\beta} = \frac{\pi}{2} \tag{5.34}$$

By adopting the sign convention stated in Fig. 15, and utilizing the relation (5.34), other orientations of meridional curve and local coordinates ξ-η can be readily treated.

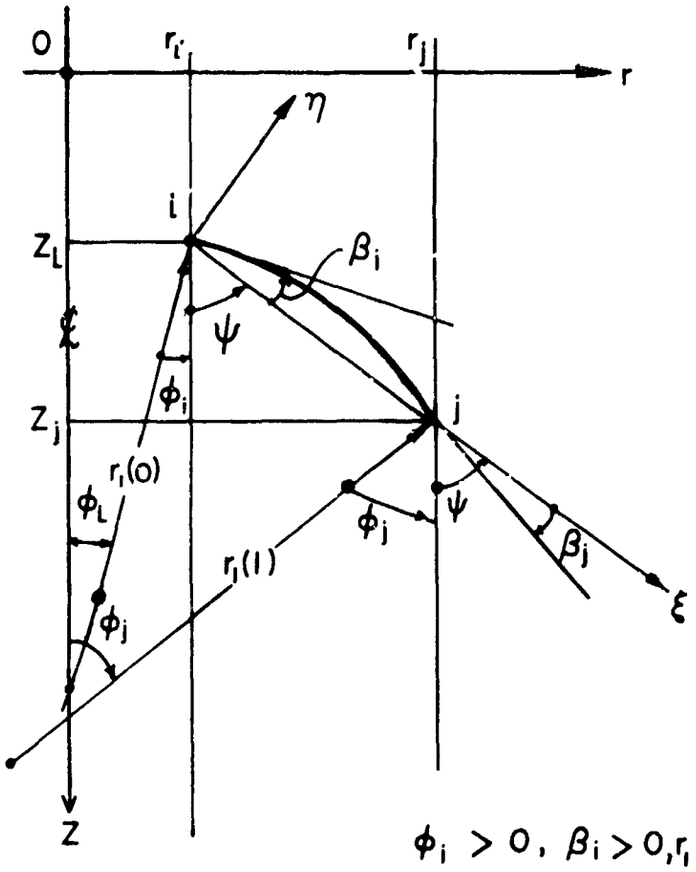

(a)

$\phi_i > 0,\ \beta_i > 0, r_1(0) > 0$

$\phi_j > 0,\ \beta_j < 0, r_1(1) > 0$ $\psi > 0$

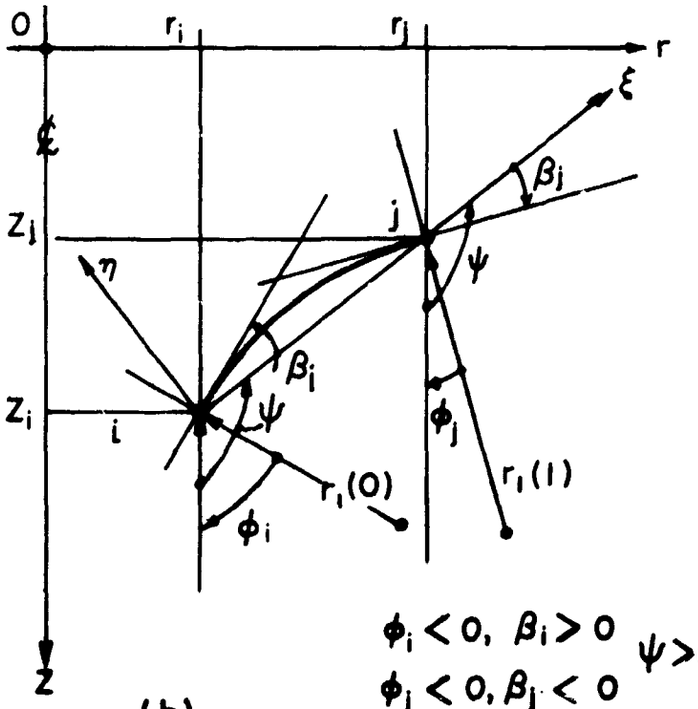

(b)

$\phi_i < 0,\ \beta_i > 0$

$\phi_j < 0, \beta_j < 0$ $\psi > 0$

$r_1(0) > 0$

$r_1(1) > 0$

FIG.15 MERIDIONAL CURVE

Two kinds of substitute curves have been utilized in this dissertation. In one, the curve passes through the given end points (nodal points) and at these points has the same slopes as those of the specified curve itself. If the normalized abscissa ξ is used - that is the abscissa is divided by the cord length -, the equation of the substitute curve may be expressed as follows

$$\eta = \xi\,(1-\xi)\,(a_1 + a_2\,\xi)$$

where

$$a_1 = \tan\,\beta_i$$

$$a_2 = -\,(\tan\,\beta_i + \tan\,\beta_j)$$

The second type of curve was chosen such that, in addition to accomodating for the specified slopes, the end (nodal point) curvatures can also take the specified values. The equation of this curve may be represented as

$$\eta = \xi\,(1-\xi)\,(a_1 + a_2\,\xi + a_3\,\xi^2 + a_4\,\xi^3) \tag{5.36}$$

where

$$a_1 = \tan\,\beta_i$$

$$a_2 = \tan\,\beta_i + \frac{1}{2}\,\eta_i''$$

$$a_3 = -\,(5\,\tan\,\beta_i + 4\,\tan\,\beta_j) + (\tfrac{1}{2}\,\eta_j'' - \eta_i'')$$

$$a_4 = 3(\tan\,\beta_i + \tan\,\beta_j) + \frac{1}{2}\,(\eta_j'' - \eta_i'')$$

$$\eta'' = \frac{d^2\eta}{d\xi^2} = -\,\frac{\ell}{r_1 \cos^3\beta}$$

ℓ is the cord length.

In the above expressions, r_1 is positive if the meridional curve is convex with respect to the positive η-axis.

The parameters in (5.35) and (5.36) can be determined from input data as follows:

$$\begin{aligned} \Delta r &= r_j - r_i \\ \Delta z &= z_j - z_i \\ \Delta s &= [\Delta r^2 + \Delta 2^2]^{\frac{1}{2}} \\ \sin \psi &= \frac{\Delta r}{\Delta s} \\ \cos \psi &= \frac{\Delta z}{\Delta s} \end{aligned} \tag{5.37}$$

$$\begin{aligned} \sin \beta_n &= \cos \varphi_n \cos \psi - \sin \varphi_n \sin \psi \\ \cos \beta_n &= \sin \varphi_n \cos \psi + \cos \varphi_n \sin \psi \end{aligned} \quad , \quad n = i, j$$

Having established the substitute curve, we can express all the geometric quantities which enter into (5.4) and (5.5) or (5.10) and (5.11) as follows

$$\begin{aligned} \tan \beta &= \eta' \\ r &= r_i + \ell\xi \, (\sin \psi + \bar{\eta} \cos \psi) \\ \frac{d}{ds} &= \frac{\cos \beta}{\ell} \, \frac{d}{d\xi} \\ \frac{1}{r_1} &= - \frac{1}{\ell} \, \frac{d^2\eta}{d\xi^2} \cos^3 \beta \end{aligned} \tag{5.38}$$

$$\cos \varphi = \sin \beta \cos \psi + \cos \beta \sin \psi = (\eta' \cos \psi + \sin \psi) \cos \beta$$

$$\sin \varphi = \cos \beta \cos \psi - \sin \beta \sin \psi = (\cos \psi - \eta' \sin \psi) \cos \beta$$

where

$$\bar{\eta} = \frac{\eta}{\xi} \quad \text{and} \quad \eta' = \frac{d\eta}{d\xi}$$

It may be noted that other substitute curves, which match with the given curve at some intermediate points, could be employed also.

5.7 Displacement Pattern

As discussed in Chapter 3, the essential feature of the displacement model of the finite element method is the expansion of displacements in terms of a relatively complete set of functions in a small sub-region. Although these base functions can be chosen arbitrarily, polynomials are the most suitable forms for numerical work.

In the analysis of shells by the finite element method using curved element the displacements may be expressed either in surface coordinates or in local Cartesian coordinates. The former is in general a curivilinear coordinates.

Expressing the displacement in the surface (curvilinear) coordinates has the advantage that the compatibility of the displacements at the interfaces of the adjoining elements can be easily achieved. But since the displacements are generally expressed in polynomial forms, the inclusion of rigid body modes creates a formidable problem.

It is possible to separate the rigid body and deformation modes in the displacement expansion. For the case of axisymmetric deformation of shells of revolution the displacements may be expressed as follows

$$\begin{aligned} u &= u_r + u_d \\ w &= w_r + w_d \end{aligned} \tag{5.39}$$

where the subscripts r and d refer to rigid body and deformation components, respectively. For the problem in question only a single rigid body mode, translation along the axis of symmetry, exists. By introducing a constraint (support) parallel to this axis at a location along the meridian, it is possible to separate these two types of modes. Imposing a constraint at the location shown in Fig. 16, the displacement components for the rigid body translation can be expressed as

$$\begin{aligned} u_r &= -\alpha_1 \sin\varphi \\ w_r &= \alpha_1 \cos\varphi \end{aligned} \tag{5.40}$$

and the one for the deformation modes as

$$\begin{aligned} u_d &= \alpha_2 \cos\varphi_i + \alpha_3 \xi \\ w_d &= \alpha_2 \sin\varphi_i + \alpha_4 \xi + \alpha_5 \xi^2 + \alpha_6 \xi^3 \end{aligned} \qquad 0 \le \xi \le 1 \tag{5.41}$$

where α's are the generalized coordinates. The number of generalized coordinates is taken to be equal to the number of degrees of freedom of the element, two displacements and one rotation at each node. It may be verified

that at node "i", Fig. 16, the component of the displacement along the axis of symmetry arising from the deformation mode vanishes

$$V_i = - u_d \sin \varphi_i + w_d \cos \varphi_i = 0$$

Although the above procedure provides a means for accomodating rigid body modes, it has a serious shortcoming. A necessary condition for a solution by the finite element method to converge uniformly is that the assumed deformation patterns should contain the constant straining modes. A close scrutiny of (5.41) reveals that it does not meet this requirement. For instance, consider the case of uniform expansion of a shell, that is when w = const. and u = o.

The second approach, that is representing the displacements in a local rectilinear coordinates, has the advantage that the requirement of the rigid body mode for each element can be automatically fulfilled. For a general type of shell, this approach has a shortcoming that it becomes difficult to satisfy the compatibility of displacements at the element interfaces. Fortunately, however, for axisymmetric deformation of rotational shells this creates no problem. Taking the ξ-η axis as the local coordinates, Fig. 12, the displacements may be expressed as

$$\begin{aligned} u_1 &= \alpha_1 + \alpha_2 \xi \\ u_2 &= \alpha_3 + \alpha_4 \xi + \alpha_5 \xi^2 + \alpha_6 \xi^3 \end{aligned} \qquad 0 \le \xi \le 1 \qquad (5.42)$$

Since the displacement patterns (5.42) are relatively complete, the uniform convergence of the solution by reducing the size of elements is assured.

Comparison of these two approaches is given in Chapter 6 in a numerical example. For the membrane type of shell the second approach was found to be superior to that of the first one.

For future reference the displacement patterns (5.39) and (5.42) will be specialized for the case of a central cap. Fig. 17. Because of symmetry, at the point located on the axis of symmetry the component of displacement perpendicular to this axis and meridional rotation vanish. Utilizing these internal boundary conditions

$$\begin{aligned} U_i &= 0 \\ \chi_i &= 0 \end{aligned} \tag{5.43}$$

where

$$U = u \cos \varphi + w \sin \varphi = u_1 \sin \psi + u_2 \cos \psi$$

$$\chi = \frac{dw}{ds} - \frac{u}{r_1} = \frac{1}{\ell} \left(- \frac{du_1}{d\xi} \tan \beta + \frac{du_2}{d\xi} \right) \cos^2 \beta$$

in connection with the expressions (5.39), one obtains

$$\alpha_2 = \alpha_4 = 0$$

Hence, for the central cap the expressions (5.41) should be replaced by

$$\begin{aligned} u_d &= \alpha_3 \xi \\ w_d &= \alpha_5 \xi^2 + \alpha_6 \xi^3 \end{aligned} \tag{5.44}$$

Similarly, the relations (5.42) given in terms of the local rectilinear coordinates specialize into the following:

$$u_1 = -\alpha_1' \cos\psi + \alpha_3\xi$$
$$u_2 = \alpha_1' \sin\psi + \alpha_3\xi \tan\beta_i + \alpha_5\xi^2 + \alpha_6\xi^3 \qquad (5.45)$$

Note that the number of generalized coordinates α's has been reduced to four which is equal to the number of degrees of freedom for the central cap.

It may be interesting to note that for a closed shell the governing differential equations expressed in finite difference forms become singular at points located on the axis of symmetry; whereas in the finite element method this singularity can be removed by imposing the internal boundary conditions and restricting the displacement field. This is important if the solution of a closed shell near the axis of symmetry is to be found and is one of the advantages of the finite element method.

Although in the above derivation the number of α's was taken to be equal to the number of degrees of freedom of the element; it is possible to take a greater number of α's and then using a general condensation procedure to establish the force displacement relations at nodal circles.

5.8 Element Stiffness Matrix

The general scheme discussed in Chapter 3, that is the procedures explained in connection with Equations (3.6) through (3.24), will be specialized for a curved element. Representation of the displacement bot

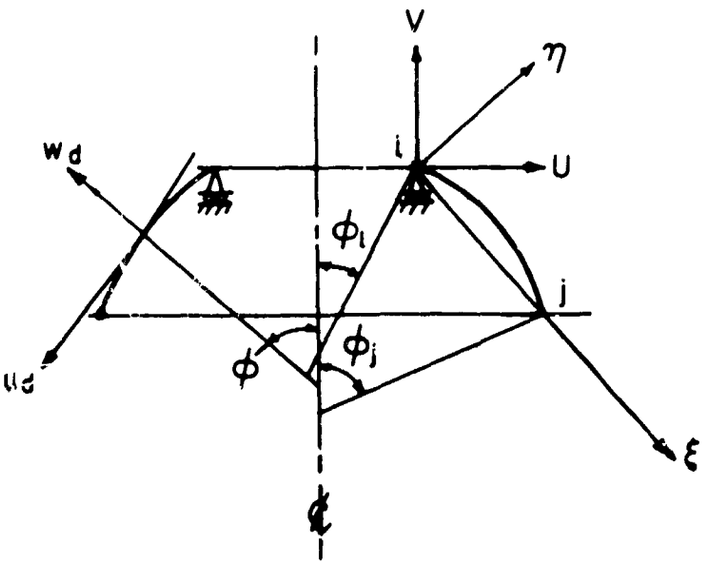

FIG. 16 DEFORMATION PARTS OF DISPLACEMENTS, u_d, w_d

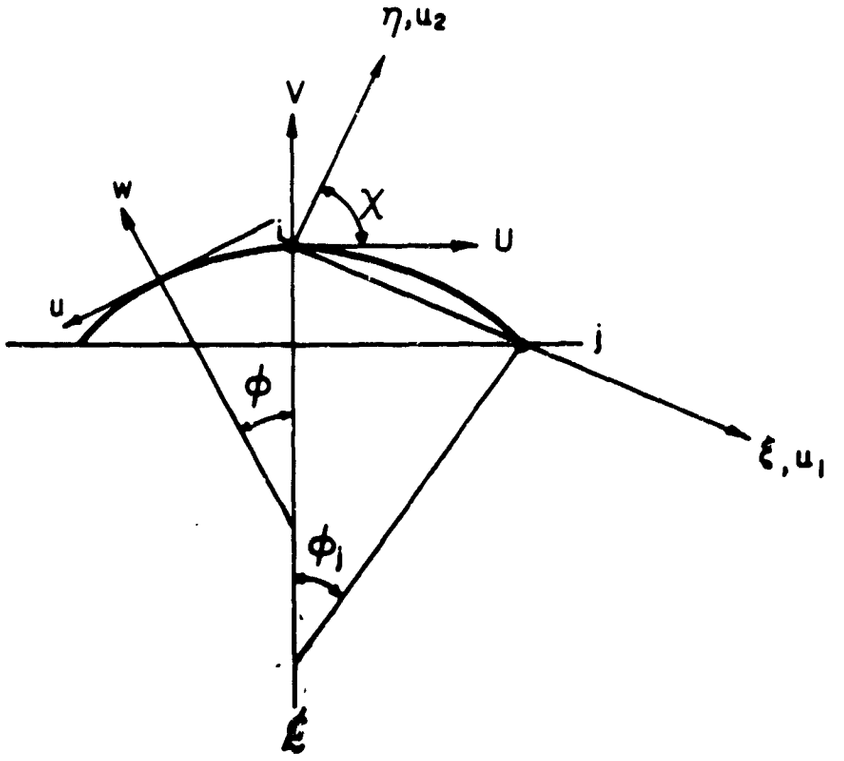

FIG. 17 CENTRAL CAP

in the surface and the local (rectilinear) coordinates will be employed. For future reference the element stiffness matrix derived through the use of displacement expressed in surface coordinats is designated by FDC (i) (Frustum whose Displacements are expressed in Curvilinear Coordinates) and the one in local Cartesian coordinates by FDR (i) (Frustum whose Displacements are expressed in Rectilinear Coordinates.) The index "i" is assigned unity for the meridional curve given in (5.35) and it is assigned 2 for the one stated in (5.36).

Utilizing Equations (5.4) and (5.5) or (5.10) and (5.11), together with (5.41) or (5.42), the strain-displacement relations may be expressed as follows

$$\underset{4x1}{\{\varepsilon\}} = \underset{4x6}{[B]}\ \underset{6x1}{\{\alpha\}} \tag{5.46}$$

where $\{\varepsilon\}$ is defined in (5.22) and the matrix [B] is given in Appendix A. For a closed cap the expression (5.44) or (5.45) are to be used and the corresponding [B] matrix is given in Appendix B.

The relations (5.39) or (5.42) together with the relative expression for meridional rotation may be represented in matrix form as

$$\underset{3x1}{\{v\}} = \underset{3x6}{[\phi(\xi)]}\ \underset{6x1}{\{\alpha\}} \tag{5.47}$$

where

$$\{v\}_C^T = \langle\ u \quad w \quad \chi\ \rangle \text{ for FDC}$$

and

$$\{v\}_R^T = \langle\ u_1 \quad u_2 \quad \chi\ \rangle \text{ for FDR}$$

The matrix $[\phi(\xi)]$ is stated in Appendix C.

The surface loads in (5.28) can be expressed in terms of interpolating functions. For a linear interpolation it may be written as

$$\underset{3x1}{\{p(\xi)\}} = (1-\xi)\ \underset{3x1}{\{p_i\}} + \xi\ \underset{3x1}{\{p_j\}} \tag{5.48}$$

For a sufficiently small element the variation of thickness and elastic-plastic moduli along the meridian may be approximated linearly

$$h(\xi) = (1-\xi)\ h_i + \xi\ h_j \tag{5.49}$$

$$\underset{2x2}{[C(\xi,\zeta)]} = (1-\xi)\ \underset{2x2}{[C(0,\zeta)]} + \xi\ \underset{2x2}{[C(1,\zeta)]} \tag{5.50}$$

Expressions (5.49) and (5.50) can be utilized to evaluate (5.32) or (5.33) explicitly. It may be noted that although linear interpolation for surface loads, thickness, and elastic-plastic moduli is suggested in (5.48) through (5.50); other interpolation formulas may be used as well. Then it is necessary to specify these values at intermediate points.

Having employed (5.26) for an element, the element stiffness matrix and generalized forces as defined in Equations (3.11) and (3.12), respectively, can be expressed as

$$\underset{6x6}{[k_\alpha]} = \int_0^1 [B(\xi)]^T\ [D(\xi)]\ [B(\xi)]\ r(\xi)\ \ell\ (1-\eta'^2)^{\frac{1}{2}}\ d\xi \tag{5.51}$$

$$\underset{6x1}{\{Q_\alpha\}} = \int_0^1 [\phi(\xi)]^T\ \{p(\xi)\}\ r(\xi)\ \ell\ (1+\eta'^2)^{\frac{1}{2}}\ d\xi \tag{5.52}$$

where the common factor of 2π in front of the integrals has been dropped. The quantities required to evaluate (5.51) and (5.52) have already been defined in (5.32), (5.33), (5.46), (5.47), and (5.48). In (5.52) it was assumed that no body force is present.

The evaluation of integrals (5.51) and (5.52) cannot be easily achieved in closed forms. However, the techniques of numerical integration can be used to advantage to evaluate these integrals. The Gauss' integration formula* was utilized in this dissertation.

Corresponding to the displacement transformation matrix [A] in (3.15) the following relations hold

$$\{q\} = \begin{Bmatrix} v_i \\ --- \\ v_j \end{Bmatrix} = \underset{6x6}{[A]} \quad \underset{6x1}{\{\alpha\}} \tag{5.53}$$

The matrix [A] and its inverse are given in Appendix D. With the aid of $[A^{-1}]$ the element stiffness matrix and generalized forces can be transformed into physical coordinates $\{v\}$ and may be stated, as in (3.17) and (3.18), as

$$\underset{6x6}{[k]} = \underset{6x6}{[A^{-1}]}^T \underset{6x6}{[k_\alpha]} \underset{6x6}{[A^{-1}]} \tag{3.17}$$

$$\{Q\} = [A^{-1}]^T \{Q_\alpha\} \tag{3.18}$$

The matrices [k] and $\{Q\}$ defined in (3.17) and (3.18) are defined in local coordinates. In order to assemble the elements, these matrices must be expressed in some global coordinates. If the r-z coordinates are taken

*See, for example, "Handbook of Mathematical Functions," edited by M. Abramowitz and I.A. Stegun, National Bureau of Standard, 1964, pp. 887.

as the global coordinates, Fig 15, the transformation can be stated as

$$\underset{6x1}{\{q\}} = \underset{6x6}{[T]}\ \underset{6x1}{\{r\}} \tag{5.54}$$

where

$$\underset{6x1}{\{r\}} = \left\langle \begin{matrix} r_1 \\ \hline \\ r_j \end{matrix} \right\rangle_{6x1} \quad ; \quad \underset{3x1}{\{r_i\}} = \left\{ \begin{matrix} u_r \\ u_z \\ \chi \end{matrix} \right\}_{3x1} i$$

The matrix [T] is given in Appendix E.

Alternatively, if the slope of the meridional curve is continuous, the surface coordinates (s,θ,ζ) at nodal circles may be employed to assemble the element stiffness matrices. The transformation is similar to that of (5.54) except that $\{r\}$ should be defined as

$$\underset{1x3}{\{r_i\}^T} = \langle\ u \quad w \quad \chi\ \rangle_j ,$$

and the corresponding [T] matrix is expressed in Appendix F.

Utilizing (5.54), the expressions (3.17) and (3.18) are transformed into

$$\underset{6x6}{[k_b]} = \underset{6x6}{[T]^T}\ \underset{6x6}{[k]}\ \underset{6x6}{[T]} \tag{5.55}$$

$$\underset{6x1}{\{Q_b\}} = \underset{6x6}{[T]^T}\ \underset{6x1}{\{Q\}} \tag{5.56}$$

With the aid of (5.55) and (5.56) expression (3.21) can be expressed as follows

$$\underset{6x6}{[k_b]}\ \underset{6x1}{\{r\}} = \underset{6x1}{\{Q_b\}} \tag{5.57}$$

Using the direct stiffness procedure, Equations (5.57) can be combined for all elements to achieve compatibility and equilibrium at nodal circles. This will lead to a set of simultaneous equations, as in (3.22)

$$\underset{NxN}{[K]} \quad \underset{Nx1}{\{r\}} = \{R\} \tag{3.22}$$

where N is the number of degrees of freedom of the system. The stiffness matrix [K] is in general a tridiagonal matrix. Having solved (3.22), the stresses can be computed as explained in (3.23).

5.9 General Procedure

The procedure to analyze the elastic-plastic deformation of shells of revolution, utilizing the scheme described in this chapter, can be outlined as follows. The shell is assumed to be initially free from residual stresses. The first increment of loading is applied and the magnitude of the load is scaled such that plastic deformation just sets in at some region within the shell. The loading is then continued in small increments. For each increment, equations (3.22) are solved for nodal displacements and the increments of the strain are determined using equations (5.46). The increments of stress and of plastic strain are obtained with the aid of (4.67) and (4.73), respectively. Then the criterion for loading (4.75) is checked. For the case of loading, the equivalent plastic strain increment (4.22)

$$\Delta\bar{\epsilon}^{p} = \frac{2}{\sqrt{3}} \sqrt{(\Delta\epsilon_1^p)^2 + (\Delta\epsilon_1^p)(\Delta\epsilon_2^p) + (\Delta\epsilon_2^p)^2}$$

is computed and is added to the previous equivalent plastic strain,

$$\bar{\epsilon}^p_{(m)} = \bar{\epsilon}^p_{(m-1)} + \Delta\bar{\epsilon}^p$$

where m refers to the number of loading increment. If the data of uniaxial test are given, the value of $\bar{\epsilon}^p_{(m)}$ is used to read tangent modulus E_t and equivalent stress $\bar{\sigma}$, Fig. 9. Since the data for uniaxial test are generally given in the form of a table, linear interpolation is used to obtain the values of E_t and $\bar{\sigma}$ for intermediate points. The value of $\bar{\sigma}$ is utilized to modify the new state of stress. The quantity E_t together with the modified state of stress is used to establish the new material properties, Equations (4.68) and (4.74). This will provide sufficient information to proceed to the next increment of loading. If the "second approximation method", Eqns. (3.50), is used, each step of loading is to be repeated as shown in Fig. 7.

The problem of convergence is largely dependent on the type of material properties and the geometry of structure. For the solution of any problem the results for different magnitude of loading increments are to be compared and the optimum size of loading increment is to be selected. It was observed that for hardening materials a larger value of loading increment can be selected compared to that of perfectly plastic materials. In addition, for loading close to the collapse load the analysis becomes very sensitive and requires a smaller size of loading increment to be used. With the availability of computer program, however, the trials for optimum loading increments are not very laborious.

6. NUMERICAL EXAMPLES

In this chapter, the procedures discussed in previous chapters are applied to some sample problems. First a brief description of the computer program is given. Then the different elements which were developed are compared, and the best element is selected. Two examples are worked out for the elastic range, and the solutions are compared with theoretical and experimental results which are available in the literature. Finally, two examples for the elastic-plastic range are analyzed.

6.1 Description of the Computer Program

A computer program using FORTRAN IV language was developed for the solution of rotational shell problems using the method discussed in the previous chapters.

The general procedures of the computer program are indicated in the concise flow chart shown in Figure 18. Each block in this chart is labeled and a few remarks concerning the blocks are mentioned below:

1. Input data are read from the input deck. The program can treat examples with number of nodes up to 100 and number of layers up to 20. The number of load increments is not restricted. However, the full capacity of the core storage, 32768 locations of IBM 7094, was not completely utilized. The dimension statements may be modified to accommodate up to 200 elements. For higher number of elements an out-of-core storage is to be employed.

The program provides for a linear variation of element thickness along the meridian. Therefore, any variation of shell thickness may be approximated by linear variation within each element.

For a closed shell, numbering of nodal points should be started from the point on the axis of symmetry.

2. The matrices [B], defined in Appendices A and B, are computed at several points within each element and are stored on tape. The tape is later read back to calculate the element stiffness matrices $[k_\alpha]$, see (3.11). The matrices $[A^{-1}]$ [T] defined in Appendices D, E, and F are also computed for each element and are stored on tape. This tape is used to transform $\{Q_\alpha\}$ and $[k_\alpha]$ to $\{Q\}$ and [k], respectively. In addition, the matrices [B] computed at the ends of each element are stored to determine the increments of strain.

3. The applied load increment which may consist of concentrated and distributed loads are read. The distributed load is transformed to equivalent nodal circle load using (5.52) and (3.18), then they are added to ring (concentrated) load to establish the load vector $\{r\}$. To facilitate the data preparation, the intensities of distributed load at nodal circles are read and linear interpolation is used to account for variation along the meridian, see (5.48).

Integration of (5.52) is carried out by Gauss' method of integration. Examples with different number of integration points were worked out and the results were compared. In most cases no significant changes in the results were observed after increasing the number of integration points above 5. For conformity with the integration of (5.51),10 integration points are taken for each element.

4. The rigidity matrices (5.25) are established using the procedure given in (5.30). A linear variation of the material properties along meridian is adopted for each element. With the aid of [B] computed in block No. 2 and rigidity matrices, the stiffness matrices $[k_\alpha]$ is computed. As mentioned before, the integration of (5.51) is achieved using Gauss' method of integration. Having obtained $[k_\alpha]$, the element stiffness matrices in global coordinates are established. The assemblage of stiffness matrices, to set up [K], is fulfilled using the direct stiffness method.

5. Solution of (3.22) for $\{r\}$ is obtained using Gauss elimination method. The properties of symmetry and band structure of [K] are taken to full advantage in storing this matrix and in the solution of the simultaneous equations (3.22). Since [K] is positive definite no pivoting is required.

6. Having determined $\{r\}$ and generalized displacements $\{\alpha\}$, the strain increments and stress resultants are obtained using (5.46) and (5.24), respectively.

7. The procedure for computing the new material properties for each load increment is illustrated in the flow chart as shown in Figure 19. The chart indicates the procedure for a typical loading increment m. Notations are mostly those used in Chapter 4. Quantities with subscript T are temporary and are adjusted. In this diagram; branch (I) indicates that the material point is still in the elastic state, branch (II) corresponds to the initiation of plastic deformation or reloading after an unloading, and branch (III) is associated with the continuation of loading. Here, the term loading signifies the loading which produces plastic deformation and corresponds to the state of stress in the neighborhood of a material point. Matrix [a], with a change of notation, is defined in (4.74). To expedite convergence the expression in block 4 is replaced by $\bar{\sigma}_T < 0.999\ \bar{\sigma}_{m-1}$.

The procedure shown in this chart is applicable to isotropic hardening as well as to perfectly plastic material, Equations (4.68) and (4.69). With a slight modification, kinematic hardening can be also treated by replacing (4.70) for (4.69) and making appropriate modification for loading criterion.

As far as computer time for the whole process is concerned, this mainly depends on the number of elements and the number of loading increments. As a guideline, for a solution with about 30 elements and 20 layers the computer time for the execution of the first loading increment is one second/element and for the execution of any other loading increment is 0.8 second/element. The execution time per element reduces if the number of elements increases.

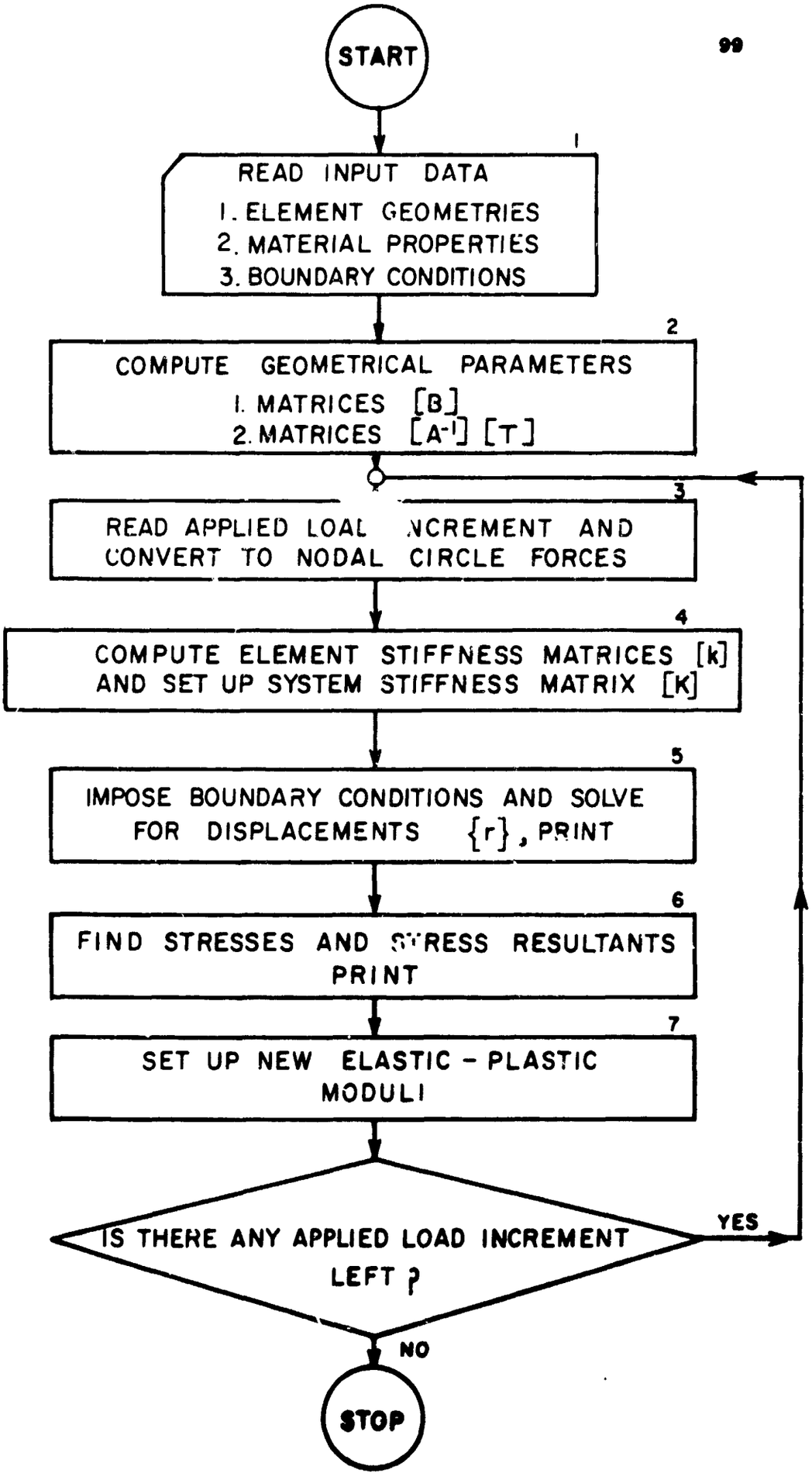

FIG. 18 A CONCISE FLOW CHART OF COMPUTER PROGRAM

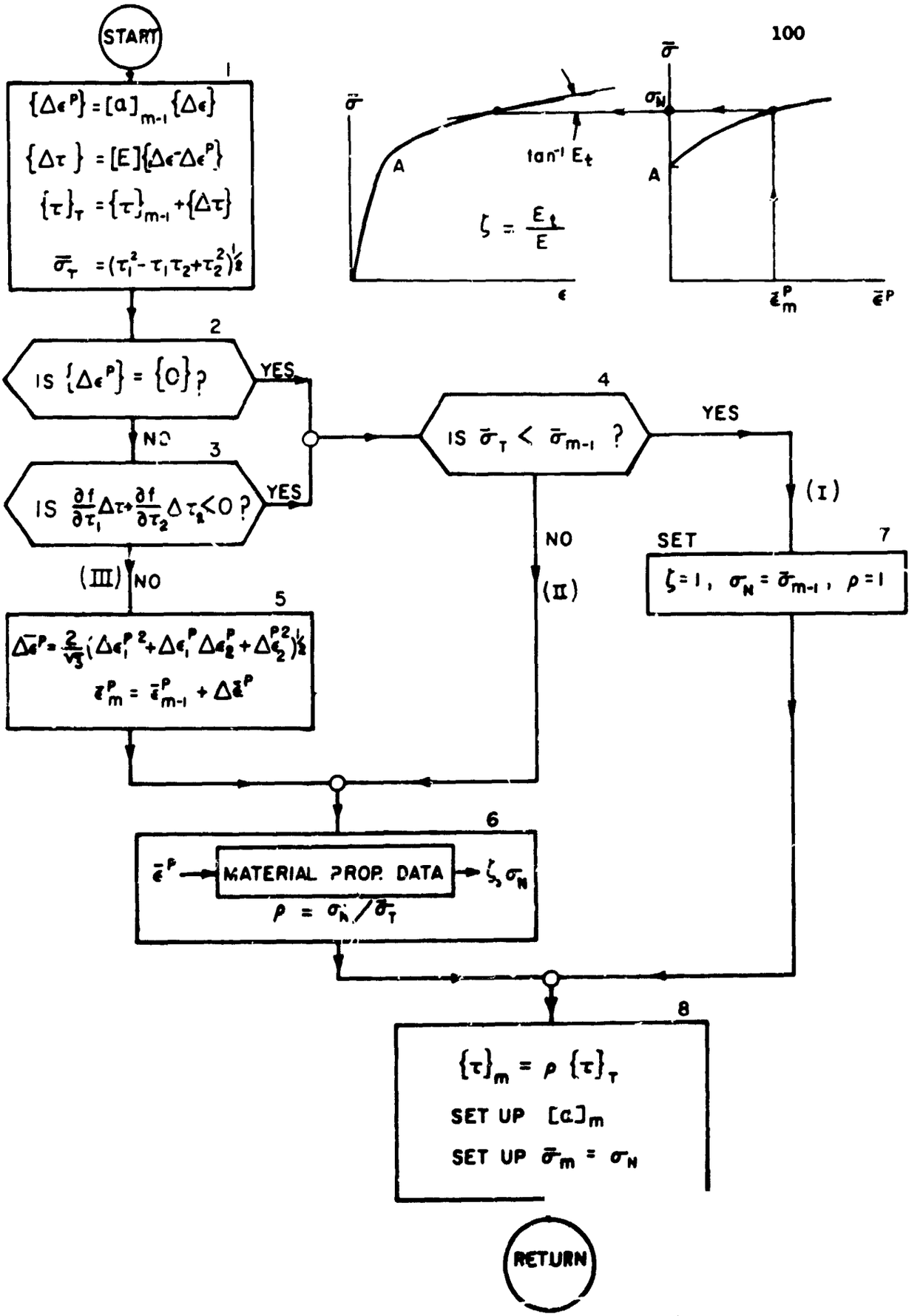

FIG. 19 FLOW CHART FOR THE MATERIAL PROPERTIES SUBROUTINE

6.2 Comparison of the Elements

Two types of elements, designated by FDR(i) and FDC(i)*, which were discussed in Chapter 5 are compared here by means of a numerical example. Geometry of all of these elements are expressed in local Cartesian coordinates ξ-η, (5.35) and (5.36). Other curved elements were also developed in terms of their intrinsic geometry. Their formulations are more involved and require some approximations. The numerical examples indicate that they yield inferior results comparing to those presented here.

For the purpose of comparison an example of a hemispherical shell under internal pressure is selected. A roller edge which does not restrain normal displacement and meridional rotation is specified. For this type of loading and support conditions the membrane theory, within the limitation of the Love's first approximation, gives the exact solution and no bending moment should appear anywhere in the shell. Its closed form solution is as follows

$$N = N_s = N_\theta = \frac{1}{2} pR$$

$$M = M_s = M_\theta = 0$$

$$w = (1-\nu) \frac{pR^2}{2Eh}$$

$$u = 0$$

---

* See, page 89

This example serves particuarly to detect any bending moment which may be generated in the shell as the result of geometrical idealization.

For the numerical computation, the following material properties and dimensions are selected

$\nu = 0.30$

$E = 10 \times 10^{6}$ psi

h = 3 in. thickness of sphere

R = 100 in. radius of sphere

p = 1 psi internal pressure

which gives

N = 50 # /in

$w = 1\text{-}1/6 \times 10^{-4}$ in.

Figures 20 through 25 show a comparison among FDR(1), FDR(2), and FDC(2) with 3 and 9 elements. The results clearly indicates that FDR(2) is superior to FDR(1) and FDC(2), in prediction of both the displacements and stresses. In this example the solution with 9 elements in a computer working with 8 deciminal digits; FDR(2) yields accurate results up to 6 digits, whereas the accuracy of FDC(2) and FDR(1) does not exceed 3 and 4 significant digits, respectively. Hence, although in some figures the plotted points for different elements coincide, the degree of accuracy is not the same. A comparison of results for FDR(1) and FDR(2) shows a relative improvement that can be achieved by matching curvatures at nodal circles.

To compare the results obtained with a curved element with those of a conical element, the same example was worked out using the computer program developed in Ref. [13]. The hemisphere was divided into 9 elements. A spherical cap was used for the central element and the remaining elements were conical. The results for displacement and meridianal bending moment are shown in Fig. 26. It indicates that the overall displacements agree closely with the exact solutions but there is a sudden jump at $\varphi = 90^{o}$ which deviates from the exact solution by 45%. The principal inaccuracy appears to be in the prediction of bending moments. The largest bending moment, which occurs at $\varphi = 10^{o}$, produces stresses at outer layers which are greater than those of membrane forces. The high concentration of bending moments at nodal circles, which are the results of idealization in geometry, is more undesirable in the plastic analysis than in the elastic analysis. Because these bending moments may cause a premature onset of plastic deformation which could lead to an overall change in the characteristic of the system.

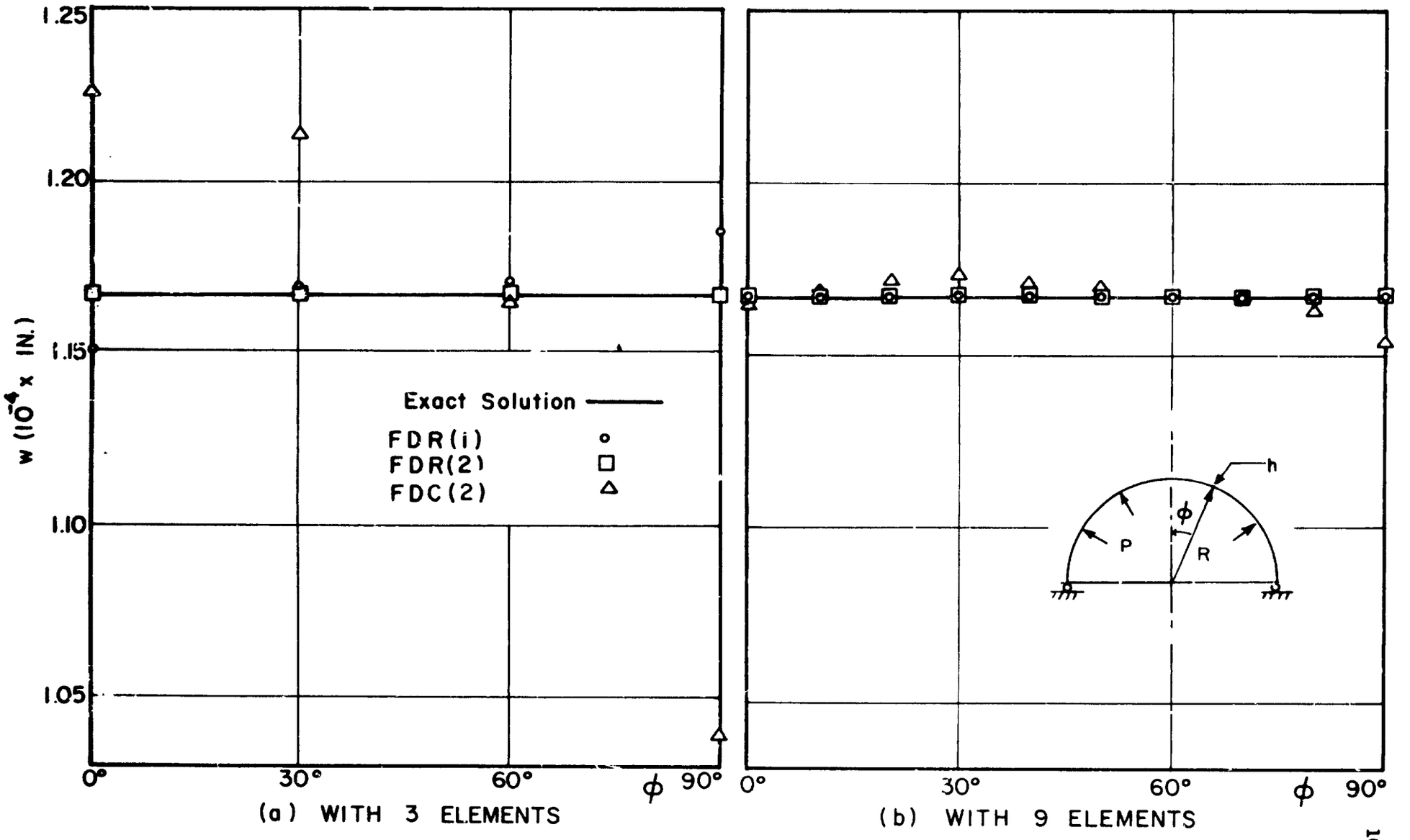

FIG. 20 NORMAL DISPLACEMENTS w VERSUS ϕ, (HEMISPHERE)

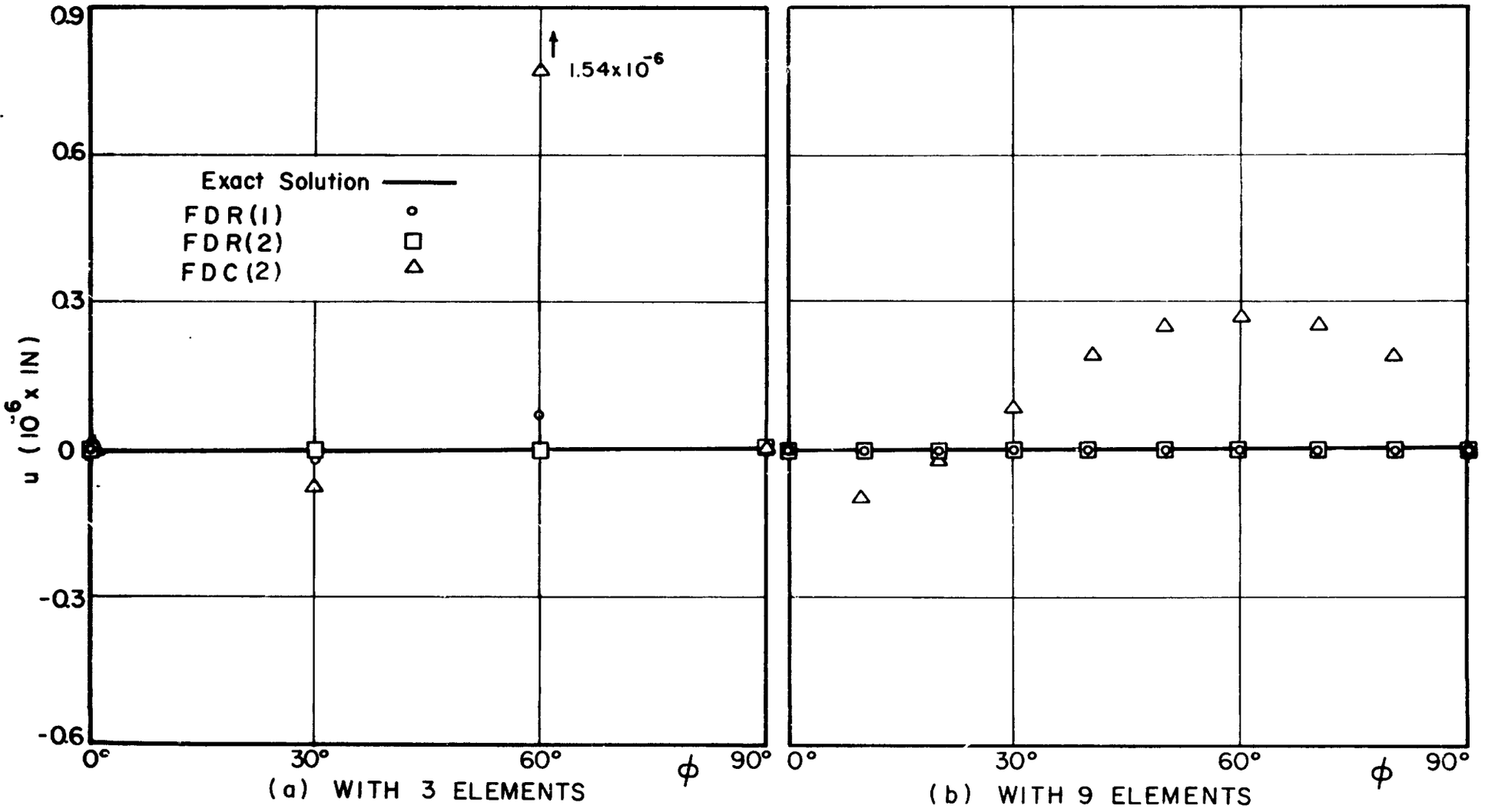

FIG. 21 MERIDIONAL DISPLACEMENT u VERSUS ϕ (HEMISPHERE)

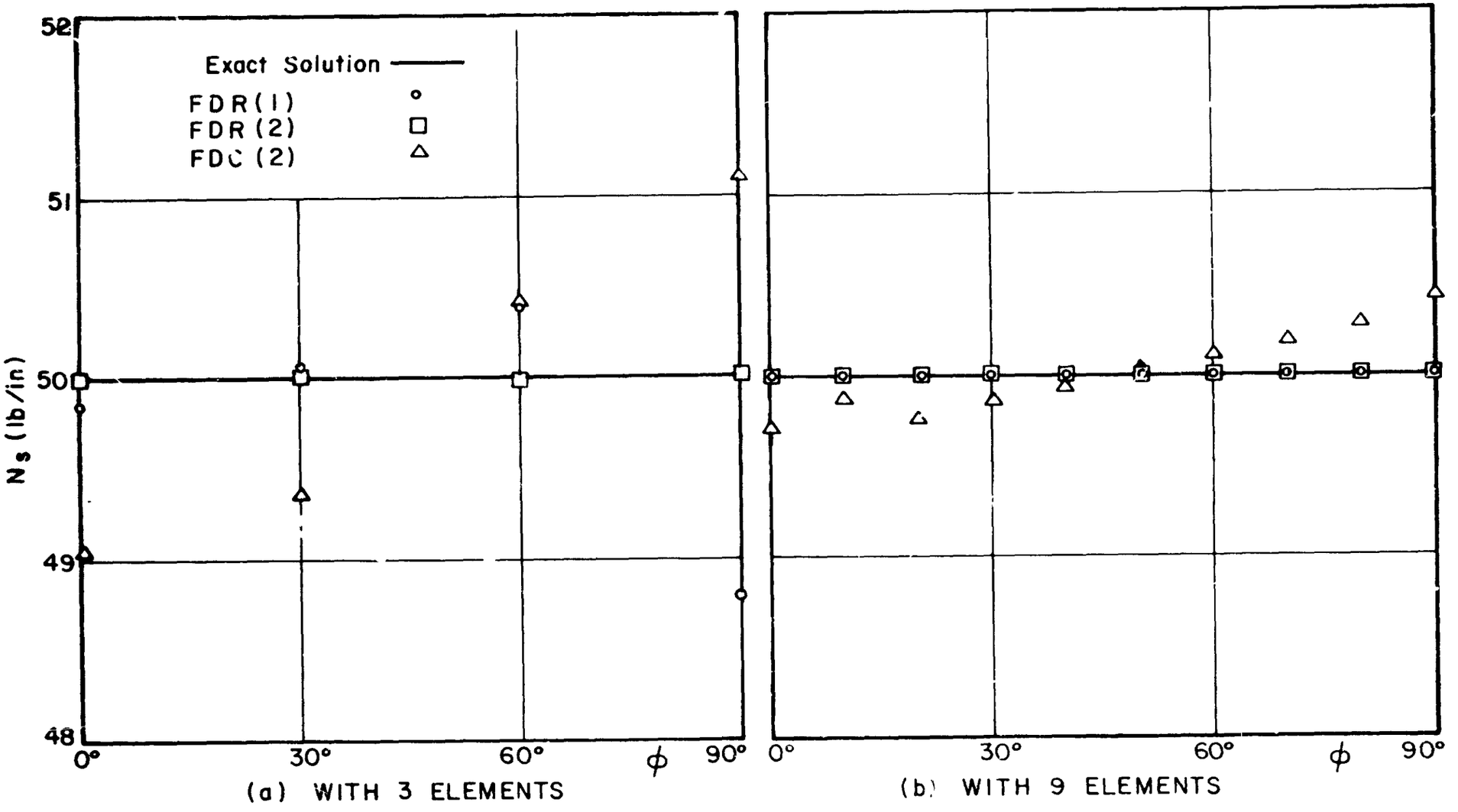

FIG. 22 MERIDIONAL MEMBRANE FORCE N_s VERSUS ϕ (HEMISPHERE)

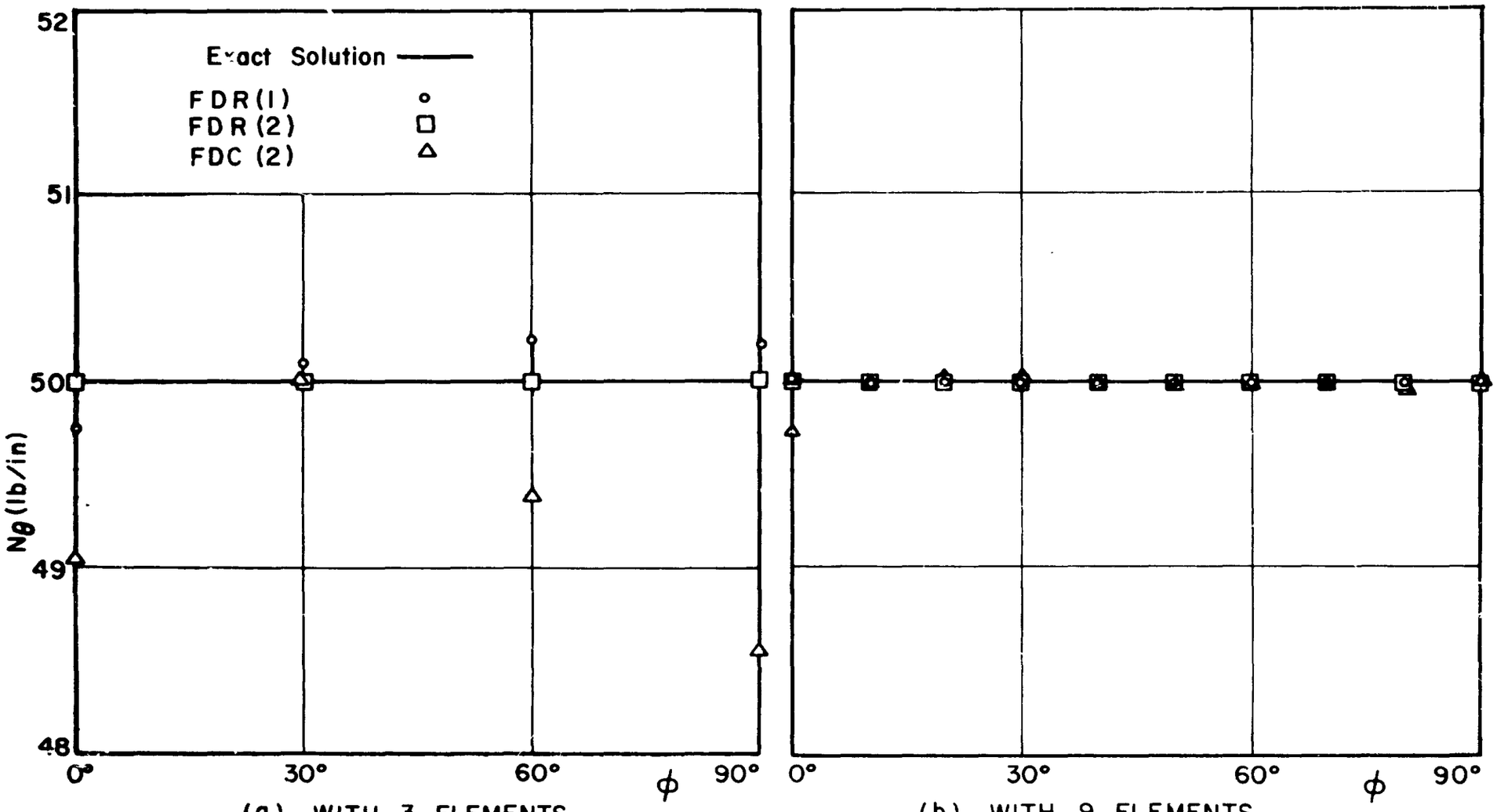

FIG.23 CIRCUMFERENTIAL MEMBRANE FORCE N_θ VERSUS ϕ (HEMISPHERE)

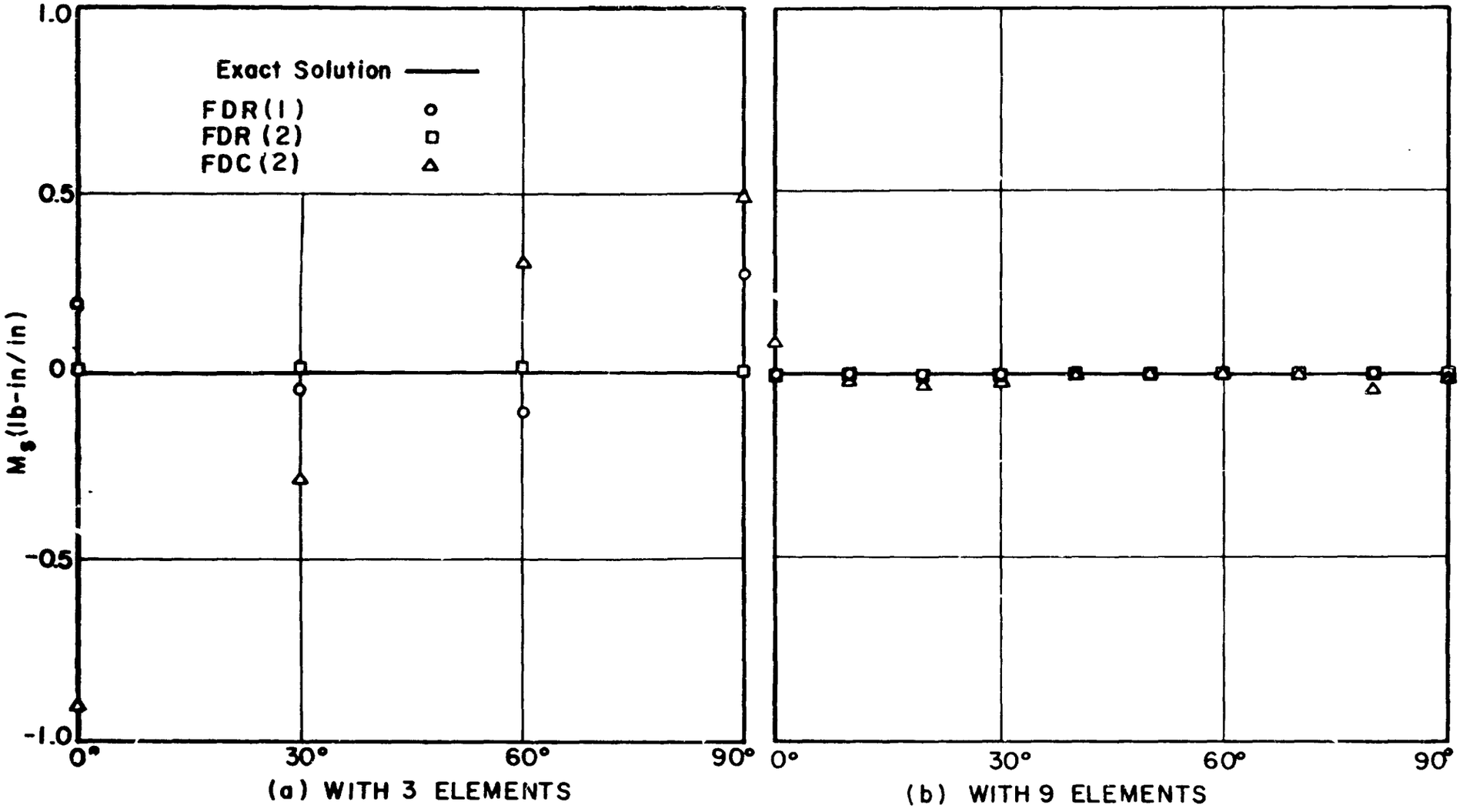

FIG.24 MERIDIONAL BENDING MOMENT M_s VERSUS ϕ (HEMISPHERE)

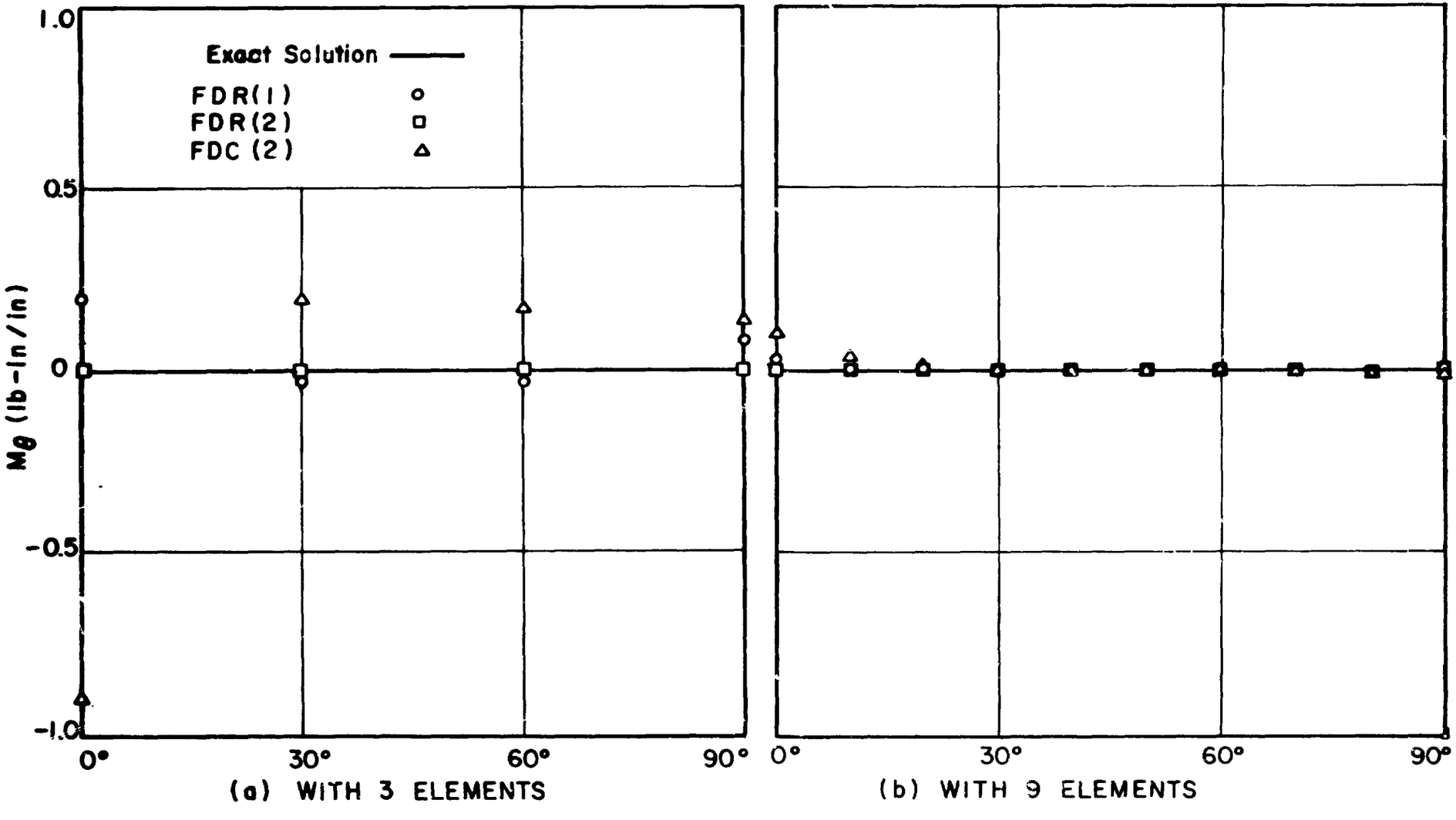

FIG. 25 CIRCUMFERENTIAL MOMENT M_θ VERSUS ϕ , (HEMISPHERE)

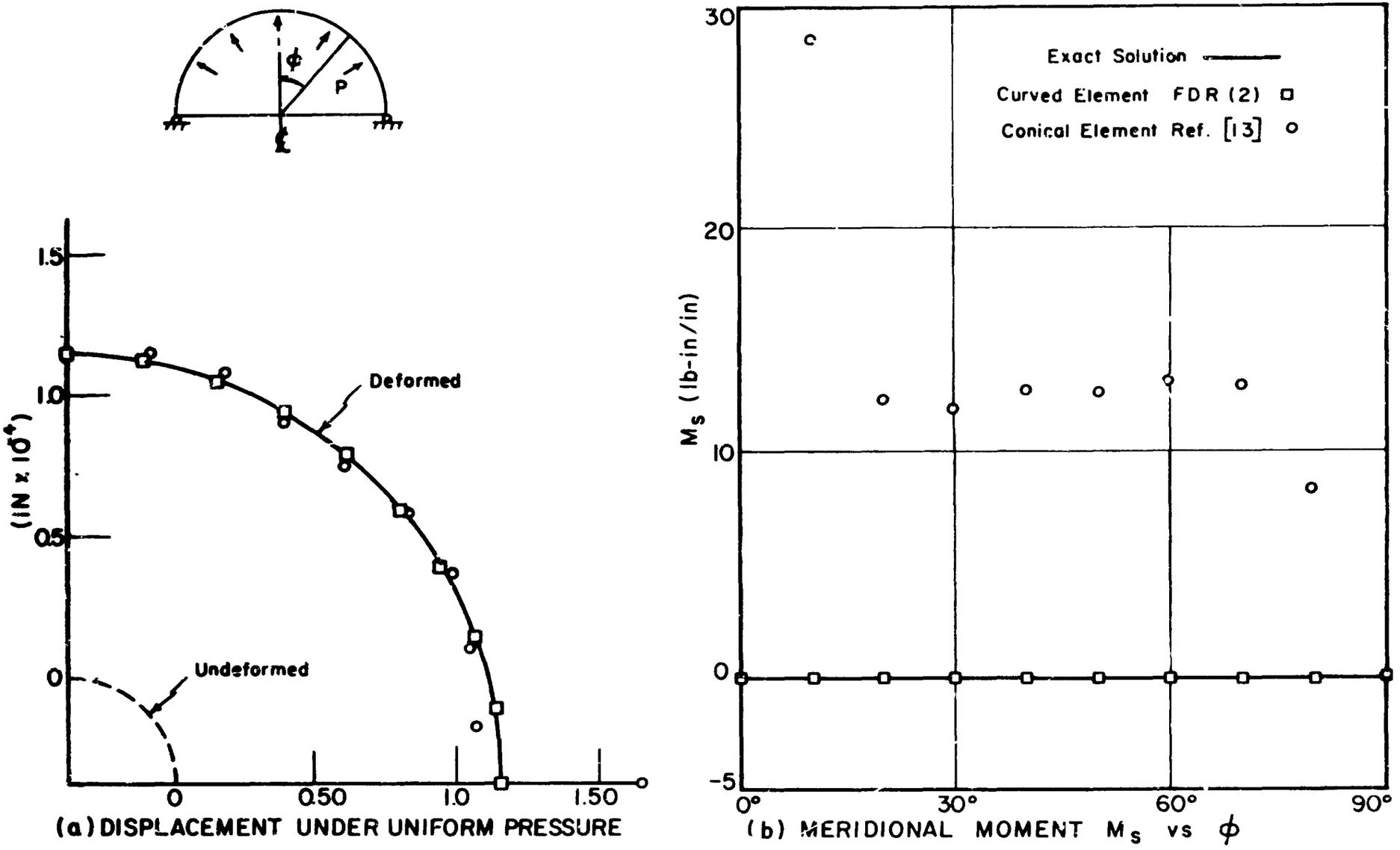

FIG.26 COMPARISON OF A CURVED AND A CONICAL ELEMENT

6.3 Comparison in the Elastic Range

The curved element developed here is compared with a theoretical solution obtained elsewhere by another method and with the results of an experiment in the elastic range. In these examples the shell geometries are relatively simple and can be managed by classical methods. The intent of comparisons given here is merely to show the reliability of the proposed approach but not its versatility. The results of these examples and those of many others, which were worked out but not reported here for the sake of brevity, show a rapid convergence of the solution. Since the curved element is employed, any shell geometry can be closely approximated. In general, the solution can be achieved with fewer number of subdivisions compared to that with conical elements. As an illustration of this, a case is cited in connection with the toroidal shell example.

6.3.1 Toroidal Shell

The shell consists of a torus which is loaded by internal pressure. A refined procedure, which combines both the direct integration and the finite-difference approach, was used in Reference [11] to achieve a solution of this problem. The results reported in [11] are compared with the results of the finite element solution developed here.

Because of symmetry only the upper half of the torus is analyzed. The internal boundary condition at the junction of the upper and the lower half, which indicate that the meridional rotation and displacement should vanish at this junction, were imposed to achieve the solution.

FDR(2) elements of several mesh sizes were employed. The comparison for the normal displacement, w, and meridional bending stress σ_{sb} are shown in Figures 27 and 28. The results by the finite element method are plotted for the number of elements equal to 16 and 30. The input data are as follows:

$E = 10 \times 10^6$ psi	$\nu = 0.30$
h = 5 in.	shell thickness
R = 100 in.	torus radius
a = 150 in.	as shown in Fig. 27
p = 1000 psi	internal pressure

The sizes of elements selected for this analysis can be inferred from the location of the points on these figures. As can be deduced from these figures, the convergence of the solution is fast and a remarkable accuracy can be achieved by taking a relatively small number of elements. It may be noted that the same problem was tackled in a graduate student research report at Berkeley* using the conical element developed in [13], where a less satisfactory result is reported even with 120 relements.

Other examples of toroidal shell with different relative geometry were also worked out. It was observed that for smaller $\frac{h}{R}$ ratios finer subdivisions should be used to obtain a comparable accuracy for bending moments. This is due to the fact that with the decrease in the $\frac{h}{R}$ ratio

*J.R. Chisholm, "Finite Element Solution of Toroidal Shells of Revolution," Graduate Student Research Report No. 225, SESM Division, Univ. of Calif., Berkeley, Fall 1965.

the membrane stresses become dominent compared to those of bending. Therefore, the order of accuracy of the digits expressing the bending stresses diminish. To recover the significant digits, it is also possible to keep the number of elements constant but to retain a larger number of digits in the computation. The increase in the required number of elements to achieve the desired accuracy, however, was found not to be excessive. The optimum element size can be easily reached by comparing the results obtained by using different element sizes.

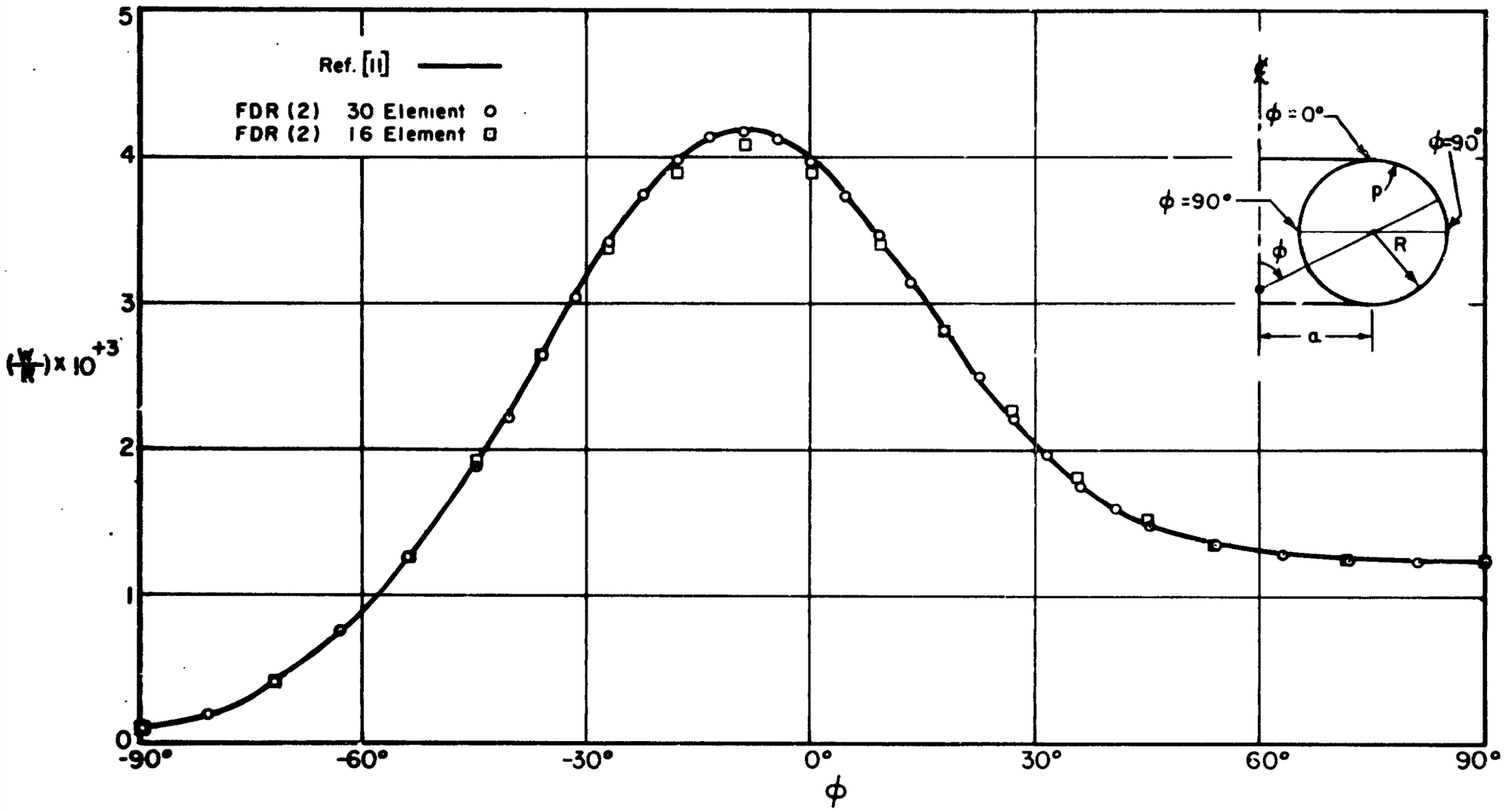

FIG. 27 NORMAL DISPLACEMENT w VERSUS ϕ (TORUS)

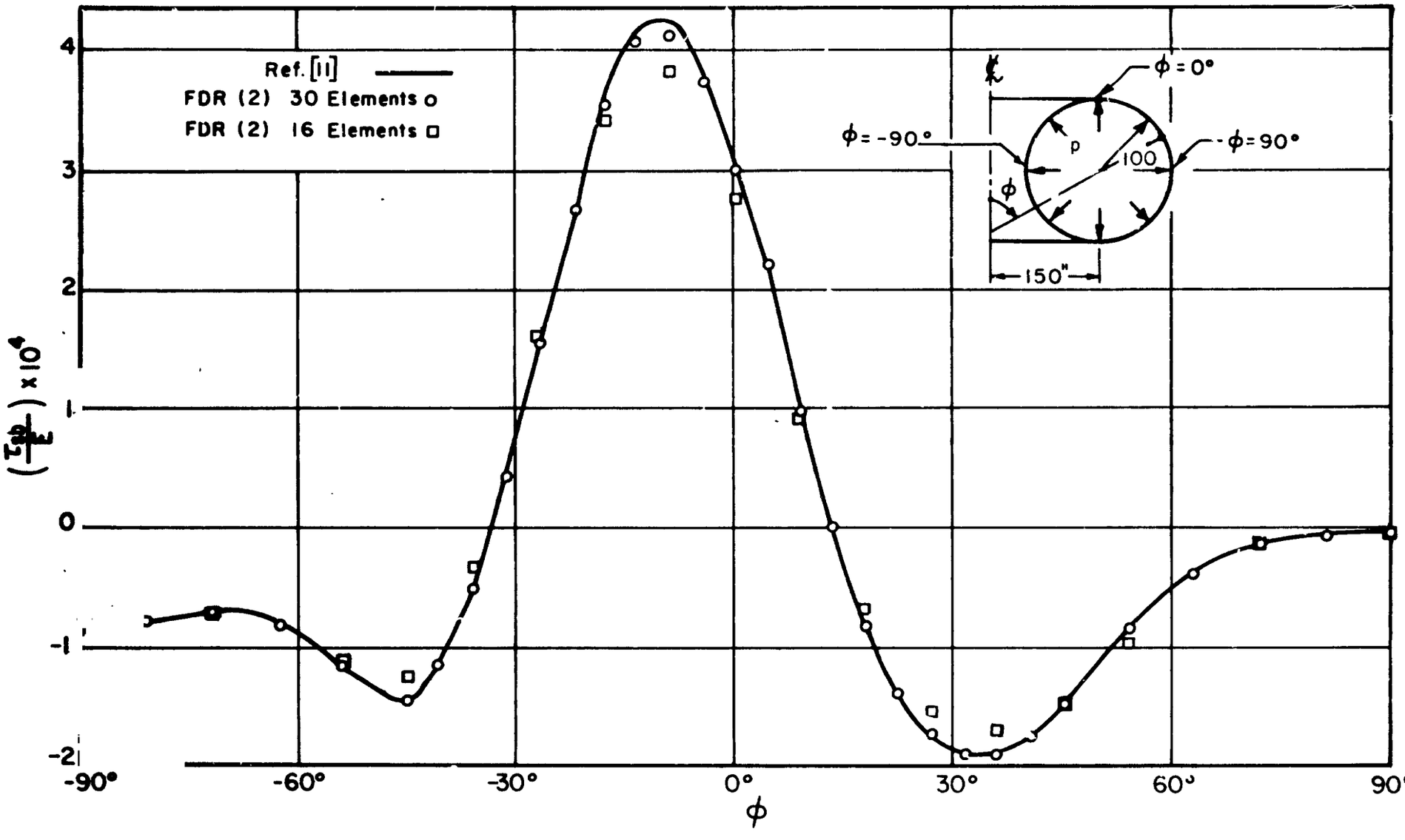

FIG.28 MERIDIONAL BENDING STRESS τ_{sb} AT OUTER FIBER VERSUS ϕ (TORUS)

6.2.2 Toriconical Shell

A special type of toriconical shell is selected. The shell consists of a cylinder which is closed at one end by a 45° spherical segment and a cone, Fig. 29. At the junctions of cylinder-to-sphere and sphere-to-cone the slopes are continuous but the meridional curvatures are not.

Two specimens of toriconical shell where tested under internal pressure in the elastic range by Morgan and Bizon* at the NASA Lewis Research Center, Cleveland, Ohio. The results of an experiment on the smaller size specimen, which was prepared with higher degree of precision in fabrication, are compared with the finite element solution.

The material properties and the dimensions of the specimen are as follows:

$E = 10 \times 10^6$ psi	$\nu = 0.30$
$h = 0.06$ in.	shell thickness
$D = 12.00$ in.	outer diameter of cylinder
$\ell = 9.50$ in..	cylinder length
$L = 18.0$ in.	total length of shell
$\phi_o = 45^{\circ}$	half-angle of the cone
$p = 250$ psi	internal pressure

The theoretical results with the aid of FDR(2) element were obtained using the above data. Two different mesh sizes were selected: one with

*W.C. Morgan and P.T. Bizon, "Experimental Evaluation of Theoretical Elastic Stress Distribution for Cylinder-To-Hemisphere and Cone-to-Sphere Junctions in Pressurized Shell Structures," NASA Technical Note, D-1565, February 1963.

34 elements;

10 elements in the conical segment

13 elements in the spherical segment

11 elements in the cylindrical segment

and the other with 46 elements;

15 elements in the conical segment

15 elements in the spherical segment

16 elements in the cylindrical segment

The results between the two solutions indicate close agreement, Figures 29 and 30 show the meridional and the circumferential stress distribution predicted by theory and that obtained in the experiment. Figure 31 is also plotted to show the distribution of the effective stress

$$\bar{\sigma}^2 = \tau_s^2 - \tau_s\tau_\theta + \tau_\theta^2$$

as was defined in (4.24). The correlation between the theory and the experiment is within the range of the test control.

It may be mentioned that the NASA paper† also reports some theoretical results which are obtained based on the classical solutions for a sphere, a cone, and a cylinder combined together by using the method of superposition.

---

†Ibid

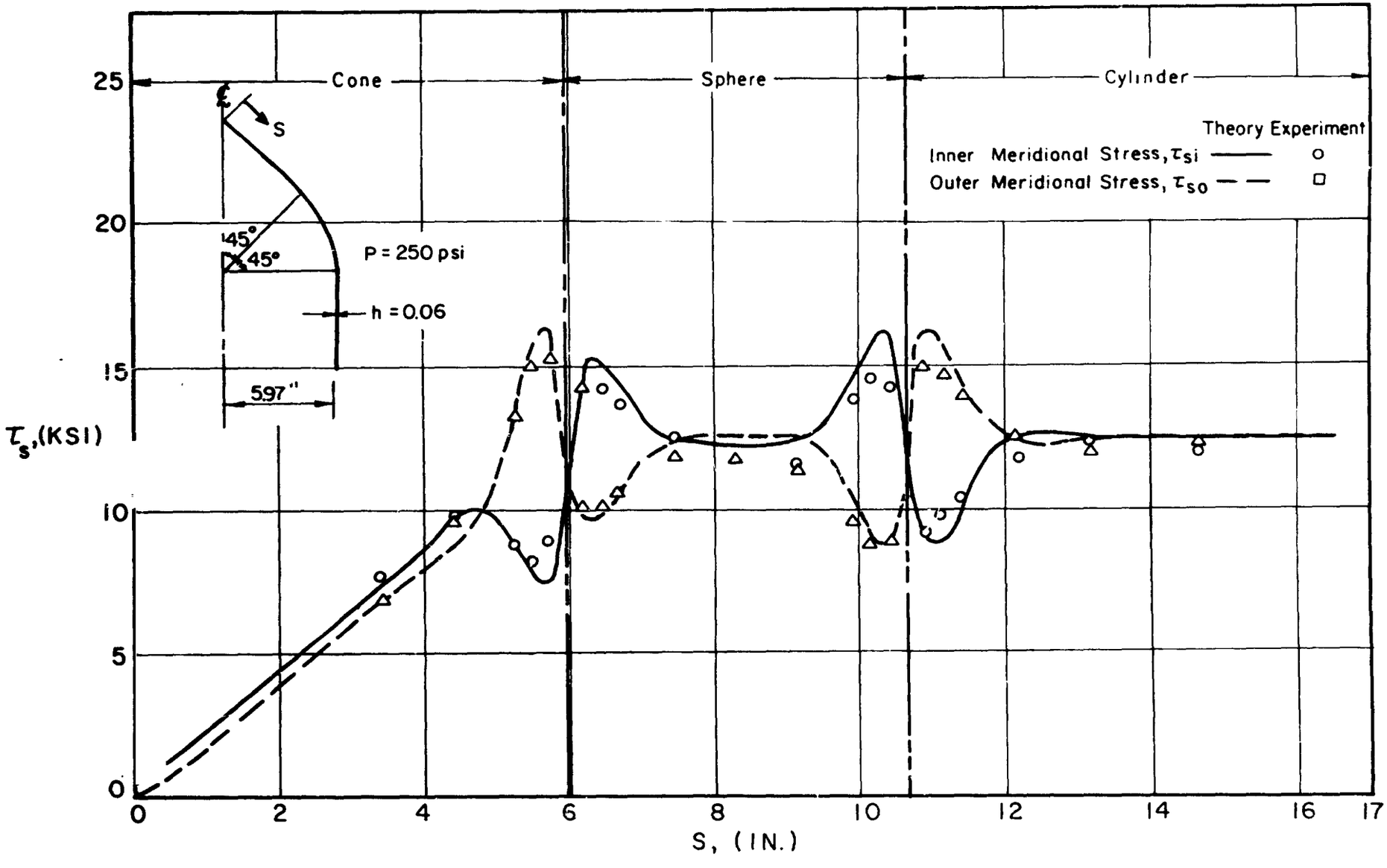

FIG.29 THEORETICAL AND EXPERIMENTAL MERIDIONAL STRESS IN TORICONICAL SHELL

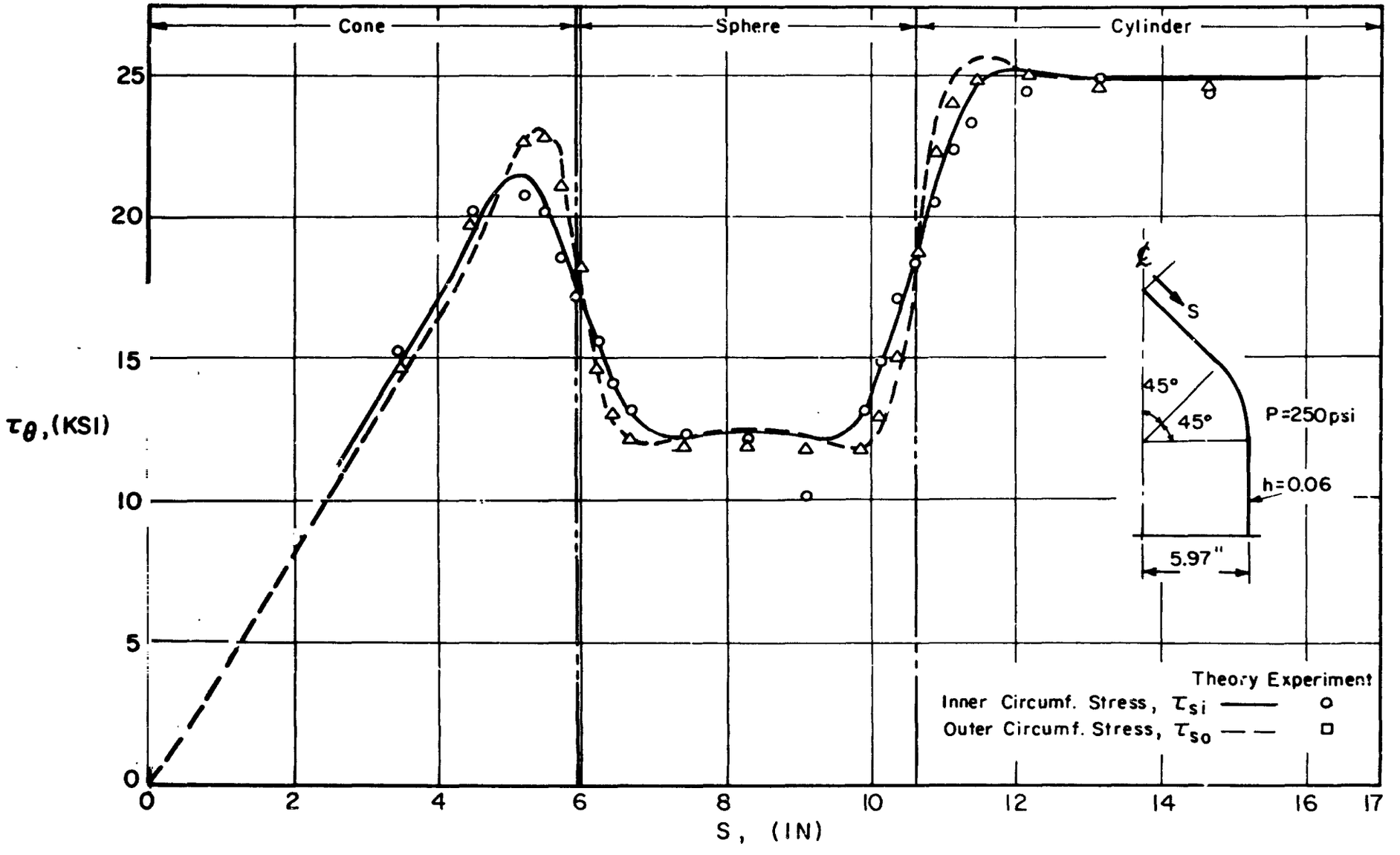

FIG.30 THEORETICAL AND EXPERIMENTAL CIRCUMFERENTIAL STRESS IN TORICONICAL SHELL

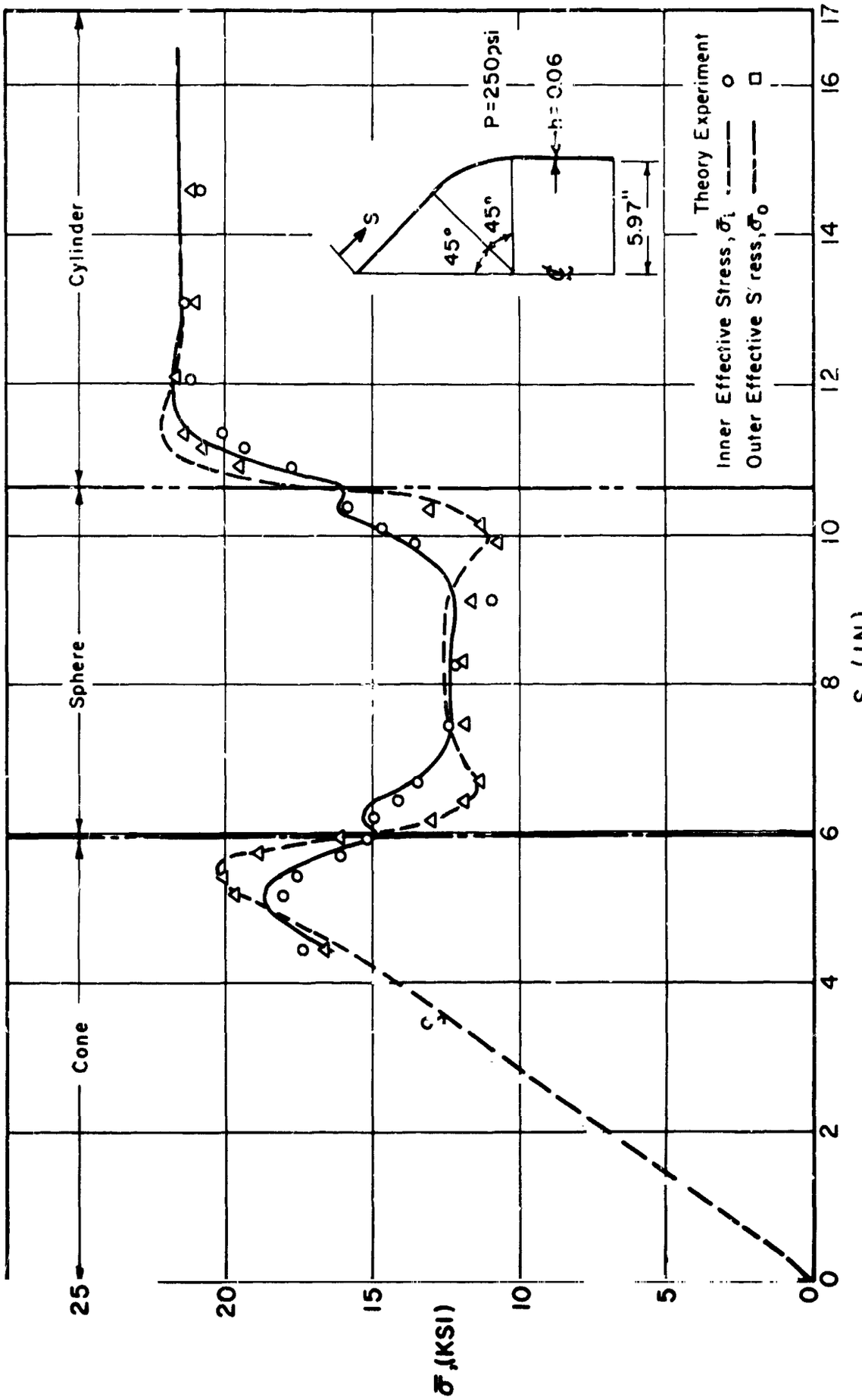

FIG.31 THEORETICAL AND EXPERIMENTAL EFFECTIVE STRESS $\bar{\sigma}$ IN TORICONICAL SHELL

6.4 Elastic-Plastic Solutions

Two examples are reported below to demonstrate the application to elastic-plastic problems. Von Mise yield condition and the associated flow rule were used in these examples. The first example is chosen to compare the result with that of a previous report where a different approach was used. The other is concerned with a case study for torispherical pressure vessel.

6.4.1 Circular Plate

A simply supported circular plate of elastic-isotropic hardening material is selected. The material properties and dimensions are the same as those reported in Examples No. 6 of Ref. [34], where

$a = 10$ in. plate radius

$h = 1$ in. plate thickness

$E = 10 \times 10^6$ psi

$\nu = 0.33$

$\sigma_y = 16{,}000$ psi elastic limit

$E_t = 3 \times 10^6$ tangent modulus

For the analysis using the finite element method, 20 elements and 20 layers were selected. After initiation of plastic deformation at the center of plate, loading was increased with increments of 10 psi.

Results of this example together with that obtained in [34] are shown in Figures 32 to 34. For comparison, solution according to elastic theory is also plotted in Figures 32 and 33. A redistribution of moment as a result of plastic deformation is apparent in Figure 33. Except for a slight change in elastic-plastic boundaries, a good correlation is obtained.

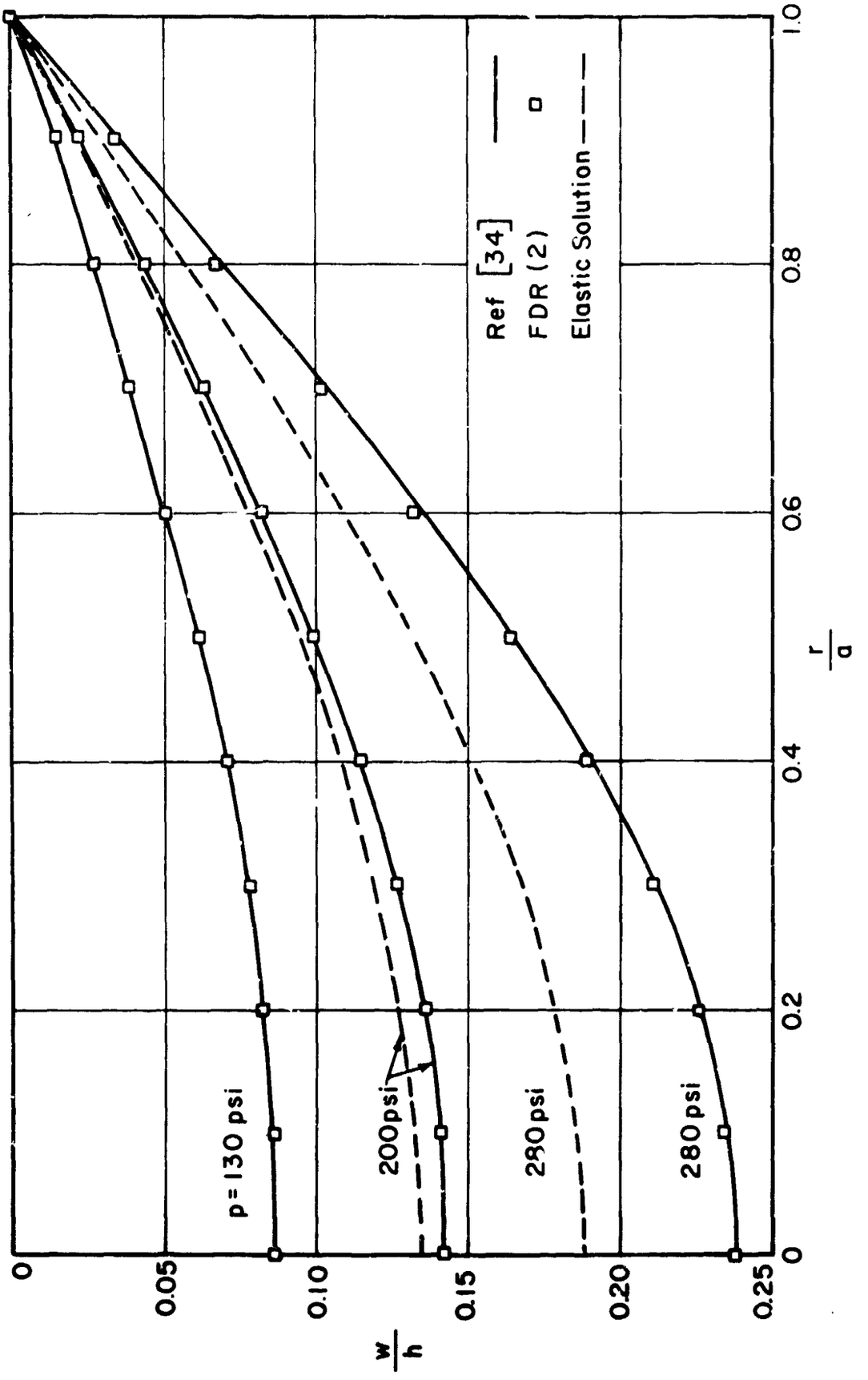

FIG. 32 NORMAL DISPLACEMENT w VERSUS $\frac{r}{a}$ (CIRCULAR PLATE)

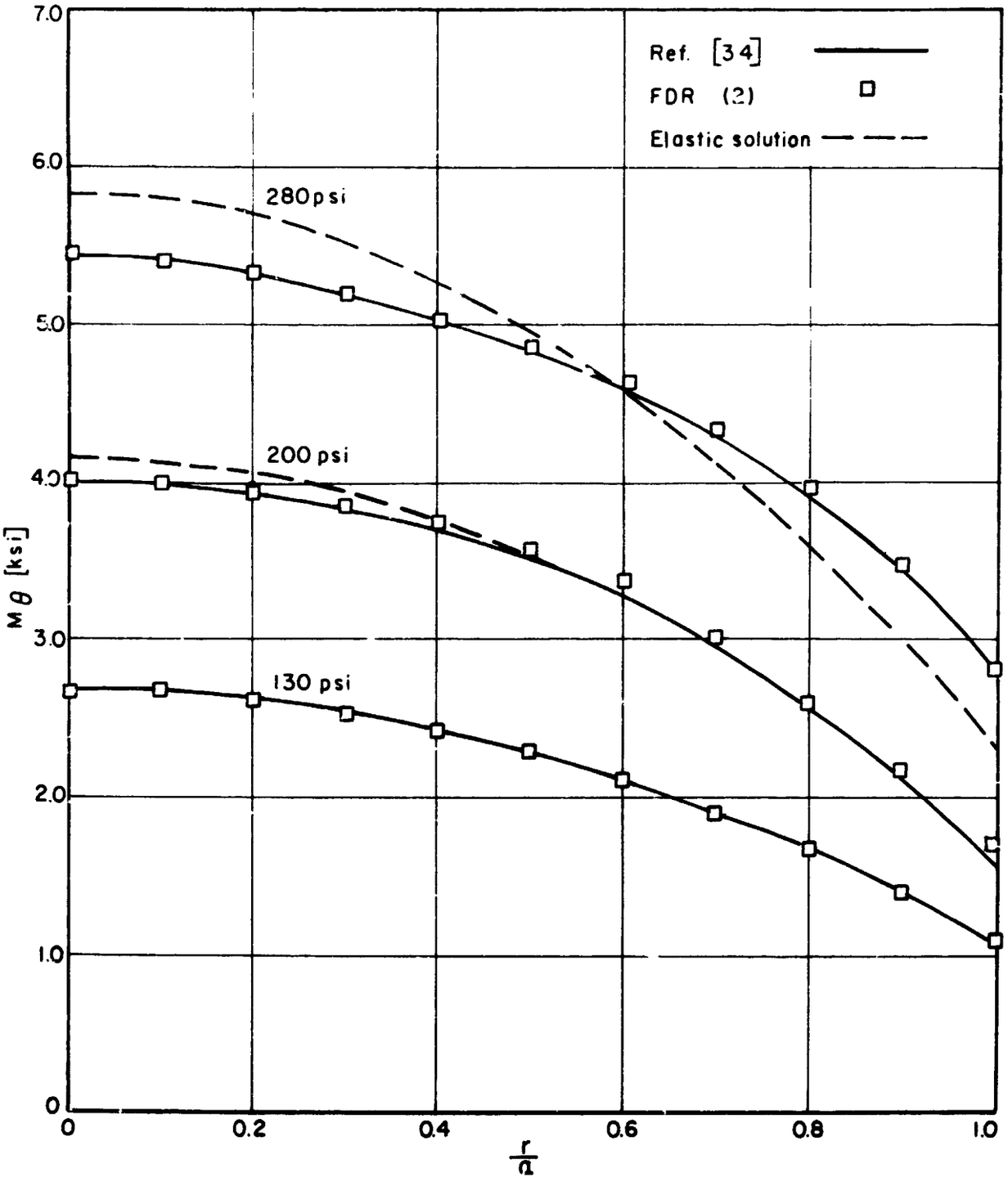

FIG.33 CIRCUMFERENTIAL BENDING MOMENT VERSUS $\frac{r}{a}$
(CIRCULAR PLATE)

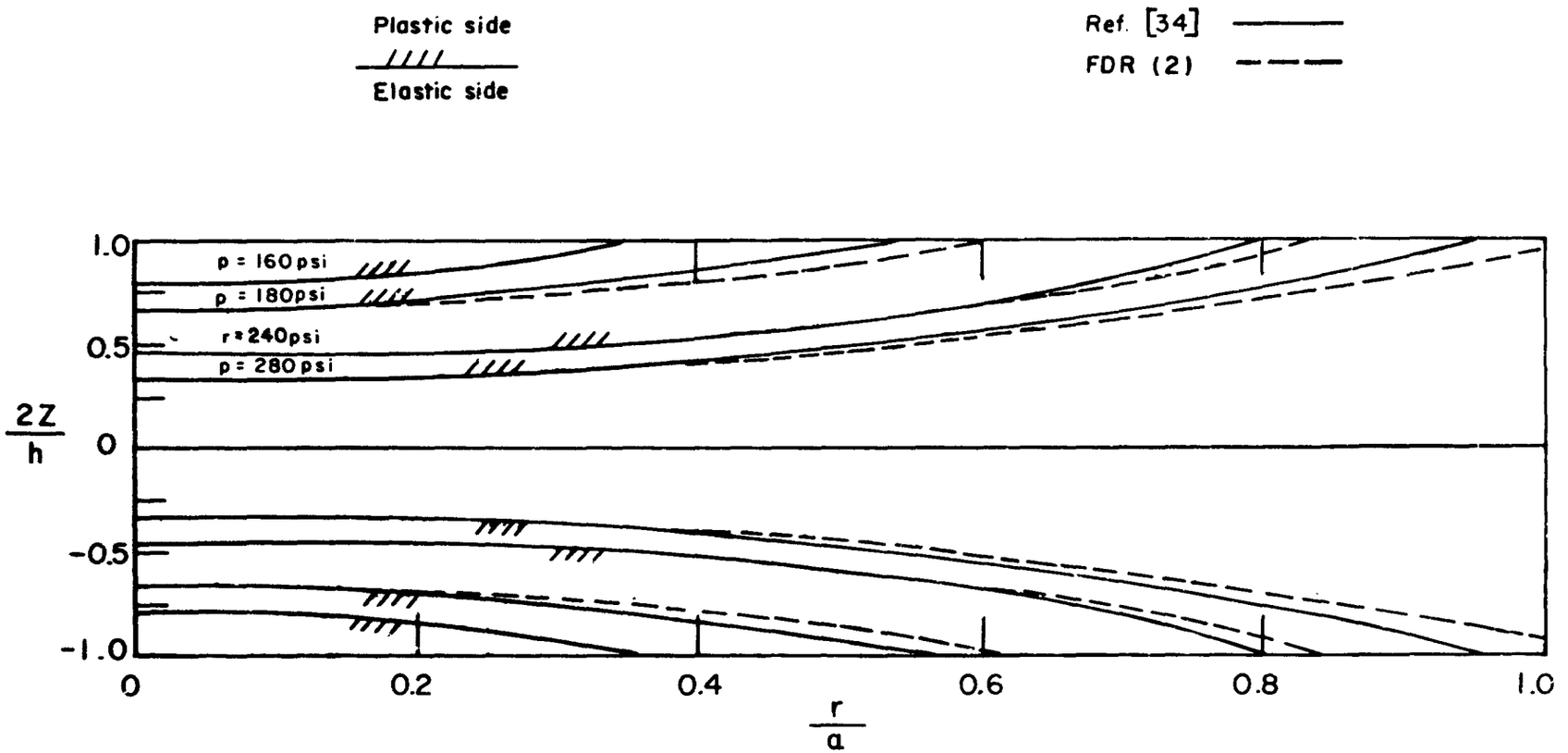

FIG. 34 ELASTIC-PLASTIC BOUNDARIES (CIRCULAR PLATE)

6.4.1 Torispherical Shell

A torispherical pressure vessel head subjected to uniform internal pressure is analyzed here. The material is assumed to be elastic-perfectly plastic. An example is worked out for a shell of uniform thickness with the following dimensions:

D = 10 in.	diameter of head skirt
L = D	radius of sphere
r = 0.06 D	meridional radius of torus
t = 0.004 D	shell thickness

The material properties are taken as follows

$E = 30 \times 10^6$ psi

$\gamma = 0.30$

$\sigma_y = 30{,}000$ psi

Three different element sizes, with 16, 32, and 47 elements; were tried for a shell under 25 psi internal pressure and the result for normal displacement w is plotted in Fig. 35, where a good convergence is observed. An example with 47 elements;

20 elements in the spherical segment

16 elements in the toroidal segment

11 elements in the cylindrical segment

and 20 layers was analyzed for elastic-plastic solution. After the application of the first increment of load of 42 psi, which is slightly less

than the yield pressure; the loading was continued with different load increments of 6, 3, and 1.5 psi. The results for normal displacement w at the center of shell, $\varphi = 0$, versus internal pressure is shown in Figure 36 where the trend of convergence can be observed. By comparing these three curves, it can be deduced that the rate of convergence increases as the magnitude of load increment decreases. The results of solution with 1.5 psi load increment are plotted in Figures 37 to 42. Figures 37, 38, and 39 show the normal displacement w, meridional moment M_s, and circumferential in plane force N_θ, respectively, for loading of 60, 81 and 102 psi. The elastic solution for 102 psi is also shown in these figures. Figures 38 and 39 clearly indicate a redistribution of stresses as the result of plastic deformation. In Figure 40 the boundaries of elastic-plastic zones are shown at several stages of loading, where a plastic region initiated at torus is propagated towards the spherical and cylindrical segments. Finally, Figures 41 and 42 show the stress path at several points along the meridian. It is interesting to note that although the external load was applied proportionally, the stress path does not remain radial. As the result, the deformation theory of plasticity is not quite suitable for this class of problem.

It may be of interest to compare the results obtained here with the limit load predicted in Ref. [62] and another paper by Shield and Drucker.* For the dimensions of shell selected here with $\frac{t}{D} = 0.004$ these

*R.T. Shield and D.C. Drucker, "Limit Strength of Thin Walled Pressure Vessels With an ASME Standard Torispherical Head," Proc. of 3rd U.S. Nat. Congr. Appl. Mech., pp. 665-672, 1958.

authors predict an ultimate pressure of

$$\frac{p^u D}{2\sigma_y t} = 0.364, \quad p^u = 87 \text{ psi}$$

This pressure is shown in Figure 36, which is lower than what might be considered as limit pressure using the procedure presented here. This might be attributed to the various approximations which were introduced in the above references namely; elimination of M_θ from the yield criterion, neglecting M_θ and M_φ in the equilibrium equations, and estimating the ultimate pressure from its bounds. In addition, the three hinge mechanism, which was assumed to achieve an upper bound, was not realized here.

The design pressure according to the ASME Unfired Pressure Vessels Code* for a torispherical shell is equal to

$$p^D = \frac{2SEt}{LM+0.2t}$$

where,

p^D - design pressure, psi

S - maximum allowable working stress, psi

E - lowest efficiency of any joint in the head

L - inside spherical radius, inches

$M = \frac{1}{4}\left(3 + \sqrt{\frac{L}{r}}\right)$

r - inside toroidal knuckle radius, inches

*ASME Boiler and Pressure Vessel Code, "Section VIII, Unfired Pressure Vessels," 1965.

t - minimum required thickness of head after forming, inches (exclusive of corrosion allowance)

and the inside diameter of the head skirt D is taken to be equal to L. Defining the load factor n

$$n = \frac{\sigma_y}{SE}$$

the above formula can be recast as

$$p^u = \frac{2\sigma_y t}{LM+0.2t}$$

where

$$p^u = np^D$$

For the example given here it turns out that

$$p^u = 135.5 \text{ psi}$$

which is higher than what might be considered as limit pressure in Fig. 36. Note that the effect of workhardening was not considered in this example.

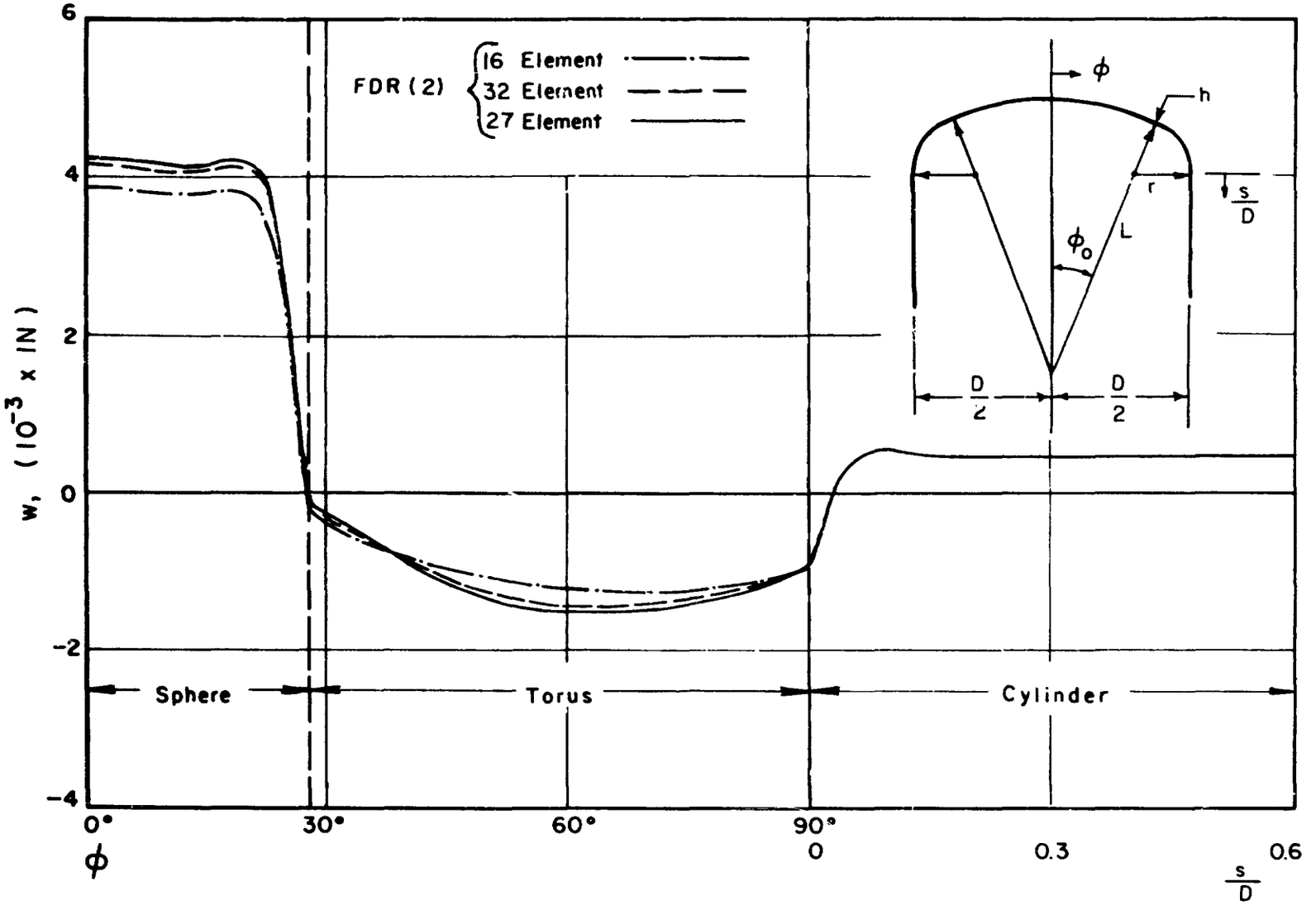

FIG 35 NORMAL DISPLACEMENT w FOR DIFFERENT NUMBER OF ELEMENT (TORISPHERICAL SHELL)

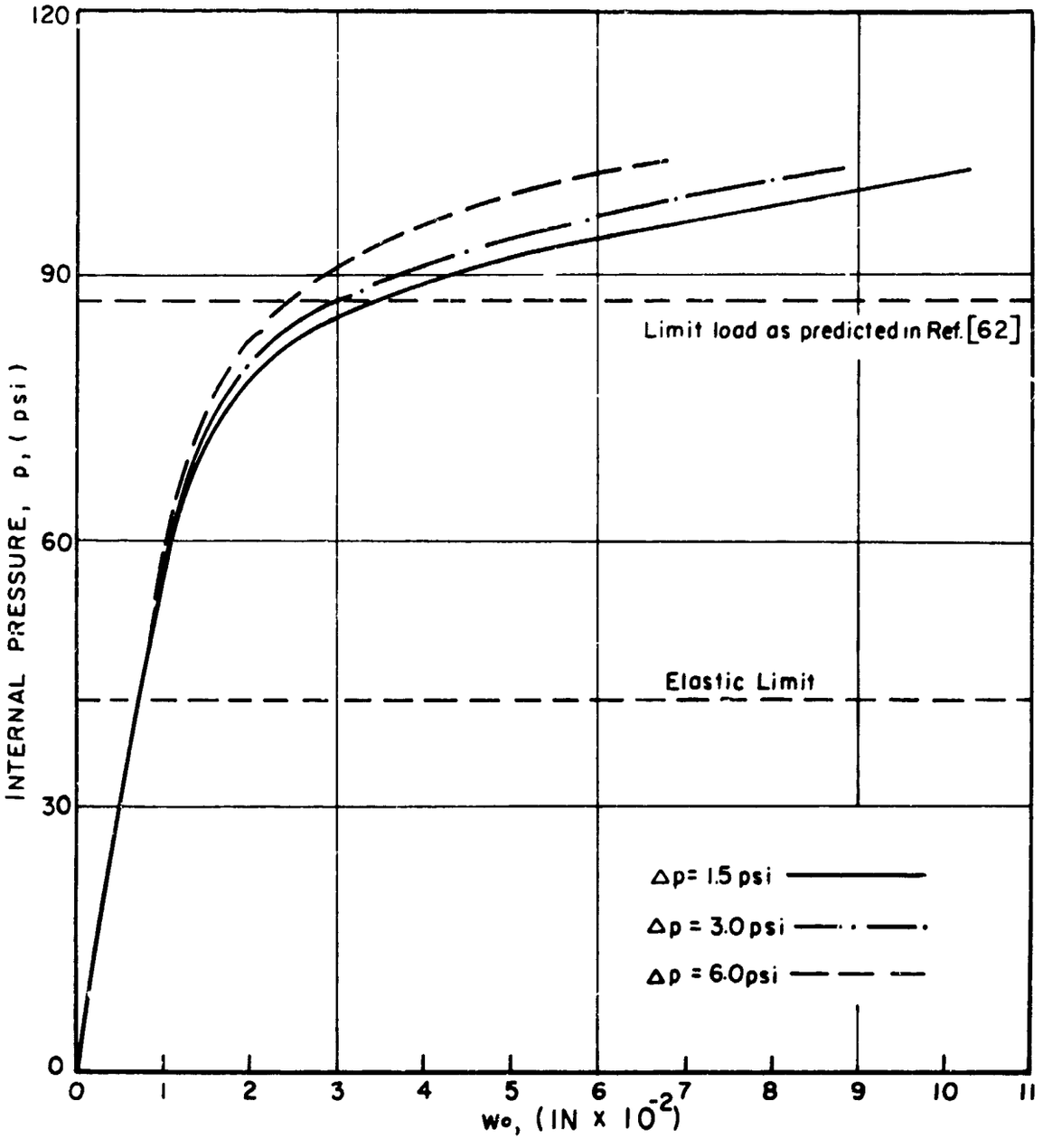

FIG. 36 PRESSURES VERSUS NORMAL DISPLACEMENT w_0 AT APEX FOR DIFFERENT LOAD INCREMENTS

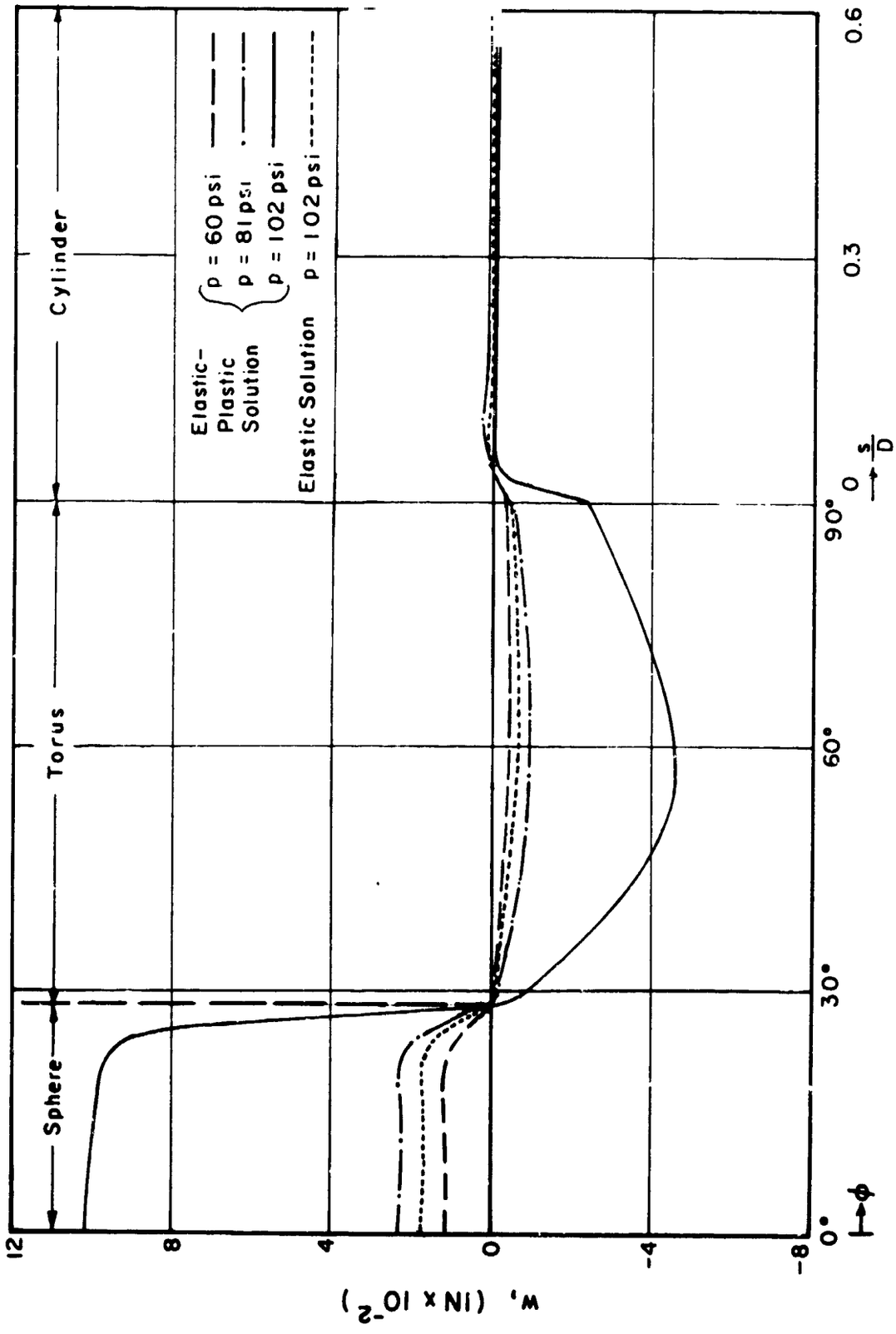

FIG. 37 NORMAL DISPLACEMENT w IN TORISPHERICAL SHELL

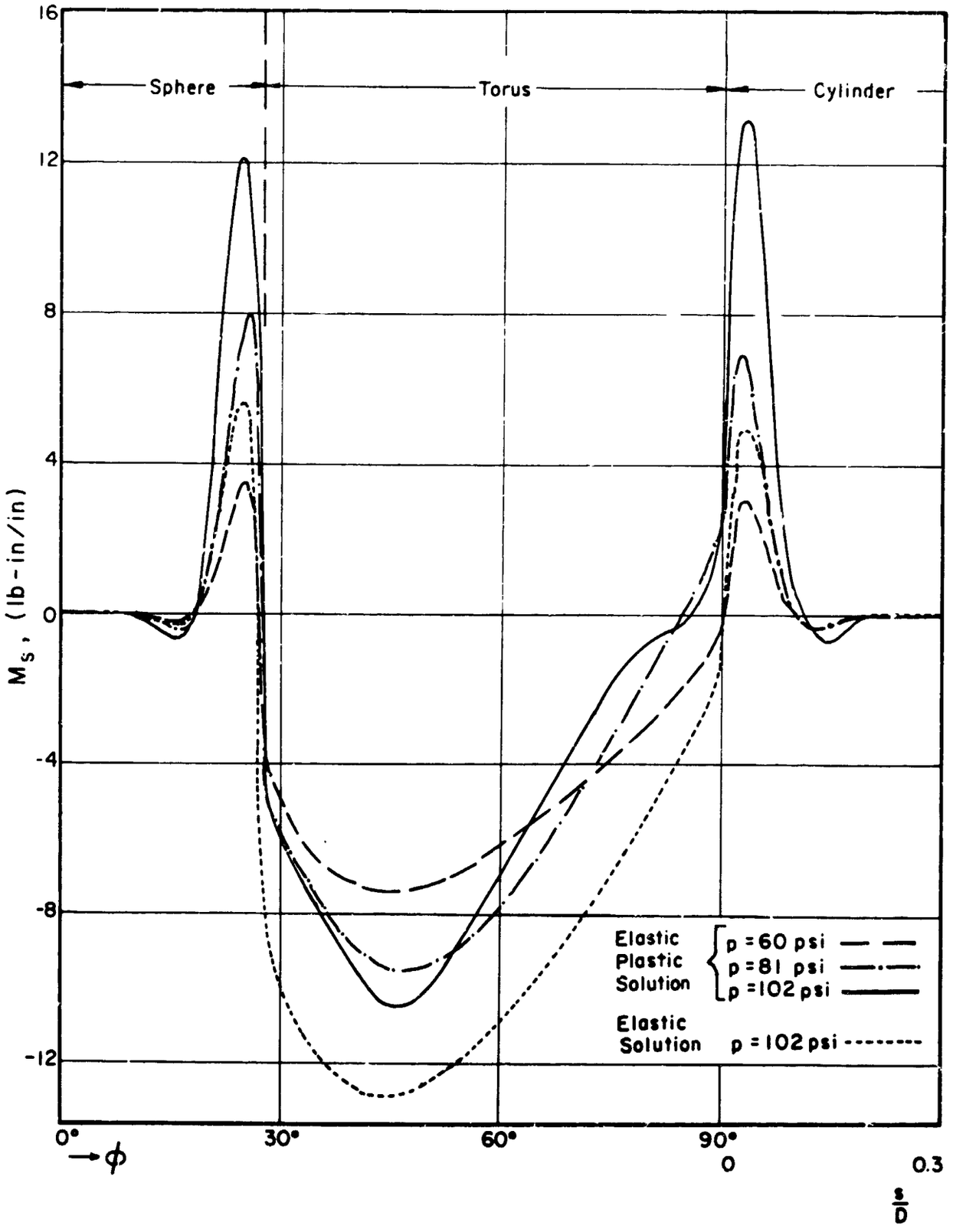

FIG. 38 MERIDIONAL BENDING MOMENT M_s IN TORISPHERICAL SHELL

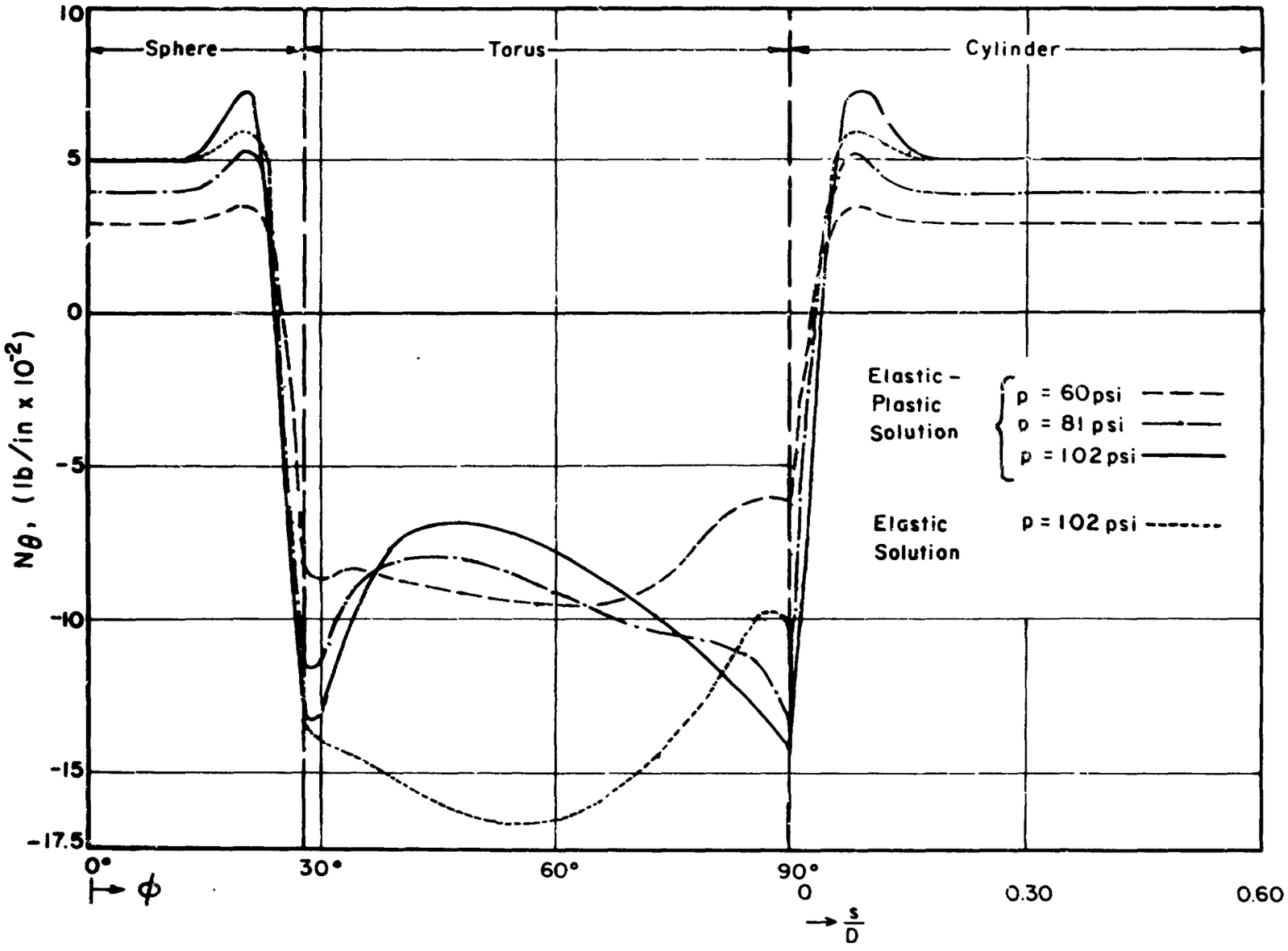

FIG. 39 CIRCUMFERENTIAL MEMBRANE FORCE IN TORISPHERICAL SHELL

Curve No.	P_i (psi)	Curve No	P_i (psi)
1	43.5	7	63.0
2	46.5	8	64.5
3	49.5	9	67.5
4	52.5	10	81.0
5	57.0	11	102.0
6	60.0		

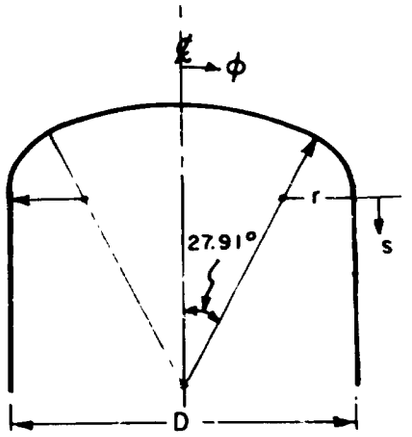

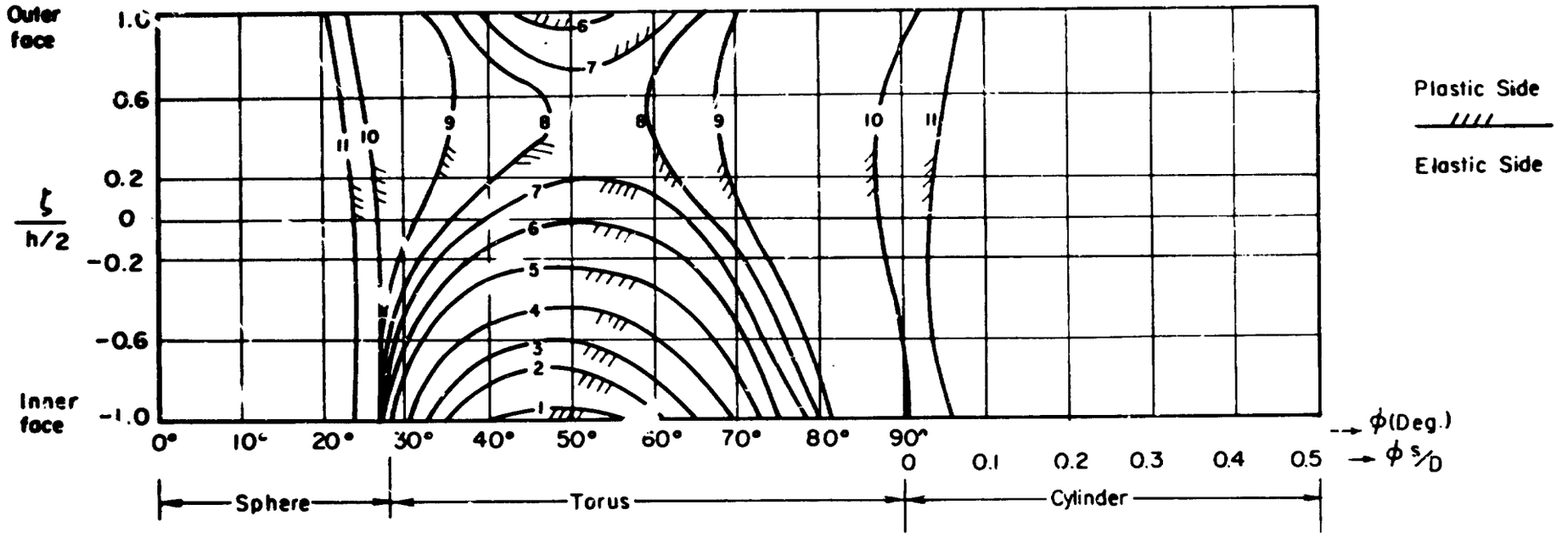

FIG. 40 ELASTIC - PLASTIC BOUNDARIES (TORISPHERICAL SHELL)

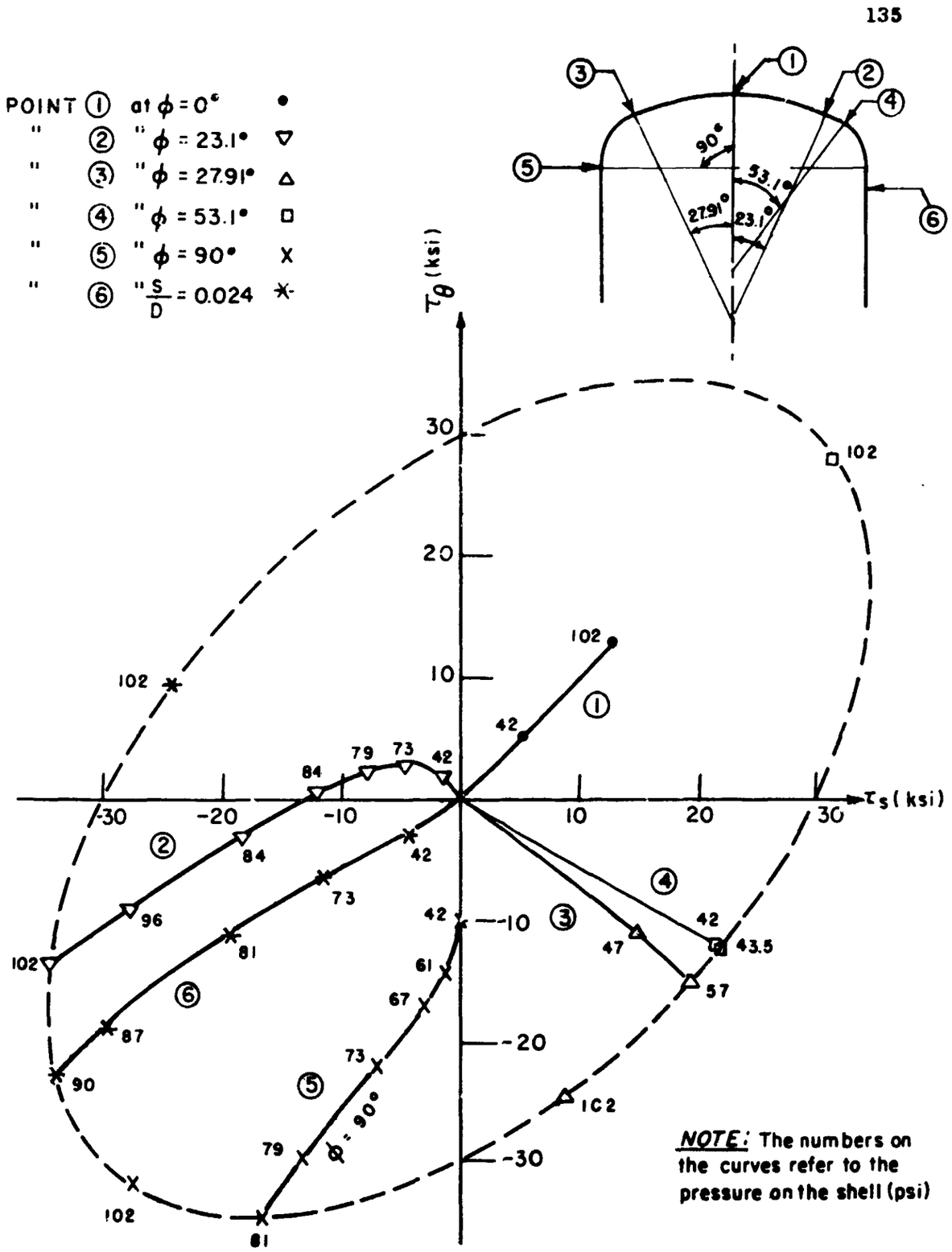

FIG. 41 STRESS PATH AT INNER FACE
(TORISPHERICAL SHELL)

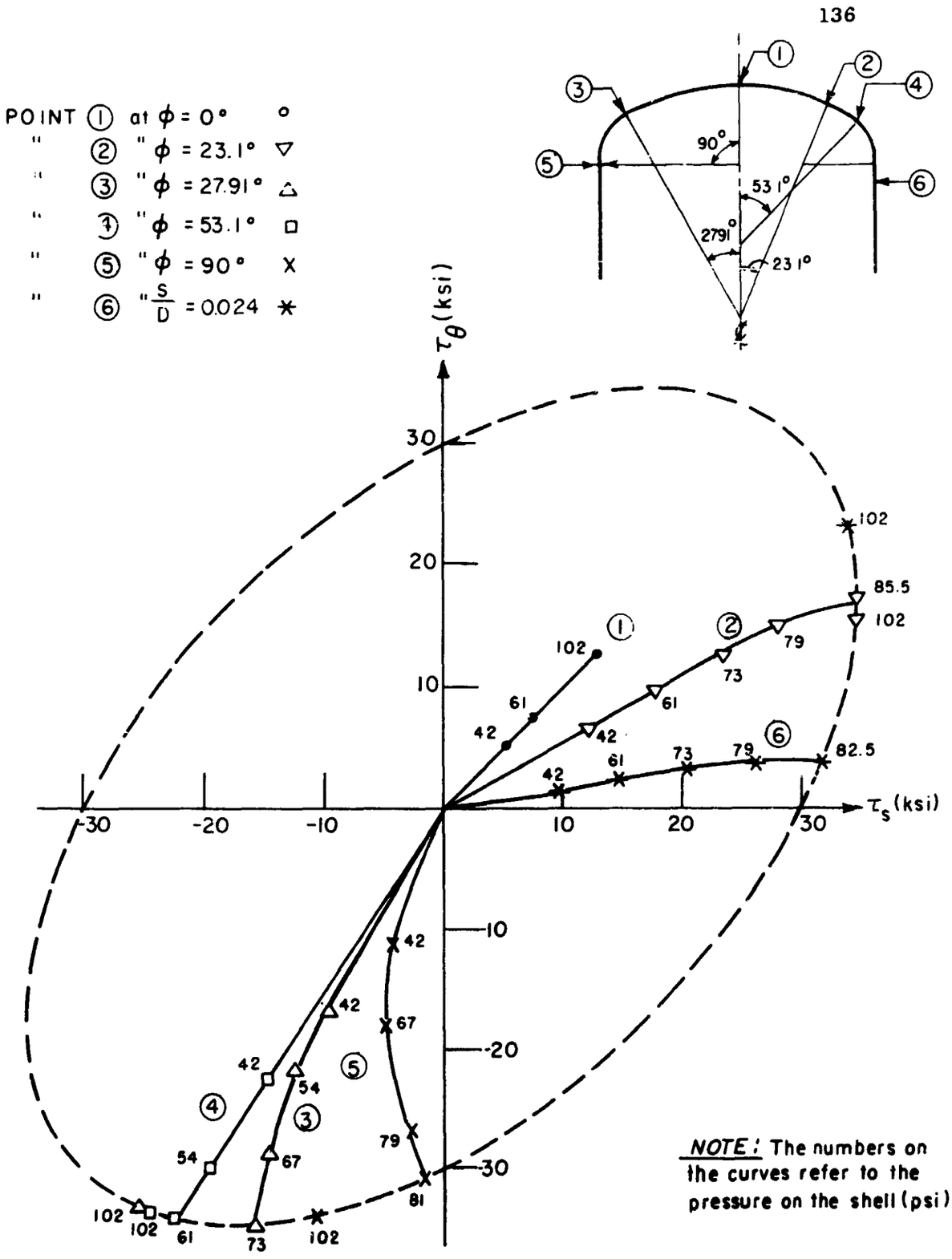

FIG. 42 STRESS PATH AT OUTER FACE
(TORISPHERICAL SHELL)

7. CONCLUSIONS

A numerical method has been presented for the analysis of elastic-plastic shells of revolution under axisymmetric loading and support conditions. The shell is assumed to be torsion-free, and Kirchhoff hypotheses together with Love's first approximation and small deflection theory are adopted. The method is quite general and is applicable to any shell geometry, loading, support conditions, and material properties; subject to the condition of axial symmetry. The approach is suitable for a routine computation on a digital computer.

The finite element method using the displacement model is selected to analyze the system. For a close idealization of the shell geometry, a curved frustum is taken as the primary element. Because the shell is axially symmetric, only the meridian is to be defined. In a search for geometric representation of a curved element, two schemes are considered. One is to express this curve in terms of its intrinsic equations. This is found to be numerically laborious and requires some approximations. The approximations are not suitable for the entire range of latitude angle. The other is to represent the curve in some local coordinates. Employing the latter approach, an element was developed which can take specified slopes and curvatures at its nodal circles and is well-conditioned for any shell geometry. It appears possible to generalize these two schemes to express the geometry of a curved element for a shell of arbitrary shape.

Representation of displacement patterns of a curved element is another important problem. The displacement patterns can be alternatively expressed in either surface (curvilinear) or local (rectilinear) coordinates. Comparison

of the two approaches was made with the aid of numerical examples. The latter was found to be superior in accommodating for rigid body translation and constant straining modes.

In general, idealization of the meridional curve with the aid of curved elements is found to greatly improve the results. The accuracy of the solution is considerably increased. At the same time, a smaller number of elements can be used in comparison to that of a conical element. Moreover, the extra effort for deriving the element stiffness matrix for a curved element and the extra computer time for execution is very small. It should be noted that for a very thin shell where the membrane forces become predominant and the bending effects are localized, a very fine mesh should be used near the boundary layer region even with a curved element. An improvement of the solution can be achieved by allowing more degrees of freedom in the displacement patterns. The solution can proceed either by a condensation technique or by including extra degrees of freedom, such as change of curvature, at nodal circles. This requires further investigations.

An incremental technique using the tangent stiffness method was utilized for the elastic-plastic solution. Flow theory of plasticity was employed which allows the trace of any loading history. Although any material properties can be specified, the examples are given for elastic-perfectly plastic and elastic-isotropic hardening materials using Mises yield condition and its associated flow rule.

Finally, a computer program was developed which can treat any rotational shells with arbitrary geometry and support conditions. The shell thickness may vary along the meridian and any distributed and/or concentrated ring loads can be specified. With the aid of numerical examples, the convergence and the accuracy of the method is found to be entirely satisfactory.

REFERENCES

General

[1] H. Reissner, "Spannungen in Kugelschalen," Müller-Breslau Festschrift, Leipzig, Germany, 1912.

[2] E. Meissner, "Das Elastizitätsgesetz für dünne Schalen von Ringflächen, Kugel- und Kegelform," Phys. Zeitschrift, Vol. 14, 1913.

[3] P.M. Naghdi and C.N. DeSilva, "Deformation of Elastic Ellipsoidal Shells of Revolution," Proc. of the Second U.S. Nat. Congr. of Appl. Mech., 1954, pp. 333-343.

[4] R.D. Schile, "Asymptotic Solution of Nonshallow Shells of Revolution Subjected to Nonsymmetric Loads," Jour. of the Aerospace Sci., Vol. 29, 1962, pp. 1375-1379.

[5] S. Timoshenko and S. Woinowsky-Krieger, "Theory of Plates and Shells," McGraw-Hill, 1960.

[6] W. Flügge, "Stresses in Shells," J. Springer, Berlin, 1960.

[7] V.Z. Vlasov, "General Theory of Shells and its Application in Engineering," Translated from Russian, NASA TT F-99, April 1964.

[8] W.K. Sepetoski, C.E. Pearson, I.W. Drigwell, and A.W. Adkins, "A Digital Computer Program for the General Axisymmetric Thin Shell Problem," Jour. of Appl. Mech., Vol. 29, Dec. 62, pp. 655-661.

[9] B. Budiansky and P.P. Radkowski, "Numerical Analysis of Unsymmetrical Bending of Shells of Revolution," AIAA Jour., Vol. 1, No. 8, Aug. 63, pp. 1833-1842.

[10] E. Klingbeil, "Zur Theorie der Rotationsschalen vom Standpunkt Numerischer Rechnungen," Ingenieur-Archiv, Vol. 27, 1959, pp. 242-249.

[11] A. Kalnins, "Analysis of Shells of Revolution Subjected to Symmetrical and Non-Symmetrical Loads," Jour. Appl. Mech., Vol. 31, No. 3, Sept. 1964, pp. 467-476.

[12] R.R. Meyer and M.B. Harmon, "Conical Segment Method for Analyzing Shells of Revolution for Edge Loading," AIAA Jour. Vol. 1, No. 4, April 1963, pp. 886-891.

[13] E.P. Popov, J. Penzien, and Z.A. Lu, "Finite Element Solution for Axisymmetrical Shells," Jour. of Eng. Mech. Div., Proc. ASCE, Vol. 90, No. 5, Oct. 1964, pp. 119-145.

[14] L.P. Felton and T.Au, "Analysis of Shells of Revolution with Arbitrary Meridians," Paper Presented at ASME meeting in New Orleans, Sept. 1966.

[15] M.J. Turner, R.W. Clough, H.C. Martin and L.J. Topp, "Stiffness and Deflection Analysis of Complex Structures," Jour. of the Aerospace Sci., Vol. 23, 1956, pp. 805-823.

[16] J.H. Argyris and S. Kelsey, "Energy Theorem and Structural Analysis," Butterworths, London, 1960.

[17] R.J. Melosh, "Bases of Derivation of Matrices for the Direct Stiffness Method," AIAA Jour., Vol. 1, No. 7, July 1963, pp. 1631-1637.

[18] B.F. deVeubeke, "Upper and Lower Bounds in Matrix Structural Analysis," Published in AGARDograph, No. 72, 1964, Edited by deVenbeke, Pergamon Press.

[19] B.F. deVeubeke, "Displacemet and Equilibrium Models in Finite Element Method," Ch. 9 of "Stress Analysis," edited by D.C. Zienkiewicz and G.S. Holister, John Wiley, 1965, pp. 145-197.

[20] L.R. Herrman, "A Bending Analysis of Plates," Proc. of the Conf. on Matrix Methods in Struct. Mech." Dayton, Ohio, Oct. 1965, AFFDL-TR-66-80, Nov. 66, pp. 577-602.

[21] P.E. Grafton and D.R. Strome, "Analysis of Axisymmetrical Shells by the Direct Stiffness Method," AIAA Jour., Vol. 1, No. 10, Oct. 1963, PP. 2342-2347.

[22] J.H. Percy, T.H.H. Pian, S. Klein, and D.R. Navaratna, "Application of Matrix Displacement Method to Linear Elastic Analyses of Shells of Revolution," AIAA Jour., Vol. 3, No. 11, Nov. 1965, pp. 2138-2145.

[23] S. Klein and R.J. Sylvester, "The Linear Elastic Dynamic Analysis of Shells of Revolution by the Matrix Displacement Method," Proc. of the Conf. on Matrix Methods in Structural Mech., Dayton, Ohio, 26-28 Oct. 1965, AFFDL-TR-66-80, Nov. 1966, pp. 299-328.

[24] S.B. Dong, "Analysis of Laminated Shells of Revolution," Jour. Eng. Mech. Div., Proc. ASCE, Vol. 92, No. 6, Dec. 1966, pp. 135-155.

[25] R.E. Jones and D.R. Strome, "A Survey of the Analysis of Shells by the Displacement Method," Proc. of the Conf. on Matrix Meth. in Struct. Mech., Dayton, Ohio, 26-28 Oct. 1965, AFFDL-TR-66-80, Nov. 1966, pp. 205-230.

[26] R.E. Jones and D.R. Strome, "Direct Stiffness Method Analysis of Shells of Revolution Utilizing Curved Element," AIAA Jour., Vol. 4, No. 9, Sept. 1966, pp. 1519-1525.

[27] E.L. Wilson, "Matrix Analysis of Nonlinear Structures," Proc. of the Second ASCE Conf. on Electronic Computation, Pittsburgh, Pa., Sept. 60.

[28] L.R. Herrman, "A Nonlinear Two-Dimensional Stress Analysis Applicable to Solid Propellant Rocket Grains," Aerojet-General Corp., T.M. No. 20, July 1965.

[29] J.H. Argyris, "Continua and Discontinua," Proc. of the Conf. on Matrix Methods in Struct. Mech., Dayton, Ohio, 26-28 Oct. 1965, AFFDL-TR-66-80, Nov. 66, pp. 126-169.

[30] A.A. Ilyushin, "Some Problems in the Theory of Plastic Deformations," (in Russian), Prikl. Mat. Mekh. Vol. 7, pp. 245-272, 1943, English translation, BMB-12, Grad. Div. Appl. Math., Brown Univ., for David W. Taylor Model Basin, 1946.

[31] J. Padlog, R.D. Huff, and G.F. Holloway, "Unelastic Behavior of Structures Subjected to Cyclic, Thermal, and Mechanical Stressing Conditions," Aero Research Lab., WADD Tech. Rep. 60-271, Dec. 60.

[32] J.H. Argyris, "Elasto-plastic Matrix Displacement Analysis of Three-Dimensional Continua," Jour. of the Royal Aeronautical Soc., Vol. 69, Sept. 1965, pp. 633-636.

[33] P.V. Marcal, "A Stiffness Method for Elastic-Plastic Problems," Int. J. Mech. Sci., Vol. 7, 1965, pp. 229-238.

[34] M. Khojasteh-Bakht, S. Yaghmai, and E.P. Popov, "A Bending Analysis of Elastic-Plastic Circular Plates," Struct. Eng. Lab., Univ. of Calif., Berkeley, SESM 66-4, April 1966.

[35] W. Lasing, W.R. Jensen, W. Falby, "Matrix Analysis Methods for Inelastic Structures," Proc. of the Conf. on Matrix Methods in Struct. Mech.," Dayton, Ohio, (Oct. 1965), AFFDL-TR-66-80, Nov. 66, pp. 605-634.

[36] R.W. Clough, "The Finite Element Method in Structural Mechanics," in "Stress Analysis," edited by O.C. Zienkiewicz and G.S. Holister, John Wiley, 1965, pp. 85-119.

[37] T.H. Lin, "In the Associated Flow Rules of Plasticity Based on Crystal Slips," Jour. of the Franklin Inst. Vol. 270, No. 4, Oct. 1960, pp. 291-300.

[38] B.F. Langer, "Design of Pressure Vessels for Cycle Fatigue," Trans. ASME, Series D, Vol. 83, 1962, pp. 389-

[39] S.S. Manson, "Thermal Stress and Low-Cycle Fatigue," McGraw-Hill, 1966.

Limit Analysis

[40] D.C. Drucker, W. Prager, and H.J. Greenberg, "Extended Limit Design Theorems for Continuous Media," Quart. Appl. Math., Vol. 9, 1952, pp. 381-389.

[41] W. Prager, "The General Theory of Limit Design," Proc. 8th Intern. Congr. Appl. Mech., Vol. 2, 1956, pp. 65-72.

[42] R.A. Meshlumyan, "Limiting Conditions for Bending and Torsion of Thin-Walled Shells Beyond the Elastic Limit," (in Russian), Prikl. Mat. Mekh., Vol. 14, No. 5, 1950. pp. 537-542.

[43] D.C. Drucker, "Limit Analysis of Cylindrical Shells under Axially Symmetric Loading," Proc. 1st Midwestern Conf. Solid Mech., Urbana, Ill., 1953, pp. 158-163.

[44] M.S. Mikeladge, "The Load Carrying Capacity or Originally Anisotropic Shells," (in Russian). DAN SSSR, Vol. 98, No. 6, 1954, pp. 921-923.

[45] E.T. Onat and W. Prager, "Limit Analysis of Shells of Revolution," Proc. of Royal Netherlands Acad. Sci., Vol. B57, 1954, pp. 534-548.

[46] P.G. Hodge, Jr., "The Rigid-Plastic Analysis of Symmetrically Loaded Cylindrical Shells," J. Appl. Mech., Vol. 21, 1954, pp. 336-342.

[47] V.J. Rosenblum, "Approximate Theory of Equilibrium of Plastic Shells," (in Russian), Prikl. Mat. Makh. Vol. 18, No. 3, 1954, pp. 289-302.

[48] E.T. Onat, "Plastic Collapse of Cylindrical Shells under Axially-Symmetrical Loading," Quart. Appl. Math., Vol. 13, 1955, pp. 63-72.

[49] G. Eason and R.T. Shield, "The Influence of Free Ends on the Load Carrying Capacities of Cylindrical Shells," J. Mech. Phys. Solids, Vol. 4, No. 1, 1955, pp. 17-27.

[50] V.V. Rozhdestvensky, "On the Problem of Limit States of Thin Shells," (in Russian) in: Investigation of Problems of Structural Mechanics and the Theory of Plasticity, Moscow, 1956.

[51] M.S. Mikeladze, "The Load Carrying Capacity of a Circular Anisotropic Cylindrical Shell Loaded Symmetrically with Respect to its Axis", (in Russian) Izv. Akad. Nauk SSSR Vol. 9, 1956.

[52] G.I. Hazalia, "Limit Analysis of Shallow Spherical Shells," (in Russian), Izv. Akad. Nauk Gruz. SSR, Vol. 17, 1956.

[53] D. Niepostyn, "The Limit Analysis of an Orthotropic Circular Cylinder," (in Polish), Arch. Mech. Stos., Vol. 8, No. 4, 1956, pp. 565-580.

[54] M.S. Mikeladze, "General Theory of Anisotropic Rigid-Plastic Shells," (in Russian), Izv. Akad. Nauk, SSSR, OTN 1957, No. 1, pp. 85-94.

[55] S.M. Feinberg, "Plastic Flow of Shallow Shells for Axisymmetric Problem," (in Russian), Prikl. Mat. Mekh. Vol. 21, No. 4, 1957, pp. 544-549.

[56] E.W. Ross, "On the Effect of Boundary and Loading Conditions in the Limit Analysis of Plastic Structures," J. Appl. Mech. Vol. 24, No. 2, 1957, pp. 314-315.

[57] V. V. Rozhdestvensky, "States of Limiting Equilibrium of Prestressed Shells of Revolution," (in Russian), Moscow 1957, C.N.I.I.S.K.

[58] M.N. Fialkov, "Limit Loads of Simply Supported Circular Shell Roofs," J. Eng. Mech. Div., Proc. ASCE, Vol. 84, July 58., pp. 1706-1, 39.

[59] P.G. Hodge, Jr., "The Linearization of Plasticity Problems by Means of Non-Homogeneous Materials," in: Non-homogeneity in Elasticity and Plasticity (Proc. IUTAM 1958) ed. W. Olzsak, 1959, pp. 147-156, Pergamon Press.

[60] A.R. Rzhanitzyn, "Analysis of Shells by the Method of Limit Equilibrium," (in Russian), Problems of the Theory of Plasticity and Strength of Structure, Moscow 1958, C.N.I.I.S.K.

[61] P.G. Hodge, Jr., "Plastic Analysis of Structures," McGraw-Hill, 1959, pp. 298-304.

[62] D.C. Drucker and R.T. Shield, "Limit Analysis of Symmetrically Loaded Thin Shells of Revolution," J. Appl. Mech., Vol. 26, No. 1, 1959, pp. 61-68.

[63] G. Eason, "The Load Carrying Capacities of Cylindrical Shells Subjected to a Ring Force," J. Mech. Phys. Solids, Vol. 7, No. 1959, pp. 169-181.

[64] P.G. Hodge, Jr., "The Collapse Load of a Spherical Cap," Proc. 4th Midwestern Conf. on Solid Mech., Austin, Texas, 1959, pp. 108-126.

[65] P.G. Hodge, Jr., "Plastic Analysis of Rotationally Symmetric Shells," DOMIIT Report No. 1-6, 1959, Ill. Inst. Tech.

[66] W. Prager, "Introduction to Plasticity," Addison-Wesley, Mass., 1959, pp. 68-76.

[67] A. Sawczuk and P.G. Hodge, Jr., "Comparison of Yield Conditions for Circular Cylindrical Shells," DOMIIT Rep. No. 7, Chicago, 1959, Ill. Inst. Tech.

[68] A. Sawczuk and J. Rychlewski, "On the Yield Surfaces for Plastic Shells," Arch. Mech. Stos., Vol. 12, No. 1, 1960, pp. 29-53.

[69] Z. Mroz, "The Load Carrying Capacity of Orthotropic Shells," Arch. Mech. Stos., Vol. 12, No. 1, 1960, pp. 85-107.

[70] P.G. Hodge, Jr., "Yield Conditions for Rotationally Symmetric Shells Under Axisymmetric Loading," J. Appl. Mech., Vol. 27, No. 2, 1960, pp. 323-331.

[71] P.G. Hodge, Jr., "Plastic Analysis of Circular Conical Shells," J. Appl. Mech., Vol. 27, No. 2, 1960, pp. 696-700.

[72] R. Sankaranarayanan, "Plastic Interaction Curves for Circular Cylindrical Shells Under Combined Lateral and Axial Pressure," J. Franklin Inst., Vol. 270, No. 5, Nov. 1960, pp. 359-366.

[73] E.T. Onat, "Plastic Analysis of Shallow Conical Shells," J. Eng. Mech. Div., Proc. ASCE, Vol. 86, No. 6, Dec. 1960, pp. 1-12, also DAM Rep. No. DA4795/3, Brown Univ., 1959.

[74] P.G. Hodge, Jr., "The Mises Yield Condition for Rotationally Symmetric Shells," Quart. Appl. Math. Vol. 18, 1961, pp. 305-311.

[75] P.G. Hodge, Jr. and C. Lakshmikantham, "Yield Point Loads of Spherical Caps with Cut Out," Proc. 4th U.S. Nat. Congr. Appl. Mech. 1962, Vol. 2, pp. 951-954 (Berkeley).

[76] P.G. Hodge, Jr. and J. Panarelli, "Interaction Curves for Circular Cylindrical Shells According to the Mises or Tresca Yield Conditions," J. Appl. Mech. Vol. 29, 1962, pp. 375-380.

[77] T. Nakamura, "Plastic Analysis of Shells of Revolution Under Axisymmetric Loads," Ph.D. Thesis, Stanford Univ., 1962.

[78] Y.R. Lepik, "On the Carrying Capacity of Inhomogeneous Plates and Shells," (in Russian), Izv. Akad. Nauk, SSSR, Otd Tekh. Mekh. i Mashinostr, No. 4, 1963, pp. 167-171.

[79] J. Panarelli and P.G. Hodge, Jr., "Plastic Analysis of Cylindrical Shells Under Pressure, Axial Load, and Torque," Proc. 8th Midwestern Mech. Conf. Cleveland, 1963.

[80] R.H. Lance and E.T. Onat, "Analysis of Plastic Shallow Conical Shells," J. Appl. Mech., Vol. 30, No. 2, March 1963, pp. 199-209.

[81] P.G. Hodge, Jr. and C. Lakshmikanthan, "Limit Analysis of Shallow Shells of Revolution," J. Appl. Mech., Vol. 30, No. 2, June 1963, pp. 215-218.

[82] P.G. Hodge, Jr. and J. DeRuntz, Jr., "The Carrying Capacity of Conical Shells Under Concentrated and Distributed Loads," DOMIIT Rep. 1-22, Ill. Inst. of Tech., 1963.

[83] Z. Mroz and B.Y. Xu, "The Load Carrying Capacities of Symmetrically Loaded Spherical Shells," Arch. Mech. Stos. Vol. 15, No. 2, 1963, pp. 245-266.

[84] R.E. Ball and S.L. Lee, "Limit Analysis of Cylindrical Shells," J. Eng. Mech. Div., Proc. ASCE, Vol. 89, No. 3, 1963, pp. 73-96.

[85] P.G. Hodge, Jr., "Limit Analysis of Rotationally Symmetric Plates and Shells," Prentice-Hall, 1963.

[86] W. Olszak, Z. Mroz, and P. Perzyna, "Recent Trends in the Development of the Theory of Plasticity," Pergamon Press, 1963, Ch. 3, pp. 84-129.

[87] M.S. Mikeladze, "Statics of Anisotropic Plastic Shells," Georgian Academy of Sciences, Tibilisi, 1963.

[88] P.G. Hodge, Jr., "Plastic Design of a Closed Cylindrical Structures," J. Mech. Phys. Solids, Vol. 12, No. 1, Feb. 1964, pp. 1-10.

[89] S.S. Gill, "The Limit Pressure for a Flush Cylindrical Nozzle in Spherical Pressure Vessel," Int. J. Mech. Sci., Vol. 6, No. 1, Feb. 1964, pp. 105-115.

[90] N.C. Lind, "Plastic Analysis of Radial Outlets From Spherical Pressure Vessels," Jour. Eng. Indust., Trans. ASME, Vol. 86, May 1964, pp. 193-198.

[91] R.L. Cloud, "Plastic Limit Analysis of Cylindrical Nozzles in Spherical Shells," Ph.D. Thesis, Univ. of Pittsburgh, 1964.

[92] B.J. Thorn, "Deformation of Perfectly Plastic and Isotropic Linear Strain Hardening Cylindrical Shells," Ph.D. Thesis, Northwestern Univ., 1964.

[93] K.S. Dinno and S.S. Gill, "The Effect of the Circumferential Bending Moment and Change of Circumferential Curvature on the Calculation of the Limit Pressure of Symmetrically Loaded Shells of Revolution," Int. J. Mech. Sci., Vol. 7, No. 1, Jan. 65, pp. 15-19.

[94] K.S. Dinno and S.S. Gill, "The Limit Analysis of a Pressure Vessel Consisting of the Junction of a Cylindrical and Spherical Shell," Int. J. Mech. Sci. Vol. 7, No. 1, Jan. 1965, pp. 21-42.

[95] W. Olszak and A. Sawczuk, Proceedings of the Symposium on "Non-Classical Shell Problems," North-Holland, 1964, pp. 619-931.

[96] R.L. Cloud, "The Limit Pressure of Radial Nozzles in Spherical Shells," Nuc. Struct. Eng., Vol. 1, No. 4, Apr. 1965, pp. 403-413.

[97] F. Ellyin and A.N. Sherbourne, "Limit Analysis of Axisymmetric Intersecting Shells of Revolution," Nucl. Struct. Eng., Vol. 2, No. 1, July 1965, pp. 86-91.

[98] F. Ellyin and A.N. Sherbourne, "The Collapse of Cylindrical/Sphere Intersecting Pressure Vessels," Nucl. Struct. Eng., Vol. 2, No. 2, Aug. 65, pp. 169-180.

[99] H.S. Ho and D.P. Updike, "Limit Analysis for Combined Loading on a Cylindrical Shell Obeying the Tresca Yield Conditions," Rep. NsG No. 9-488, Brown Univ., Aug. 1965.

[100] F.A. Leckie, "The Plastic Analysis of a Spherical Shell Subjected to a Radial Load Applied Through a Rigid Boss," Rep. NSF GP-1115/23, Brown Univ., Aug. 65.

[101] M. Duszek, "Effect of Geometry Changes on the Carrying Capacity of Cylindrical Shells," Polska Akad. Nauk, Warsaw, Vol. 13, No. 4, 1965, pp. 183-191.

[102] W. Flügge and T. Nakamura, "Plastic Analysis of Shells of Revolution under Axisymmetric Loads," Ing. Arch., Vol. 34, July 1965, pp. 238

[103] R.W. Kuech and S.L. Lee, "Limit Analysis of Simply Supported Conical Shells Subjected to Uniform Internal Pressure," J. Franklin Inst. Vol. 280, No. 1, July 1965, pp. 71-87.

[104] L.C. Lee and E.T. Onat, "Analysis of Plastic Spherical Shells," Div. Eng., Brown Univ., NSF GP 1115/27, Nov. 1965.

[105] J.A. DeRuntz, Jr. and P.G. Hodge, Jr., "The Signifiance of the Concentrated Load in the Limit Analysis of Conical Shells," J. Appl. Mech., Vol. 30, No. 1, March 1966, pp. 93-101.

[106] J.C. Gerdeen, "Shell Plasticity-Piecewise Smooth Trajectories on the Nakamura Yield Surface," Ph.D. Thesis, Stanford Univ., 1966.

Rigid-Work Hardening

[107] W. Prager, "A New Method of Analyzing Stresses and Strains in Work-Hardening Plastic Solids," Jour. Appl. Mech., Vol. 23, No. 4, Dec. 1956, pp. 493-496; also Brown Univ., Rep. A 11-123, 1955.

[108] P.G. Hodge, Jr., "The Theory of Piecewise Linear Isotropic Plasticity," in Deformations and Flow of Solids, Colloq., Madrid, Edited by Grammell, Springer, 1955.

[109] P.G. Hodge, Jr., "A General Theory of Piecewise Linear Plasticity Based on Maximum Shear," J. Mech. Phys. Solids, Vol. 5, No. 4, 1957, pp. 242-260.

[110] E.T. Onat, "Analysis of Shells of Revolution Composed of Work-Hardening Material," J. Mech. and Phys. Solids, Vol. 7, Nov. 1958, pp. 45-49.

[111] B.J. Thorn and S.L. Lee, "Linear Strain Hardening of Cylindrical Shells," Jour. Eng. Mech. Div., Proc. ASCE, Vol. 90, No. 4, Aug. 64, pp. 97-122.

Elastic-Plastic Analysis Using Deformation Theory

[112] A.A. Ilyushin, "Plasticity," (in Russian), Moscow 1948; (in French), Paris, 1956, edited by Eyroller.

[113] R.A. Meshlumyan, "Applied Theory of Elastic-Plastic Shells and its Application to the Computation of Shells," (in Russian), Inzh. Sborn. Vol. 10, 1951, pp. 35-70.

[114] Yu. N. Rabotnov, "Approximate Technical Theory of Elastic-Plastic Shells," (in Russian), Prickl. Mat. Mekh., Vol. 15, 1951, pp. 167-175.

[115] A.J. Rosenblum, "Approximate Theory of Equilibrium of Plastic Shell," (in Russian), Prickl. Mat. Mekh., Vol. 18, No. 3, 1954, pp. 289-302.

[116] A.N. Ananina, "Axisymmetric Deformation of Cylindrical Shell with Elastic-Plastic Deformation," (in Russian) Inzh. Sborn., Vol. 18, 1954, pp. 157-160.

[117] I.S. Tsurkov, "Elastic-Plastic Equilibrium of Shells of Revolution With Small Axisymmetric Deformation," (in Russian) Izv. Akad. Nauk SSSR, OTN, No. 11, 1956, pp. 106-110.

[118] I.S. Tsurkov, "Elastic-Plastic Equilibrium of Shallow Shells with Small Deformations," (in Russian) Izv. Akad. Nauk SSSR, OTN, 1956, No. 6, pp. 139-142.

[119] L.V. Ershov and D.D. Ivlov, "Elastic-Plastic State of a Conical Tube Under the Action of Internal Pressure," (in Russian), Vestn. Mosk, Gros. Univ., No. 2, 1957, pp. 51-52.

[120] M.S. Mikeladze, "Elastic-Plastic Equilibrium of Anisotropic Shells," (in Russian), Izv. Akad. Nauk Gruz. SSR, 1958.

[121] A. Mendelson and S.S. Manson, "Practical Solution of Plastic Deformation Problems in Elastic-Plastic Range," NASA TR-R-28, 1959.

[122] P. Stern, "Elastic-Plastic Analysis of Shells of Revolution by a Finite Difference Method," Rep. LMSD-288183, Lockheed Aircraft Corp., Jan. 1960.

[123] A.V. Odinets, "Elastic-Plastic Symmetric Strain of Constructionally Orthotropic Cylindrical Shells," (in Russian), Sh. Nauk, Trudi Kievsk, Stroit. In'ta, part 20, 1962, pp. 191-199; Rev. Zh. Mekh. No. 1, 1964.

[124] D.A. Spera, "Analysis of Elastic-Plastic Shells of Revolution Containing Discontinuities," AIAA Jour. Vol. 1, No. 11, Nov. 63, pp. 2583-2589.

[125] S.B. Roberts, "Elastic-Plastic Analysis of Symmetrically Loaded Shells of Revolution," Rept AMR 5109-3003, May 1965.

Elastic-Plastic Analysis Using Flow Theory

[126] P.G. Hodge, Jr. and F. Romano, "Deformations of an Elastic-Plastic Cylindrical Shells with Linear Strain Hardening," J. Mech. and Phys. Solids, Vol. 4, No. 3, May 1956, pp. 145-161.

[127] P.G. Hodge, Jr., "Displacement in an Elastic-Plastic Cylindrical Shell," J. Appl. Mech., Vol. 23, No. 1, 1956, pp. 73-79.

[128] P.G. Hodge, Jr. and S.V. Nardo, "Carrying Capacity of an Elastic-Plastic Cylindrical Shell with Linear Strain Hardening," Jour. Appl. Mech., Vol. 25, No. 1, 1958, pp. 79-85.

[129] B. Paul and P.G. Hodge, Jr., "Carrying Capacity of Elastic-Plastic Shells Under Hydrostatic Pressure," Proc. Third U.S. Nat. Congr. Appl. Mech., 1958, pp. 631-640.

[130] E.T. Onat and S. Yamantürk, "On Thermally Stressed Elastic-Plastic Shells," J. Appl. Mech., Vol. 29, No. 1, Mar. 1962, pp. 108-114.

[131] B.W. Shaffer and M. Senator, "An Elastic-Plastic Analysis of Cylindrical Shell with Partially Plastic Cross Section," Proc. Fourth U.S. Nat. Congr. Appl. Mech., Vol. 2, June 1962, pp. 1121-1131.

[132] E.A. Witmer, H.A. Balmer, J.W. Leech, and T.H.H. Pian, "Large Dynamic Deformations of Beams, Rings, Plates and Shells," AIAA Jour., Vol. 1, No. 8, Aug. 63, pp. 1848-1857.

[133] P.V. Marcal and C.E. Turner, "Numerical Analysis of the Elastic-Plastic Behavior of Axisymmetrically Loaded Shells of Revolution," The Jour. of Mech. Eng. Sci., Vol. 5, No. 3, Spet. 63, pp. 232-237.

[134] P. Stern, "Stresses and Displacements in Elastic-Plastic Shells of Revolution with Temperature-Dependent Properties," Tech. Rept. 6-62-90-123, Jan. 1963, Lockheed Missiles and Space Co.

[135] S.L. Lee and B.J. Thorn, "Deformation of Axisymmetrically Loaded Cylindrical Shells at Incipient Plastic Collapse," Inter. Jour. of Mech. Sci., Vol. 6, 1964, pp. 247-256.

[136] J.A. Stricklin, P.T. Hsu, and T.H.H. Pian, "Large Elastic, Plastic, and Creep Deflections of Curved Beams and Axisymmetric Shells," AIAA Jour., Vol. 2, No. 9, Sept. 64, pp. 1613-1620; see Also, J.A. Stricklin, Ph.D. Thesis, MIT, Jan. 1964.

[137] W.B. Stephens, "Analysis of Elastic-Strain Hardening Behavior of Symmetrically Loaded Conical Shells," Thesis, Univ. of Virginia, Charlotessville, 1965.

[138] B.J. Thorn, J.S. Kao, and S.L. Lee, "Isotropic Linear Strain-Hardening of Cylindrical Shells Based Upon Tresca Yield Criterion," J. Franklin Inst., Vol. 280, No. 6, Dec. 1965, pp. 530-547.

[139] P.V. Marcal and W.R. Pilgrim, "A Stiffness Method for Elastic-Plastic Shells of Revolutions," Jour. of Strain Analysis, Vol. 1, No. 4, 1966, pp. 339-350.

[140] W.B. Stephens and J.A. Friedericy, "Elastic-Strain Hardening Behavior of Symmetrically Loaded Shells of Revolution Undergoing Large Deflection," to be published in AIAA Jour., see also, Proc. 5th U.S. Nat. Congr. Appl. Mech. 1966, pp. 591.

Experiments

[141] K.H. Gerstle, R. Lance and E.T. Onat, "Plastic Behavior of Conical Shells," Proc. First Southeastern Conf. on the Theoretical and Appl. Mech. May 62; in Dev. in Theo. and Appl. Mech., Vol. 1, May 62, Plenum Press (1963).

[142] H.H. Demir and D.C. Drucker, "An Experimental Study of Cylindrical Shells Under Ring Loading," in Progress in Appl. Mech., Prager Anniv. Volume, MacMillan, 1963, pp. 205-220.

[143] G. Augusti and S. d'Agostino, "Tests of Cylindrical Shells in the Plastic Range," J. of Eng. Mech. Div., Proc. ASEE, Vol. 90, Feb. 64, pp. 69-81.

[144] D.C. Drucker, "The Experimental and Analytical Significance of Limit Pressure for Cylindrical Shells - A Discussion," Rept. NSF GP 1115/6, March 64, Brown University.

[145] S.T. Wasti, "Finite Plastic Deformation of Spherical Shells," Ph.D. Thesis, Cambridge 1964.

[146] A. Kaufman and D.A. Spera, "Investigation of the Elastic-Plastic Stress State Around A Reinforced Opening in a Spherical Shell," NASA TN D-2672, Feb. 1965.

[147] P.V. Marcal and C.E. Turner, "Limit Life of Shells of Revolution Subjected to Severe Local Bending," J. Mech. Eng. Sci., Vol. 7, No. 4, Dec. 1965, pp. 408-423.

[148] J.S. Stoddart and B.S. Owen, "Stresses in a Tori-Spherical Pressure Vessel Head," Inst. of Physics, Stress Analysis Group, Meeting on Stress Analysis Today, 1965.

[149] K.S. Dinno and S.S. Gill, "An Experimental Investigation into the Plastic Behavior of Flush Nozzles in Spherical Pressure Vessels," Int. J. Mech. Sci., Vol. 7, No. 12, Dec. 1965, pp. 817-839.

[150] F. Ellyin and A.N. Sherbourne, "An Experimental Study of Plastic Deformation of Intersecting Shells," Proc. 5th U.S. Nat. Cong. Appl. Mech., June 66, pp. 551.

Constitutive Laws of Plasticity

[151] Tresca, "Mémoire Sur l'écoulement des Corps Solides," Mérn. Press, par div., San. 18, 1868, pp. 733-799.

[152] R.V. Mises, "Mechanik der Fester Koerper in Plastisch Deformation Zustand," Goettinger, Nachr. Math-Phys., Kh., 1913, pp. 582-592.

[153] P.W. Bridgman, "The Compressibility of Thirty Metals as a Function of Pressure and Temperature," Proc. Am. Acad. Sci., Vol. 58, 1923, pp. 163-242.

[154] R.V. Mises, "Mechanik der Plastischen Formanderung von Kristaleen," Z. Angew. Math. Mech., Vol. 8, 1928, pp. 161-

[155] W. Prager, "Strain Hardening Under Combined Stresses," Jour. Appl. Phys., Vol. 16, 1945, pp. 837-840.

[156] R. Hill, "A Theory of the Yielding and Plastic Flow of Anisotropic Metals," Proc. of the Royal Soc., London, England, Series A, Vol. 193, 1948, pp. 281-299.

[157] R. Hill, "The Mathematical Theory of Plasticity," Oxford, Clarendon Press, 1950.

[158] D. C. Drucker, "A More Fundamental Approach to Plastic Stress-Strain Relations," Proc. 1st U.S. Nat. Congr. Appl. Mech. (Chicago, 1951), pp. 487-491, New York, 1952.

[159] W. Prager, "The Theory of Plasticity: A Survey of Recent Achievements," (James Clayton Lecture) Proc. Inst. Mech. Eng., Vol. 169, 1955, pp. 41-52.

[160] D.R. Bland, "The Two Measures of Work-Hardening," Proc. 9th Int. Congr. Appl. Mech. (Brussels, 1956), Vol. 8, 1957, pp. 45-50.

[161] H. Ziegler, "A Modification of Prager's Hardening Rule," Quart. Appl. Math., Vol. 17, 1959, pp. 55-65.

[162] W.T. Koiter, "General Theorems of Elastic-Plastic Solids," in Progress in Solid Mech., Vol. 1, (Edited by I.N. Sneddon and R. Hill), North-Holland, 1960.

[163] P.M. Naghdi, "Stress-Strain Relations in Plasticity and Thermo-Plasticity," in Plasticity, Proc. 2nd Symp. on Naval Struct. Mech., pp. 121-167, Pergammon, 1963.

APPENDIX A

[B] Matrices For a Frustum Element (See pp. 89)

$$(5.46)\quad \underset{4\times1}{\{\varepsilon\}} = \underset{4\times6}{[B]}\ \underset{6\times1}{\{\alpha\}}$$

(1) FDC Element

$$\begin{bmatrix} 0 & \frac{\sin\varphi_i}{r_1} & \frac{1}{\ell} & \frac{\xi}{r_1} & \frac{\xi^2}{r_1} & \frac{\xi^3}{r_1} \\ 0 & \frac{\cos(\varphi-\varphi_i)}{r} & \frac{\cos\varphi}{r}\xi & \frac{\sin\varphi}{r}\xi & \frac{\sin\varphi}{r}\xi^2 & \frac{\sin\varphi}{r}\xi^3 \\ 0 & \frac{d}{ds}(\frac{1}{r_1})\cos\varphi_i & \frac{d}{ds}(\frac{\xi}{r_1}) & 0 & -\frac{2}{\ell^2} & -\frac{6\xi}{\ell^2} \\ 0 & \frac{\cos\varphi\ \cos\varphi_i}{rr_1} & \frac{\xi\cos\varphi}{rr_1} & -\frac{\cos\varphi}{\ell r} & -\frac{2\xi\ \cos\varphi}{\ell r} & -\frac{3\xi^2\ \cos\varphi}{\ell r} \end{bmatrix}$$

(2) FDR Element

$$\begin{bmatrix} 0 & \rho & 0 & \eta'\rho & 2\xi\eta'\rho & 3\xi^2\eta'\rho \\ \frac{\sin\psi}{r} & \frac{\sin\psi}{r}\xi & \frac{\cos\psi}{r} & \frac{\cos\psi}{r}\xi & \frac{\cos\psi}{r}\xi^2 & \frac{\cos\psi}{r}\xi^3 \\ 0 & (1-\eta'^2)\Phi & 0 & 2\eta'\Phi & 4\xi\eta'\Phi-\mu & 3\xi(2\xi\eta'\Phi-\mu) \\ 0 & \eta'\Psi & 0 & -\Psi & -2\xi\Psi & -3\xi^2\Psi \end{bmatrix}$$

where

$$\rho = \frac{1}{\ell(1+\eta'^2)} \qquad \mu = \frac{2}{\ell^2(1+\eta'^2)^{3/2}} \qquad \Phi = \frac{\eta''}{\ell^2(1+\eta'^2)^{5/2}} \qquad \Psi = \frac{\sin\psi+\eta'\cos\psi}{\ell r(1+\eta'^2)^{3/2}}$$

APPENDIX B

[B] Matrices For a Cap Element (see pp. 89)

$$(5.46)\quad \underset{4x1}{\{\varepsilon\}} = \underset{4x6}{[B]}\ \underset{6x1}{\{\alpha\}}$$

(1) FDC Element

$$\begin{bmatrix} 0 & 0 & \frac{1}{\ell} & 0 & \frac{\xi^2}{r_1} & \frac{\xi^3}{r_1} \\ 0 & 0 & \frac{\cos\varphi}{\bar{r}} & 0 & \frac{\xi}{\bar{r}}\sin\varphi & \frac{\xi^2}{\bar{r}}\sin\varphi \\ 0 & 0 & \frac{d}{ds}\left(\frac{\xi}{r_1}\right) & 0 & -\frac{2}{\ell^2} & -6\frac{\xi}{\ell^2} \\ 0 & 0 & \frac{\cos\varphi}{\bar{r}r_1} & 0 & -2\frac{\cos\varphi}{\bar{r}\ell} & -3\frac{\xi\cos\varphi}{\bar{r}\ell} \end{bmatrix}$$

where

$$\bar{r} = \frac{r}{\xi}\ ,\ \text{Note } r(0) = 0$$

(2) FDR Element

$$\begin{bmatrix} 0 & 0 & 0 & \rho(1+\eta'\tan\beta_i) & 2\xi\eta'\rho & 3\xi^2\eta'\rho \\ 0 & 0 & 0 & \frac{\cos\varphi_i}{\bar{r}\cos\beta_i} & \frac{\xi\cos\psi}{\bar{r}} & \frac{\xi^2\cos\psi}{\bar{r}} \\ 0 & 0 & 0 & (1+2\eta'\tan\beta_i-\eta'^2)\Phi & 4\xi\eta'\Phi-\mu & 3\xi(2\xi\eta'\Phi-\mu) \\ 0 & 0 & 0 & \frac{\eta'-\tan\beta_i}{\xi}\Psi & -2\Psi & -3\xi\Psi \end{bmatrix}$$

where

$$\rho = \frac{1}{\ell(1+\eta'^2)} \qquad \mu = \frac{2}{\ell^2(1+\eta'^2)^{3/2}} \qquad \Phi = \frac{\eta''}{\ell^2(1+\eta'^2)^{5/2}} \qquad \Psi = \frac{\sin\psi+\eta'\cos\psi}{\ell\bar{r}(1+\eta'^2)^{3/2}}$$

APPENDIX C

[$\phi(\xi)$] Matrices For a Frustum Element (see pp. 89)

$$(5.47)\quad \underset{3\times1}{\{v(\xi)\}} = \underset{3\times6}{[\phi(\xi)]}\ \underset{6\times1}{\{\alpha\}}$$

(1) FDC Element

$$\begin{Bmatrix} u \\ w \\ \chi \end{Bmatrix} = \begin{bmatrix} -\sin\varphi & \cos\varphi_i & \xi & 0 & 0 & 0 \\ \cos\varphi & \sin\varphi_i & 0 & \xi & \xi^2 & \xi^3 \\ 0 & -\dfrac{\cos\varphi_i}{r_1} & -\dfrac{\xi}{r_1} & \dfrac{1}{\ell} & \dfrac{2\xi}{\ell} & \dfrac{3\xi^2}{\ell} \end{bmatrix} \begin{Bmatrix} \alpha_1 \\ \alpha_2 \\ \alpha_3 \\ \alpha_4 \\ \alpha_5 \\ \alpha_6 \end{Bmatrix}$$

(2) FDR Element

$$\begin{Bmatrix} u_1 \\ u_2 \\ \chi \end{Bmatrix} = \begin{bmatrix} 1 & \xi & 0 & 0 & 0 & 0 \\ 0 & 0 & 1 & \xi & \xi^2 & \xi^3 \\ 0 & -\dfrac{\eta'}{\ell(1+\eta'^2)} & 0 & \dfrac{1}{\ell(1+\eta'^2)} & \dfrac{2\xi}{\ell(1+\eta'^2)} & \dfrac{3\xi^2}{\ell(1+\eta'^2)} \end{bmatrix} \begin{Bmatrix} \alpha_1 \\ \alpha_2 \\ \alpha_3 \\ \alpha_4 \\ \alpha_5 \\ \alpha_6 \end{Bmatrix}$$

APPENDIX C (Con't)

[$\phi(\xi)$] Matrices for a Cap Element (see pp. 89)

$$(5.47)\quad \underset{3x1}{\{v(\xi)\}} = \underset{3x6}{[\phi(\xi)]}\ \underset{6x1}{\{\alpha\}}$$

(1) FDC Element

$$\begin{Bmatrix} u \\ w \\ \chi \end{Bmatrix} = \begin{bmatrix} -\sin\varphi & 0 & \xi & 0 & 0 & 0 \\ \cos\varphi & 0 & 0 & 0 & \xi^2 & \xi^3 \\ 0 & 0 & -\frac{\xi}{r_1} & 0 & \frac{2\xi}{\ell} & \frac{3\xi^2}{\ell} \end{bmatrix} \begin{Bmatrix} \alpha_1 \\ \alpha_2 \\ \alpha_3 \\ \alpha_4 \\ \alpha_5 \\ \alpha_6 \end{Bmatrix}$$

(2) FDR Element

$$\begin{Bmatrix} u_1 \\ u_2 \\ \chi \end{Bmatrix} = \begin{bmatrix} 0 & 0 & -\cos\psi & \xi & 0 & 0 \\ 0 & 0 & \sin\psi & \xi\tan\beta_i & \xi^2 & \xi^3 \\ 0 & 0 & 0 & \frac{\tan\beta_i - \eta'}{(1+\eta'^2)} & \frac{2\xi}{(1+\eta'^2)} & \frac{3\xi^2}{(1+\eta'^2)} \end{bmatrix} \begin{Bmatrix} \alpha_1 \\ \alpha_2 \\ \alpha_3 \\ \alpha_4 \\ \alpha_5 \\ \alpha_6 \end{Bmatrix}$$

Note that the order of $\{\alpha\}$ has been changed for compactness from Frustum to Cap element. This is consistent with [A] matrix.

APPENDIX D

Displacement Transformation Matrices [A] for a Frustum Element (See pp. 91)

$$(5.53)\quad \underset{6\times1}{\{q\}} = \underset{6\times6}{[A]}\ \underset{6\times1}{\{\alpha\}} \qquad \{q\} = \begin{Bmatrix} v_i \\ \hline v_j \end{Bmatrix} \quad \underset{6\times6}{[A]} = \begin{bmatrix} \Phi(0) \\ \hline \Phi(1) \end{bmatrix}$$

(1) FDC Element

$$\begin{bmatrix}
-\sin\varphi_i & \cos\varphi_i & 0 & 0 & 0 & 0 \\
\cos\varphi_i & \sin\varphi_i & 0 & 0 & 0 & 0 \\
0 & -\dfrac{\cos\varphi_i}{r_1(0)} & 0 & \dfrac{1}{\ell} & 0 & 0 \\
-\sin\varphi_j & \cos\varphi_i & 1 & 0 & 0 & 0 \\
\cos\varphi_j & \sin\varphi_i & 0 & 1 & 1 & 1 \\
0 & -\dfrac{\cos\varphi_i}{r_1(1)} & -\dfrac{1}{r_1(1)} & \dfrac{1}{\ell} & \dfrac{2}{\ell} & \dfrac{3}{\ell}
\end{bmatrix}$$

(2) FDR Element

$$\begin{bmatrix}
1 & 0 & 0 & 0 & 0 & 0 \\
0 & 0 & 1 & 0 & 0 & 0 \\
0 & -\dfrac{\sin\beta_i\cos\beta_i}{\ell} & 0 & \dfrac{\cos^2\beta_i}{\ell} & \dfrac{2\xi\cos^2\beta_i}{\ell} & \dfrac{3\xi^2\cos^2\beta_i}{\ell} \\
1 & 1 & 0 & 0 & 0 & 0 \\
0 & 0 & 1 & 1 & 1 & 1 \\
0 & -\dfrac{\sin\beta_j\cos\beta_j}{\ell} & 0 & \dfrac{\cos^2\beta_j}{\ell} & \dfrac{2\xi\cos^2\beta_j}{\ell} & \dfrac{3\xi^2\cos^2\beta_j}{\ell}
\end{bmatrix}$$

APPENDIX D (Con't)

$[\bar{A}] \equiv [A^{-1}]$ Matrices For a Frustum Element (see pp. 91)

(1) FDC Element

$$\begin{bmatrix}
-\sin\varphi_i & \cos\varphi_i & 0 & 0 & 0 & 0 \\
\cos\varphi_i & \sin\varphi_i & 0 & 0 & 0 & 0 \\
\bar{a}_{31} & \bar{a}_{32} & 0 & 1 & 0 & 0 \\
\dfrac{\ell\cos^2\varphi_i}{r_1(0)} & \dfrac{\ell\sin\varphi_i\cos\varphi_i}{r_1(0)} & \ell & 0 & 0 & 0 \\
\bar{a}_{51} & \bar{a}_{52} & -2\ell & -\dfrac{\ell}{r_1(1)} & 3 & -\ell \\
\bar{a}_{61} & \bar{a}_{62} & \ell & \dfrac{\ell}{r_1(1)} & -2 & \ell
\end{bmatrix}$$

where

$$\bar{a}_{31} = -1 - (\sin\varphi_j - \sin\varphi_i)\sin\varphi_i$$

$$\bar{a}_{32} = (\sin\varphi_j - \sin\varphi_i)\cos\varphi_i$$

$$\bar{a}_{51} = \left[3\cos\varphi_j - 3\cos\varphi_i + \frac{\ell\sin\varphi_j}{r_1(1)}\right]\sin\varphi_i - 2\frac{\ell\cos^2\varphi_i}{r_1(0)}$$

$$\bar{a}_{61} = -\left[2\cos\varphi_j - 2\cos\varphi_i + \frac{\ell\sin\varphi_j}{r_1(1)}\right]\sin\varphi_i + \frac{\ell\cos^2\varphi_i}{r_1(0)}$$

$$\bar{a}_{52} = -3 - \left[3\cos\varphi_j - 3\cos\varphi_i + \frac{\ell\sin\varphi_j}{r_1(1)}\right]\cos\varphi_i - 2\frac{\ell\sin\varphi_i\cos\varphi_i}{r_1(0)}$$

$$\bar{a}_{62} = 2 + \left[2\cos\varphi_j - 2\cos\varphi_i + \frac{\ell\sin\varphi_j}{r_1(1)}\right]\cos\varphi_i + \frac{\ell\sin\varphi_i\cos\varphi_i}{r_1(0)}$$

APPENDIX D (Con't)

$[\bar{A}] \equiv [A^{-1}]$ Matrices For a Frustum Element (See pp. 91)

(2) FDR Element

$$\begin{bmatrix}
1 & 0 & 0 & 0 & 0 & 0 \\
-1 & 0 & 0 & 1 & 0 & 0 \\
0 & 1 & 0 & 0 & 0 & 0 \\
-\tan\beta_i & 0 & \ell(1+\tan^2\beta_i) & \tan\beta_i & 0 & 0 \\
2\tan\beta_i+\tan\beta_j & -3 & -2\ell(1+\tan^2\beta_i) & -2\tan\beta_i-\tan\beta_j & 3 & -\ell(1+\tan^2\beta_j) \\
-\tan\beta_i-\tan\beta_j & 2 & \ell(1+\tan^2\beta_i) & \tan\beta_i+\tan\beta_j & -2 & \ell(1+\tan^2\beta_j)
\end{bmatrix}$$

$[\bar{A}] = [A^{-1}]$ Matrices For a Cap Element (See pp. 91)

(1) FDC Element

$$\begin{bmatrix}
0 & 1 & 0 & 0 & 0 & 0 \\
0 & 0 & 0 & 0 & 0 & 0 \\
0 & \sin\varphi_j & 0 & 1 & 0 & 0 \\
0 & 0 & 0 & 0 & 0 & 0 \\
0 & -\dfrac{\ell\sin\varphi_j}{r_1(1)} - 3\cos\varphi_j & 0 & -\dfrac{\ell}{r_1(1)} & 3 & -\ell \\
0 & \dfrac{\ell\sin\varphi_j}{r_1(1)} + 2\cos\varphi_j & 0 & \dfrac{\ell}{r_1(1)} & -2 & \ell
\end{bmatrix}$$

Note - The value $\bar{a}_{12} = 1$ only contributes to rigid body translation.

Appendix D (Con't)

$[\bar{A}] = [A^{-1}]$ Matrices For a Cap Element (see pp. 91)

(2) FDR Element

$$\begin{bmatrix}
0 & 0 & 0 & 0 & 0 & 0 \\
0 & 0 & 1 & 0 & 0 & 0 \\
0 & 0 & 0 & 0 & 0 & 0 \\
0 & 0 & \cos\Psi & 1 & 0 & 0 \\
0 & 0 & -2\dfrac{\cos\varphi_i}{\cos\beta_i} - \dfrac{\cos\varphi_j}{\cos\beta_j} & -2\tan\beta_i + \tan\beta_j & 3 & -\ell(1+\tan^2\varphi_j) \\
0 & 0 & \dfrac{\cos\varphi_i}{\cos\beta_i} + \dfrac{\cos\varphi_j}{\cos\beta_j} & \tan\beta_i + \tan\beta_j & -2 & \ell(1+\tan^2\varphi_j)
\end{bmatrix}$$

Note - For a Cap Element

$$\{\alpha\} = [A^{-1}]\ \{q\}$$

$$\{q\}^T = \langle\ 0\ \ V(0)\ \ 0\ \ u_1(1)\ \ u_2(1)\ \ \chi(1)\ \rangle$$

APPENDIX E

Transformations To Global Coordinates (r-Z)

$$(5.54) \qquad \underset{6x1}{\{q\}} = \underset{6x6}{[T]}\ \underset{6x1}{\{r\}}$$

(1) FDC Element

Equation (5.54) may be expressed as

$$\begin{Bmatrix} v_i \\ \hline v_j \end{Bmatrix} = \left[\begin{array}{c|c} T_i & 0 \\ \hline 0 & T_j \end{array}\right] \begin{Bmatrix} r_i \\ \hline r_j \end{Bmatrix}$$

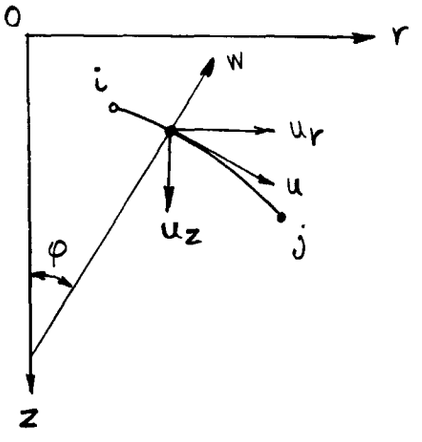

where

$$\{v_i\}^T = \langle\, u \quad w \quad \chi \,\rangle_i$$

$$\{r_i\}^T = \langle\, u_r \quad u_z \quad \chi \,\rangle_i$$

$$[T(\xi)] = \begin{bmatrix} \cos\varphi & \sin\varphi & 0 \\ \sin\varphi & -\cos\varphi & 0 \\ 0 & 0 & 1 \end{bmatrix}$$

$$\underset{3x3}{[T_i]} = \underset{3x3}{[T(0)]} \qquad \underset{3x3}{[T_j]} = \underset{3x3}{[T(1)]}$$

APPENDIX E (Con't)

(2) FDR Element

Similar to the previous case

$$\{v\}^T_{i,j} = \langle u_1 \quad u_2 \quad \chi \rangle_{i,j}$$

$$[T] = [T_i] = [T_j] = \begin{bmatrix} \cos\psi & \sin\psi & 0 \\ \sin\psi & -\cos\psi & 0 \\ 0 & 0 & 1 \end{bmatrix}$$

3x3 3x3 3x3

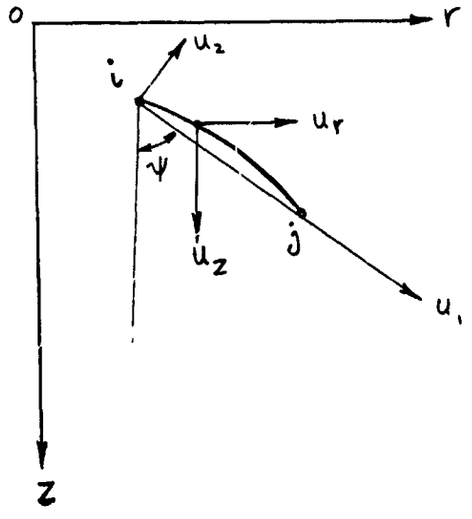

APPENDIX F

Transformation to Surface Coordinates (u,w)

$$(5.54) \quad \underset{6x1}{\{q\}} = \underset{6x6}{[T]} \; \underset{6x1}{\{r\}}$$

or

$$\begin{Bmatrix} v_i \\ \hline v_j \end{Bmatrix} = \left[\begin{array}{c|c} T_i & 0 \\ \hline 0 & T_j \end{array}\right] \begin{Bmatrix} r_i \\ \hline r_j \end{Bmatrix}$$

$$\{r\}^T_{i,j} = \langle\, u \quad w \quad \chi \,\rangle_{i,j}$$

(1) FDC Element

$$\{v\}^T = \langle u \quad w \quad \chi \rangle$$

$$\underset{3x3}{[T_i]} = \underset{3x3}{[T_j]} = \underset{3x3}{[I]}$$

where $[I]$ is the identity matrix

(2) FDR Element

$$\{v\}^T = \langle\, u_1 \quad u_2 \quad \chi \,\rangle$$

$$[T(\xi)] = \begin{bmatrix} \cos\beta & -\sin\beta & 0 \\ \sin\beta & \cos\beta & 0 \\ 0 & 0 & 1 \end{bmatrix}$$

$[T_i] = [T(0)]$, $[T_j] = [T(1)]$